การวิเคราะห์ออกซิไดซ์อะโปโปรตีน B-100 โดยแมสสเปกโทรเมทรี

นางสาวศิริพร แสงสุธรรม

วิทยานิพนธ์นี้เป็นส่วนหนึ่งของการศึกษาตามหลักสูตรปริญญาวิทยาศาสตรมหาบัณฑิต
สาขาวิชาเทคโนโลยีชีวภาพ หลักสูตรเทคโนโลยีชีวภาพ
คณะวิทยาศาสตร์ จุฬาลงกรณ์มหาวิทยาลัย
ปีการศึกษา 2546

ISBN 974-17-3884-6

ANALYSIS OF OXIDIZED APOPROTEIN B-100 BY MASS SPECTROMETRY

Miss Siriporn Sangsuthum

A Thesis Submitted in Partial Fulfillment of the Requirements

for the Degree of Master of Science in Biotechnology

Program of Biotechnology

Faculty of Science

Chulalongkorn University

Academic Year 2003

ISBN 974-17-3884-6

Thesis Title	ANALYSIS OF OXIDIZED APOPROTEIN B-100 BY MASS SPECTROMETRY
By	Miss Siriporn Sangsuthum
Field of Study	Biotechnology
Thesis Advisor	Assistant Professor Dr. Polkit Sangvanich
Thesis Co-advisor	Associate Professor Dr. Winai Dahlan

Accepted by the Faculty of Science, Chulalongkorn University in Partial Fulfillment of the Requirements for the Master 's Degree

..... Dean of Faculty of Science

(Professor Dr. Piamsak Menasveta)

THESIS COMMITTEE

..... Chairman

(Professor Dr. Sophon Roengsumran)

..... Thesis Advisor

(Assistant Professor Dr. Polkit Sangvanich)

..... Thesis Co-advisor

(Associate Professor Dr. Winai Dahlan)

..... Member

(Associate Professor Dr. Amorn Petsom)

..... Member

(Assistant Professor Dr. Nattaya Ngamrojanavanich)

ศิริพร แสงสุธรรม : การวิเคราะห์ออกซิไดซ์อะโปโปรตีนB-100 โดยแมสสเปกโทรเมทรี. (ANALYSIS OF OXIDIZED APOPROTEIN B-100 BY MASS SPECTROMETRY) อ. ที่ปรึกษา : ผศ.ดร.พลกฤษณ์ แสงวณิช, อ.ที่ปรึกษาร่วม : รศ.ดร.วินัย ดะห์ลัน, 85 หน้า. ISBN 974-17-3884-6.

ไลโปโปรตีนชนิดความหนาแน่นต่ำ (Low density lipoprotein, LDL) ทำหน้าที่ขนส่งคอเลสเทอรอลในกระแสเลือด เมื่อ LDL เกิดออกซิเดชัน จะผลิตสารเคมีที่เป็นพิษหลายตัว เช่น 4-hydroxy-2-nonenal (HNE), malondialdehyde (MDA) ซึ่งสารเคมีดังกล่าว โดยเฉพาะ HNE จะเข้าทำปฏิกิริยากับอะโปโปรตีน B-100 (apoprotein B-100, apoB-100) ส่งผลให้โครงสร้างของ apoB-100 เปลี่ยนไป ทำให้รีเซพเตอร์ไม่สามารถรับ LDL เข้าเซลล์ได้ตามปกติ อันเป็นปัจจัยสำคัญที่ก่อให้เกิดการสะสมของไขมันบนผนังหลอดเลือด และก่อให้เกิดโรคหลอดเลือดตีบแข็ง (atherosclerosis) ดังนั้น การวิเคราะห์ผลของการเกิดออกซิเดชันของ LDL จึงมีความสำคัญในการอธิบายสาเหตุของการเกิดโรคดังกล่าว

ในการทดลองครั้งนี้ได้ทำการแยก LDL จากพลาสมาซึ่งใช้ EDTA เป็นสารกันเลือดแข็ง โดยวิธี sequential ultracentrifugation ทำการออกซิไดซ์ LDL ด้วย $CuSO_4$ และ รีดิวซ์ด้วย $NaBH_4$ แล้วสกัดแยกออกซิไดซ์ apoB-100 ออกจากออกซิไดซ์ LDL ด้วย $CHCl_3$/MeOH (2/1) หลังจากนั้น ย่อยออกซิไดซ์ apoB-100 ที่ได้ด้วยทริปซิน แล้วแยกเปปไทด์ผสมออกจากกันด้วย reverse phase HPLC โดยใช้ ACN/H_2O เป็นตัวชะแบบ gradient และนำไปวิเคราะห์ต่อด้วย tandem mass spectrometry ตรวจหาเปปไทด์ที่ HNE เข้าไปทำปฏิกิริยากับหมู่ histidine โดยตรวจหาเปปไทด์ที่แตกตัวที่ m/z 268 ซึ่งเป็นตำแหน่งของ immonium ion ของ histidine ที่ HNE เข้าทำปฏิกิริยา หลังจากนั้น ทำการหาลำดับกรดอะมิโนในเปปไทด์นั้น เพื่อยืนยันตำแหน่ง histidine ที่ HNE เข้าทำปฏิกิริยา พบเปปไทด์ของออกซิไดซ์ apoB-100 ที่ HNE เข้าทำปฏิกิริยากับหมู่ histidine จำนวน 2 เปปไทด์ คือ T198 และT103 ซึ่งมีลำดับกรดอะมิโน LH*VAGNLK และ LLSGGNTLH*LVSTTK ตามลำดับ โดย * คือตำแหน่งที่ HNE เข้าไปทำปฏิกิริยา

หลักสูตร เทคโนโลยีชีวภาพ	ลายมือชื่อนิสิต.....
สาขาวิชา เทคโนโลยีชีวภาพ	ลายมือชื่ออาจารย์ที่ปรึกษา.....
ปีการศึกษา 2546	ลายมือชื่ออาจารย์ที่ปรึกษาร่วม.....

4372538623 : MAJOR BIOTECHNOLOGY

KEY WORD: OXIDIZED APOB-100 / OXIDIZED LDL / MASS SPECTROMETRY / HNE / LDL

SIRIPORN SANGSUTHUM: ANALYSIS OF OXIDIZED APOPROTEIN B-100 BY MASS SPECTROMETRY. THESIS ADVISOR: ASSISTANT PROFESSOR DR. POLKIT SANGVANICH, THESIS COADVISOR : ASSOCIATE PROFESSOR DR. WINAI DAHLAN, 85 pp. ISBN 974-17-3884-6.

Oxidatively modified LDL is likely to be the main source of cholesterol that accumulates in arteriosclerotic plaques. Trace amount of copper can induce LDL oxidation that generate the lipid peroxidation products such as malondialdehyde (MDA) and 4-hydroxy-2-nonenal (HNE). These aldehydes especially HNE modify apoB-100 results in an increasing in net negative charge of apoB-100, leads to the decreased or completely lost recognition by LDL receptor. Leading to the accumulation of cholesterol or cholesterol esters in the arterial wall and formation of fatty streak in the arterial wall and served as the first stage of atherogenesis.

In this research, LDL was prepared from EDTA plasma by sequential ultracentrifugation, and HNE/protein product was prepared from copper-mediated oxidized LDL and reduced with $NaBH_4$, following extraction of oxidized apoB-100 with CH_3Cl/MeOH (2/1) and trypsin digestion. Later, the tryptic peptides were separated by reverse phase HPLC with ACN/H_2O gradient elution. Finally, tandem mass spectrometry in precursor ion scanning of m/z 268 that correspond to the reduced form of the immonium ion of HNE-modified histidine, was used to determine the sites of modification on oxidized apoB-100. The modified peptides, T198 and T103 were found. Later the modified peptides were sequenced in product ion scanning mode to confirm the sites of modification. T198 and T103 with the sequence LH*VAGNLK and LLSGGNTLH*LVSTTK were presented (where * indicates adduction by HNE).

Program Biotechnology Student's signature.....

Field of study Biotechnology Advisor's signature.....

Academic year 2003 Co-advisor's signature.....

ACKNOWLEDGEMENTS

I would like to express my sincere thanks and appreciation to my thesis advisor, Assistant Professor Dr. Polkit Sangvanich for his continue guidance, thoughtful, help, encouragement and attention throughout this thesis. I also thank my thesis co-advisor Associate Professor Dr. Winai Dahlan.

I would like to thank Mr. Phayungsak Tanglukmongkol and Dr. Jaran Jainhaknan for their guidance and help about mass spectrometry. I also thank Mr. Nattawat Sukthouryart who donates plasma for this research and all my colleagues for their help.

Additionally, I would like to thank Department of Pharmacology, Faculty of Medicine Siriraj Hospital, Mahidol University and Department of Transfusion Medicine, Faculty of Allied Health Sciences for allowing me to use their instruments for this thesis.

I wish to thank Department of Clinical Chemistry, Faculty of Allied Health Sciences, Chulalongkorn University for allowing me to take a leave of absence for a higher degree.

Finally, I would like to thank my family for their love, encouragement and everything that I can't express in all.

This thesis is supported by a grant from the Faculty of Allied Health Sciences, Chulalongkorn University.

CONTENTS

Page

LIST OF FIGURES

Figure Page

Figure page

LIST OF TABLE

Table Page

LIST OF ABBREVIATIONS

Abs	absorbance
ACN	acetronitrile
Ang II	angiotensin II
ApoB-100	apolipoproteinB-100
BSA	bovine serum albumin
CAD	coolision Activated Dissociation
$CHCl_3$	chloroform
$CuSO_4$	copper sulphate
EDTA	ethylenediamine tetraacetic acid
ELISA	enzyme-linked immunosorbent assay
ESI	electrospray ionization
FAB	fast atom bombardment
HDL	high-density lipoprotein
4-HNE, HNE	4-hydroxy nonenal
HPLC	high performance liquid chromatography
IDL	intermediate-density lipoprotein
KBr	potassium bromide
KH_2PO_4	potassium dihydrogen phosphate
K_2HPO_4	dipotassium hydrogen phosphate
LDL	low-density lipoprotein
MCA	multi-channel analyzer
MDA	malondialdehyde
MeOH	methanol
m/z	mass-to-charge
MS	mass spectrometry
min	minute
$NaBH_4$	sodium borohydride
NaCl	sodium chloride
NaH_2PO_4	sodium dihydrogen phosphate

Na_2HPO_4	disodium hydrogen phosphate
PUFA	polyunsaturated fatty acid
TFA	trifluoroacetic acid
UV	ultraviolet
VLDL	very low –density lipoprotein
v/v	volume by volume
μl	microlitre
μM	micromolar

Chapters I

Introduction

Low density lipoprotein (LDL) is one class of the lipoproteins found in bloodstream that plays essential role in the transport of cholesterol to tissues. Like the others lipoprotein, LDL is a spherical shape particle consists of neutral lipid core composed of triacylglycerols and/or cholesterol esters surrounded by polar portions of protein, phospholipids, and cholesterol. But LDL is a richest in cholesterol. One LDL particle contains a single molecule of apoprotein B-100, apoB-100, as its primary protein component.

Cells obtain exogenous cholesterol mainly through the action of a specific receptor, the **LDL receptor**. When LDL specifically binds to its receptor, through recognition of the apoB-100 the entire LDL molecule is engulfed and taken into the cell in a process called receptor - mediated endocytosis. In addition to receptor-mediated LDL uptake, cells can also internalize LDL by a bulk-phase pinocytosis of macrophage or **scavenger receptor**, which does not require specific cell - surface binding.

Oxidatively modified LDL is likely to be the main source of cholesterol that accumulates in arteriosclerotic plaques. Trace amount of copper can induce LDL oxidation that generate the lipid peroxidation products such as malondialdehyde (MDA), 4-hydroxy-2-nonenal (HNE). And these aldehydes especially HNE modify apoB-100 results in an increase in net negative charge of apoB-100, leads to the decreased or completely lost recognition by LDL receptor. But the scavenger receptor increases recognition and accelerated uptakes of cholesterol by macrophages. Later macrophages that contain so much cholesterol become foam cells. Leading to the accumulation of cholesterol or cholesterol esters in the arterial wall and formation of fatty streak in the arterial wall and served as the first stage of atherogenesis. Atherosclerotic plaques may promote occlusive clot formation and/or so reduce the size of the blood-vessel lumen that areas of heart muscle become deprived of oxygen leads to tissue death.

The methods frequency used for determine the sites of HNE adducts on apoB-100 are amino acid analysis or edman degradation and reverse phase HPLC -

mass spectrometry. Although, edman degradation is one popular approach, but it ‘s a time consuming method and frequent fails to obtain amino acid sequence results from a blocked N-terminus of the protein. In contrast, mass spectrometry not only overcomes this problem but it ’s also the high sensitivity, rapid and high efficiency technique.

The main objective of this research was the characterization of lipid/protein conjugates in oxidized LDL by mass spectrometry technique.

The experiment begins with preparation HNE/protein product from copper-mediated oxidized LDL, following enzymatic digestion of modified apoB-100 and separation of tryptic digest of apoB-100 by reverse phase HPLC. Finally, using mass spectrometry to determine the sites of modification on apoB-100 by HNE.

The results from the investigation of oxidized LDL may represent an evidence supporting an important hypothesis concerning the initiation of atherosclerosis.

Chapters II

Literature Review

1. Lipoproteins

Lipids play roles in energy metabolism and in a variety of other processes include their roles as membrane constituents, hormones, fat-soluble vitamins, thermal insulators, and biological regulators such as the prostaglandin.

The amounts and types of lipids found in human plasma fluctuate according to the dietary habits and metabolic states of the individual. The normal ranges for lipid levels in plasma are shown in table 2.1.

Table 2.1 Normal concentrations of the major lipid classes in plasma in humans (1)

Lipid	Concentration (g/l)
Total lipid	3.6-6.8
Cholesterol and cholesterol ester	1.3-2.6
Triacylglycerol	0.8-2.4
Phospholipid	1.5-2.5

After an average meal, there is a transient elevation of blood lipids. The peak level of lipids in blood plasma usually occurs after ½ to 3 hours and returns to normal in 5 to 6 hours. But dietary lipids are insoluble in aqueous media, so they are transported by the circulation as components of **plasma lipoproteins** or **lipoproteins**.

1.1 Structure of Lipoproteins

Lipoproteins are spherical shape and vary in diameter from 10 nm to as much as 1,000 nm, depending on the particular proteins and lipids. The structures of the various lipoproteins appear to be similar. Each of the lipoprotein classes consists of neutral lipid core composed of triacylglycerols and/or cholesterol esters surrounded by polar portions of protein, phospholipids, and cholesterol (figure 2.1).

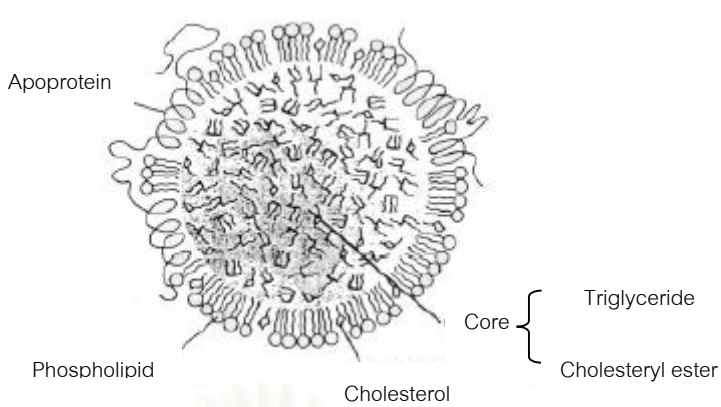

Figure 2.1 Generalized structure of lipoproteins. The spherical particle contains neutral lipids in the interior and protein, phospholipids, and cholesterol at the surface.

1.2 Classification and Functions of Lipoproteins

Lipoproteins are classified into five major types on the basis of their density, as determined by centrifugation, and physical properties (table 2.2).

Table 2.2 Composition and density of human lipoproteins (1,2)

	Chylomicron	VLDL	IDL	LDL	HDL
Density (g/ml)	< 0.95	0.95-1.006	1.006-1.019	1.019-1.063	1.063-1.210
Diameter (nm)	75-1,200	30-80	25-35	18-25	5-12
Component (% dry weight)	2	8	15	22	40-55
Protein[a]	86	55	31	6	4
Triacylglycerols[b]	2	7	7	8	4
Free cholesterol[a]	3	12	23	42	12-20
Cholesterol esters[b]	7	18	22	22	25-30
Phospholipids[a]	A-I,A-II,B-48,	B-100, C-I,	B-100, C-I,	B-100	A-I, A-II, C-I,
Apoprotein composition	C-I,C-II,C-III	C-II,C-III,E	C-II,C-III,E		C-II,C-III,D,E
Classification by Electrophoresis	Omega	Pre-beta	Between beta and pre-beta	Beta	Alpha

[a] Surface components

[b] Core lipids

Lipoproteins in each class contain characteristic apoproteins and have distinctive lipid compositions make they have different physiological functions.

1. **Chylomicrons**, which transport exogenous (externally supplied; in this case, dietary) triacylglycerols and cholesterol from the intestine to the tissues.

2-4. **Very low density lipoproteins (VLDL), intermediate density lipoproteins (IDL), and low density lipoproteins (LDL)**, a group of related particles that transport endogenous (internally produced) triacylglycerols and cholesterol from the liver to the tissues (the liver synthesizes triacylglycerols from excess carbohydrates).

5. **High density lipoproteins (HDL)**, which transport endogenous cholesterol from the tissues to the liver.

1.3 Transport and Utilization of Lipoproteins

Begin with **chylomicrons**, the largest in size and contain the most lipids and the smallest percentage of protein, transport dietary fat from the intestine to peripheral tissues, notably heart, muscle, and adipose tissues. **VLDL** plays a comparable role for triacylglycerols synthesized in liver. The triacylglcerols in both lipoproteins are hydrolyzed to glycerol and fatty acids at the inner surface (endothelium) of capillaries in the peripheral tissues. This hydrolysis involves activation of the extracellular enzyme, **lipoprotein lipase (LPL)**, which is most active within the capillaries of adipose tissue, cardiac muscle, skeletal muscle, and lactating mammary gland. The enzyme is specifically activated by **apoprotein C-II**, which is associated with chylomicrons, and VLDL. Some of the released fatty acids are absorbed by nearby cells, while others, rather insoluble, become complexed with serum albumin for transport to more distant cells. After absorption into the cell, the fatty acids derived from lipoprotein lipase action can be either catabolized to generate energy or, in adipose cells, used to resynthesize triacylglycerols. Glycerol is returned from adipocytes to liver, for resynthesis of glucose by gluconeogenesis.

As a consequence of triacylglycerol hydrolysis in the capillaries, both chylomicrons and VLDL are degraded to protein – rich remnants. The **IDL** class of lipoprotein is derived from VLDL, and chylomicrons are degraded to what are simply called **chylomicron remnants.** Both classes of remnants are taken up by the liver through interaction with specific receptors and further degraded in the liver lysosomes. **Apoprotein B-100** is reused for synthesis of **LDL** (via IDL). LDL is the principal form in which cholesterol is transported from liver to tissues, and **HDL** plays the primary role in returning excess cholesterol from tissues to the liver for metabolism or excretion. The overall aspects of lipoprotein metabolism and transport are summarized in figure 2.2.

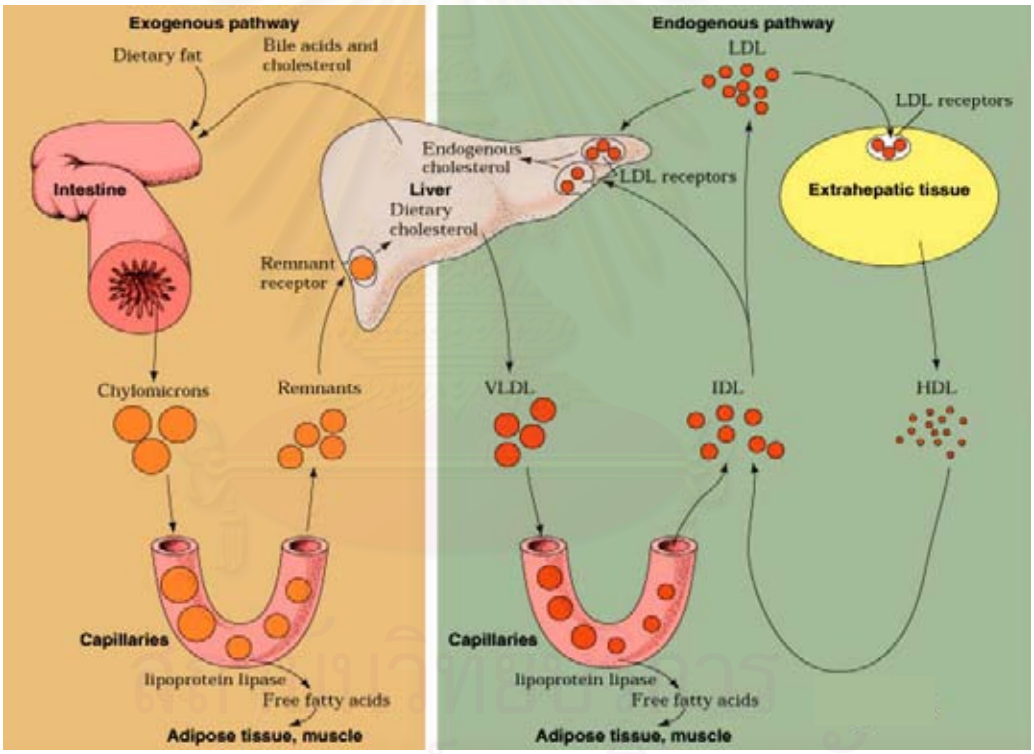

Figure 2.2 Overview of lipoproteins transport pathways and fates (3).

1.4 Apolipoproteins

" **Apolipoproteins** " or " **apoproteins** " are the protein components of lipoproteins. A total of nine major apoproteins are found in human lipoproteins. Their properties are summarized in table 2.3.

Table 2.3 Apoproteins of the human plasma lipoproteins (2,3)

Apoprotein	Molecular weight	Characteristics
A-I	28,300	Major protein in HDL; Activates LCAT[a]
A-II	17,400	Major protein in HDL; Inhibits LCAT, Activates hepatic lipase
B-48	241,000	Found exclusively in chylomicrons, Cholesterol clearance
B-100	513,000	Major protein in LDL, Cholesterol clearance
C-I	7,000	Found in chylomicrons; Activates LCAT and LPL[b]
C-II	10,000	Found primarily in VLDL; Activates LPL
C-III	9,300	Found primarily in chylomicrons, VLDL and HDL; Inhibits LPL
D	35,000	HDL protein, also called cholesterol ester transfer protein
E	33,000	Found in VLDL, LDL, and HDL, Cholesterol clearance

[a] LCAT; Lecithin-cholesterol acyl transferase

[b] LPL; Lipoprotein lipase

The structure and function of these apoproteins has been intensely studied in the past decade, and most of the apoproteins have been sequenced. The synthesis of the apoproteins takes place on ribosomes that are bound to the liver endoplasmic reticulum. All apoproteins are monomers except apoprotein A-II, which is a disulfide-linked dimer. Most of them are water-soluble and associate rather weakly with lipoproteins. Hence, they readily transfer between lipoprotein particles via the aqueous phase. Circular dichroism (CD) measurements indicated that apoproteins have a high helix content, which increased when they are incorporated in lipoproteins. Apoprotein alpha helices float on phospholipid surfaces of lipoprotein, much like logs on water. The phospholipids are arrayed with their charged groups bound to oppositely charged residues on the polar face of the helix and with the first few methylene groups of their fatty acid residues in hydrophobic association with the nonpolar face of the helix (1-4).

2. Low Density Lipoprotein

2.1 The LDL Receptor and Cholesterol Homeostasis

Cholesterol in plasma lipoproteins exists both as the free cholesterol and as cholesterol esters. Cholesterol esters are synthesized in plasma from cholesterol and acyl chain on phosphatidylcholine, through the action of lecithin: cholesterol acyltransferase (LCAT), an enzyme that is secreted from liver into bloodstream :

$$\text{Phosphatidylcholine + cholesterol} \xrightleftharpoons{\text{LCAT}} \text{lysolecithin + cholesterol ester}$$

Cholesterol esters are considerably more hydrophobic than cholesterol itself.

Of the five-lipoprotein classes, LDL is the richest in cholesterol. LDL particles have an average diameter of 22 nm, the core consisting of about 170 triglyceride and 1600 cholesteryl ester molecules and the surface monolayer comprising about 700 phospholipid molecules, 600 usesterified cholesterol molecules and a single copy of apoprotein B-100 (figure 2.3). The amounts of cholesterol and cholesterol esters associated with LDL about two-thirds of the total plasma cholesterol. The main phospholipid components are phosphatidylcholine (about 450 molecules/LDL particle) and sphingomyelin (about 185 molecules/LDL particle). The LDL particles also contain polyunsaturated fatty acids (PUFAs), mainly linoleic acid (18:2) and arachidonic acid (20:4). In addition to lipids, LDL also carries lipophilic antioxidants such as α-tocopherol, γ-tocopherol, carotenoids, oxycarotenoids and ubiquinol-10 (3,6,7).

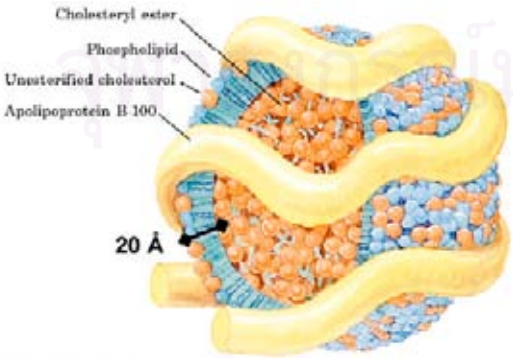

Figure 2.3 LDL particle consists of some 1500 cholesteryl ester molecules surrounded by an amphiphilic coat of 800 phospholipid molecules, 600 cholesterol molecules, and a single 513-kDa molecule of apoprotein B-100 (4536 amino acid residue) (3).

Cholesterol esters are too hydrophobic to traverse cell membranes, so LDL is function as the cholesterol transport vesicle. Michael Brown and Joseph Goldstein (A Nobel Prize) have extensively described the mechanism for the uptake of LDL in extrahepatic tissue. Cells obtain exogenous cholesterol mainly through the action of a specific receptor, the **LDL receptor** that congregates in areas of the plasma membrane. The receptors are clustered in a structure called a coated pit, an invagination whose most abundant protein is clathrin, a self-interacting protein capable of forming a cagelike structure. When LDL specifically binds to its receptor, through recognition of the apoprotein B-100, the entire LDL molecule is engulfed and taken into the cell (in a process called **receptor - mediated endocytosis**) to form coated vesicle, which is directed toward and fuses with lysosome. The LDL particle is degraded within the lysosomes by the action of protease and lysosomal acid lipases (lipid degradative enzymes). The LDL apoprotein is hydrolyzed to amino acids, and the cholesterol esters are hydrolyzed to give free cholesterol. The receptor itself is recycled, moving back to the plasma membrane to pick it up more LDL.

Much of the cholesterol released moves to the endoplasmic reticulum, where it is used for membrane synthesis. The internalized cholesterol exerts three regulatory effects.

1. Suppresses endogenous cholesterol synthesis, by inhibiting hydroxy methylglutaryl-CoA reductase (HMG-CoA reductase), and by suppressing transcription of the gene for this enzyme and accelerating degradation of the enzyme protein.
2. Activates acyl-CoA: cholesterol acyltransferase (ACAT), an intracellular enzyme that synthesizes cholesterol esters from cholesterol and a long chain acyl-coA. This promotes the storage of excess cholesterol in the form of droplets of cholesterol esters.
3. Regulates the synthesis of the LDL receptor itself, by lowering the content of mRNA for the receptor. Decreased synthesis of the receptor ensures that cholesterol will not be taken into the cell in excess of the cell ' s needs, even when extracellular levels are very high (8).

2.2 Scavenger Receptors

In addition to receptor-mediated LDL uptake, cells can also internalize LDL by a bulk-phase pinocytosis of macrophage (a type of white blood cell that ingests and destroys a variety of foreign and endogenous substances) or **scavenger receptor**, which does not require specific cell - surface binding. However, the classical LDL receptor recognizes a specific domain of positive charges from lysine, arginine, and histidine residues at the apoprotein B-100. If the domain is altered, the recognition is decreased or completely lost results in an increased recognition by the scavenger receptor and an unlimited uptake of cholesterol (3).

The scavenger receptor also mediates the endocytosis of several forms of modified LDL. In culture, the uptake of modified LDL by the scavenger receptor can lead to the accumulation of cholesterol which is then stored in the form of lipids droplets, which macrophages converts these cells to a cholesterol-engorges species called **foam cells**. This scavenger receptor pathway was discovered in experiments with LDL, which had been pretreated in vitro with acetic acid anhydride, acetylated LDL. Such a treatment leads to the acetylation of ε-amino groups of lysine residues at the apoprotein B-100 and causes a loss of positive charges and a net increase of negative surface charges in LDL (7,9,10).

Scavenger receptors are proteins that mediate the endocytosis of diverse group of polyanions. From the past to now, there are many experiments to solve the possible role of scavenger receptors in the uptake of modified LDL. Conclusion, there are three classes of cloned scavenger receptors, the first class, Class A receptors, includes the type I and II macrophage scavenger receptors (SR-AI and SR-AII). They are found predominantly on macrophages and activated smooth muscle cells. Ligands for class A receptors include acetylated LDL, oxidized LDL, fucoidan and carrageenan. The second class, Class B scavenger receptors, includes CD36 and SR-B1, which are found in adipose tissue, lung, liver and macrophages. These receptors bind oxidized LDL, apoptotic cells and anionic phospholipids. The third class, macrosialin/CD68, a family of endosomal proteins with sequence homology similar to the lysosomal - associated

membrane proteins. The role of these receptors in the uptake of oxidized LDL remains to be elucidated.

These scavenger receptors for oxidized LDL share one common characteristic: they are all multiligand receptors. Although they can all bind to and take up oxidized LDL, it is not known whether this is an important physiological function of any of these receptors in vivo (11,12).

2.3 LDL Dysfunction in Atherosclerosis

Atherosclerosis is a disease primarily of the elastic arteries, large and medium-sized muscular arteries. The basic lesion – the **atheroma**, or fibrofatty plaque – consists of a raised focal plaque within the intima, having a core of lipid (mainly cholesterol and cholesterol esters) and a covering fibrous cap. The resultant roughening of the arterial wall promotes the formation of blood clots, which may also occlude the artery. A blood flow stoppage, known as an **infarction**, causes the death of the deprived tissues. Although atheromas can occur in many different arteries, they are most common in the coronary arteries, The arteries supplying the heart. This results in myocardial infarctions or “heart attacks”. Atherosclerosis is the most common and important form of arteriosclerosis.

Arteriosclerosis means hardening of the arteries. Arteriosclerosis marked by proliferative or hyaline thickening of the walls of small arteries and arterioles (3,5).

The initial pathogenesis of atherogenesis has been considered by the accumulation of lipids within the artery walls, called lipid-filled foam cells. Later foam cells develop into fatty streaks (grossly flat, lipid-rich lesion consisting of both macrophages and some smooth muscle) and the fatty streak is the first signs of atherosclerosis. Later, the fibrous plaque begins as changes in the structure of the artery or fatty streaks. As atherosclerosis progresses, the streaks gradually change, becoming larger and more complex, turning into intermediate lesions. When a fibrous plaque becomes unstable and breaks or tears, thrombi can form on the surface of the plaque. If these clots are large enough, they can block the artery that has already been narrowed by the fibrous plaque (13-16).

An increase in plasma LDL levels lead to an increased rate of entry of LDL into the arterial wall (17,18) and at the same time to an increase in the adherence of circulating monocytes to arterial endothelial cells. There are evidences suggested that modified LDL be converted to foam cells by macrophages that derived from monocytes in the blood. Leading to the accumulation of cholesterol or cholesterol esters in the arterial wall (19,20). Oxidized LDL was demonstrated to incorporate with fatty streak formation in the arterial wall and served as the first stage of atherogenesis (21). The hypothesis of foam cells is illustrated in figure 2.4. The uptake of cholesterol - containing lipoproteins by macrophages in arterial intima is believed to be an important step in the pathogenesis.

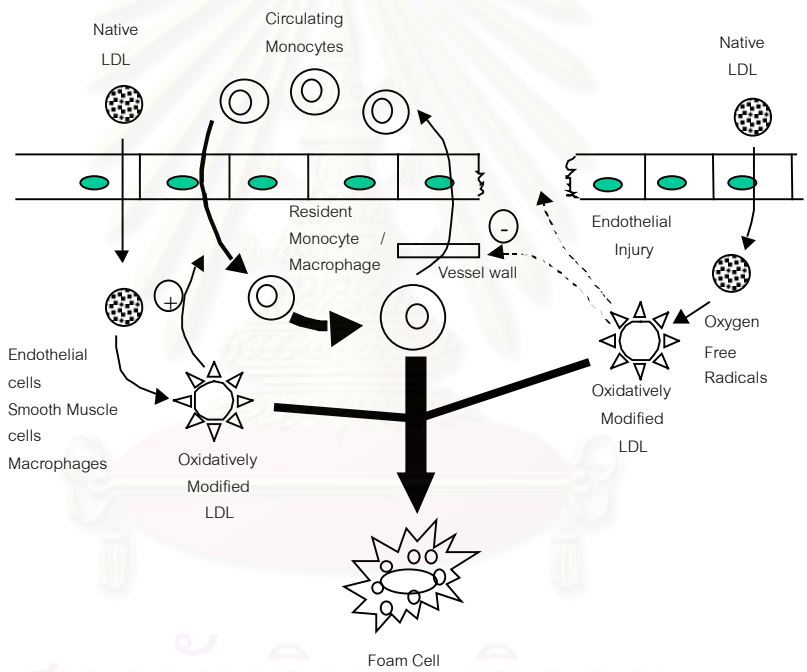

Figure 2.4 Schematic of a hypothesis of atherosclerosis and the formation of fatty streaks (21).

There are several forms of modified LDL such as non-enzymatic modifications (proteoglycans, glycosylation, immune complexes, endothelial cells), enzymatic modifications (lipases, oxygenases) and oxidative modification of LDL which was demonstrated to occur in vivo. The mechanism of this process involves cellular lipid peroxidation. Previous studies have shown that during LDL oxidation lipid peroxidation products, generated from phospholipids of LDL, become covalently attached to

apoprotein B-100. And requires the binding of LDL to its receptor on macrophages that accumulate at sites of arterial injury (22,23).

2.4 Lipid Peroxidation

The formation of lipid peroxidation products in the body is accelerated by transition metal ions such as Cu^{+}, Fe^{3+} promoting formation of lipid alkoxyl radicals, in a Fentone-type reaction,

$$Cu^{+} + LOOH \longrightarrow Cu^{2+} + OH^{-} + LO^{\cdot}$$

β-Cleavage reaction (homo-scission) of either of the two C-C bonds on each side of alkoxyl group radical will follow to yield aldehydes and carbon center lipid radicals (figure 2.5). The aldehydes can be classified to two groups; the first are aliphatic aldehydes derived from the methyl terminus of the fatty acid chain and the second group, called core aldehydes, are the aldehydes that are still bound to the parent lipid molecules.

When LDL is oxidized by radical generating substances such as Cu^{2+} ions, three consecutive phases of the reaction can be observed in kinetic experiments by measuring compositional changes of LDL. Initially, lipid peroxidation proceeds with a low rate because the antioxidants contained in LDL inhibit the chain reaction, this period is called the lag phase or lag time. As the antioxidants are used up, the propagation phase begins and the rate of lipid peroxidation rapidly accelerates. Follow by the decomposition phase where the lipid hydroperoxides formed break down to a wide range of products (25).

For the oxidative modifications of LDL, the conjugation between lipid peroxidation products to LDL was considered one of the most significant types of reaction. The decomposition of lipid hydroperoxides to aldehyde is a general phenomenon in fat autoxidation and lipid peroxidation in biological systems. The aliphatic aldehydes found in oxidized LDL are listed in table 2.4.

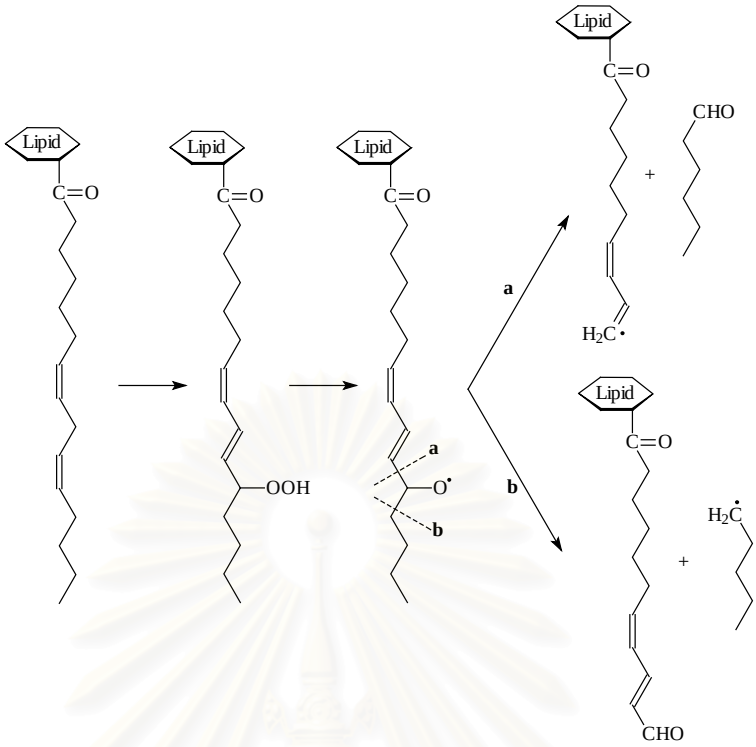

Figure 2.5 Decomposition of lipid hydroperoxides by β-cleavage yields aldehydes a, aldehyde derived from the methyl terminus of the fatty acids and b, core aldehydes bounds to the parent lipid molecule (24)

Table 2.4 Aldehydes in LDL oxidized in the presence of copper ion (24)

Aldehyde products	Composition (nmol/mg of protein)	
	4-5 hr	20-24 hr
Hexanal	52	229
Malondialdehyde (MDA)	86	114
4-hydroxynonenal (HNE)	25	114
nonanal	10	27
4-hydroxyhexenal	8	49
4-hydroxyoctenal	7	not detected
propanal	6	not detected
pentanal	5	not detected
2,4-heptadienal	5	not detected
butanal	4	not detected
octanal	1	5
Total aldehydes	209	538

The mechanism of autoxidation of common polyunsaturated fatty acids (PUFA), linoleic acid, linolenic acid and arachidonic acid, to produce HNE are shown in figure 2.6. It involves the formation of an alkoxyl radical from the n-6 hydroperoxide (in the case of arachidonic acid corresponding to 15-hydroperoxide-eicosatetraenoic acid). Reduction of this hydroperoxide gives an alkoxyl radical, **3**, that can cyclyze to give the epoxy-hydroperoxide, **4**. This compound can be converted in several steps to the epoxyaldehyde, **9**, with Lewis or Bronsted acid catalysis. Epoxyaldehydes are usually unstable compounds with respect to ring opening even under very mild conditions. HNE is the expected product of opening of **9** (26).

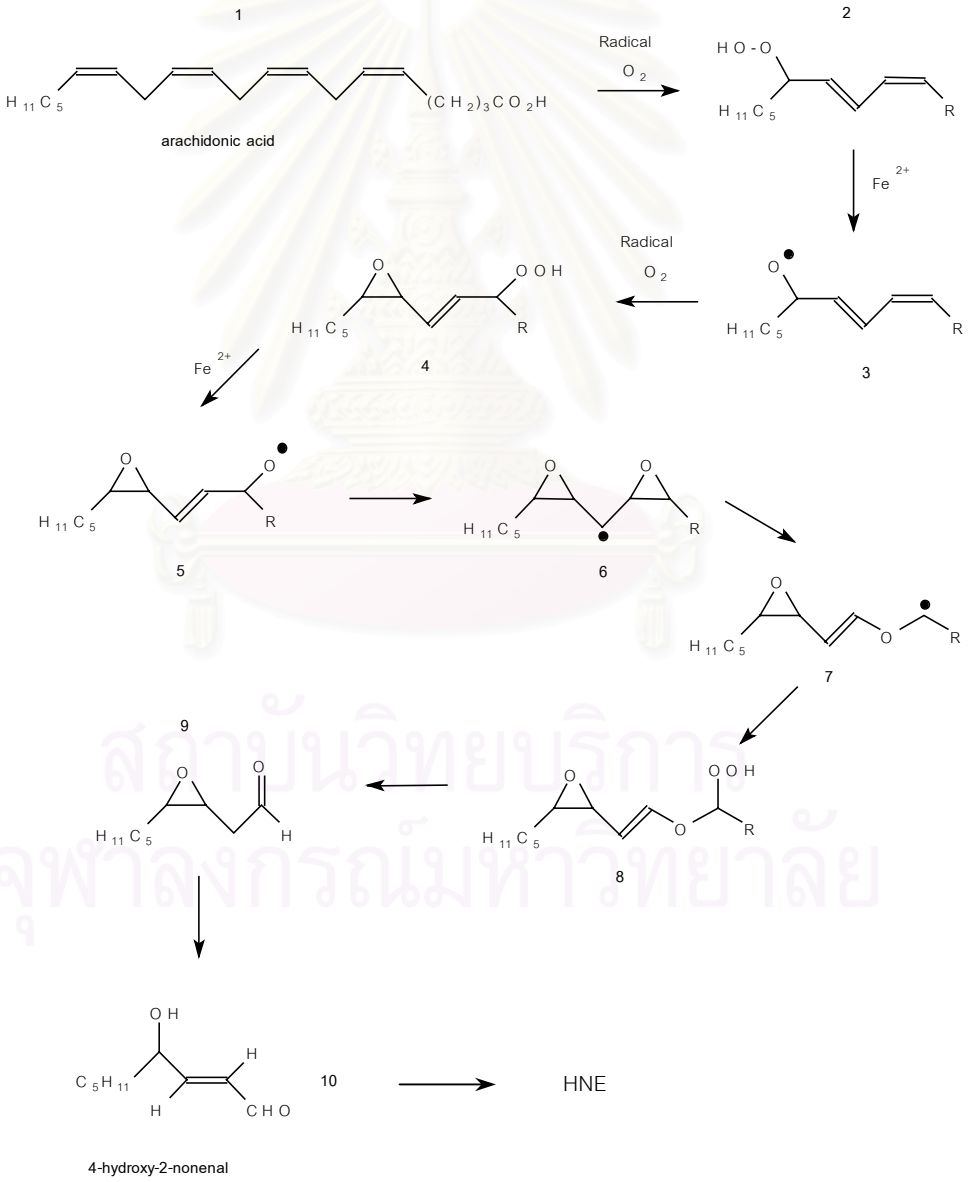

Figure 2.6 Proposed mechanism for the production of 4-hydroxy-2-nonenal from arachidonic acid (26).

Some experiments in vitro suggested that HNE exhibit high capacity to modify LDL and apoprotein B-100. Experiments that modified LDL directly with HNE at low concentrations of HNE resulted in the covalent binding of HNE to apoprotein B-100 by block ε-lysine residue. This lead to an increase of the negative charge of the LDL particles as evidenced by its increased electrophoretic mobility. In addition, modification of LDL by incubation with the high concentrations of HNE resulted in LDL aggregation and partial conversions of the apoprotein B-100 into a higher-molecular weight form (probably apoproteinB-126 and B-151). These forms of LDL also contained inter - or intra - molecular crosslinked apoB molecules. And it is believed that LDL modification response for lipid peroxidation conditions in vivo. By amino acid analysis revealed that HNE attacks mainly the lysine and tyrosine residues and to a lesser extent also serine, histidine and cysteine (27-30).

Same of modified LDL directly with HNE, the autoxidation of LDL catalyzed by metal ions results in a previous papers suggested the oxidation of LDL decrease in free lysine groups and binding of lipid peroxidation products to apoprotein B-100. Amino acid analysis of apolipoprotein B-100 revealed that HNE attached mainly to lysine and tyrosine residues and to a lesser extent to serine, histidine and cysteine (31-36).

But the quantification of HNE-histidine and HNE-lysine adducts in apoprotein B-100 oxidized by Cu^{2+} using enzyme-linked immunosorbent assay (ELISA) and sodium-dodecyl sulphate-polyacrylamide gel electrophoresis (SDS-PAGE). The data suggested the mainly presence of HNE-histidine adducts and a trace amount of HNE-lysine adducts (37).

Through the reaction of insulin (no sulphydryl groups) with HNE and reduced the HNE protein adducts with $[^3H]NaBH_4$ which analyzed by reversed-phase HPLC and fast atom bombardment mass spectrometry (FAB-MS), demonstrated that histidine as the only amino acid modified by HNE via a Michael-type addition reaction. The mechanism was proposed in figure 2.7.

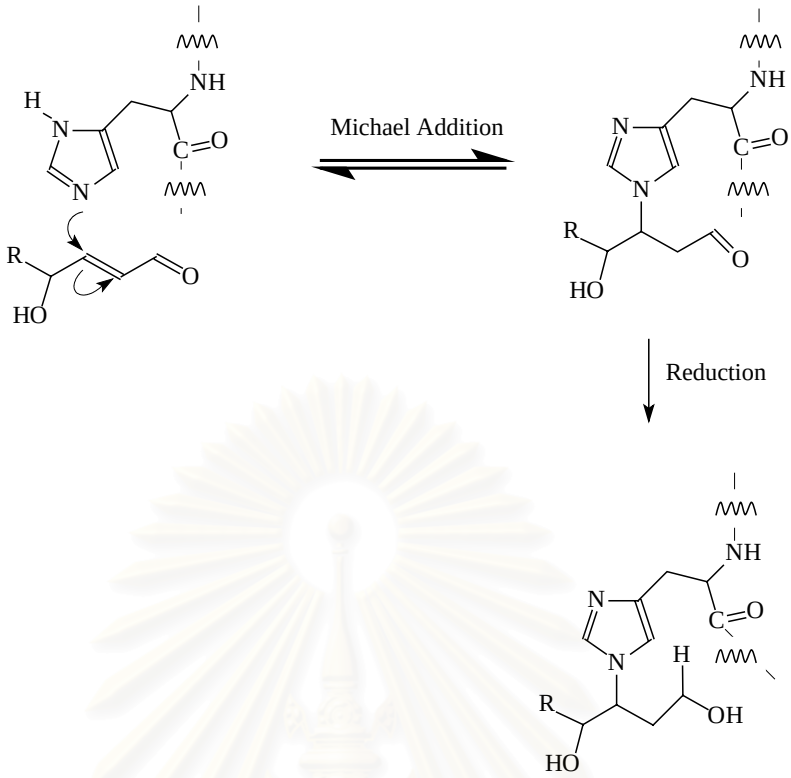

Figure 2.7 Proposed mechanism for formation of HNE-histidine adducts and their reduction (38).

Moreover, histidine was confirmed as a target of HNE in apoprotein B-100 and apomyoglobin via Michael addition (39,40). Electrospray ionization mass spectrometry (ESI-MS) and ESI tandem MS techniques were used to determination the attachment sites of HNE adducts. Precursor ion scanning of m/z 268 corresponding to the reduced form of immonium ion of HNE-modified histidine (figure 2.8) was used to screen for the HNE-adducted apomyoglobin tryptic fragment. The numbers of modified histidine residues in an apomyoglobin tryptic fragment were observed in table 2.5.

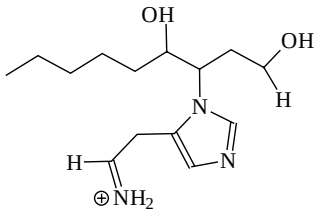

Figure 2.8 The immonium ion of HNE-modified histidine (39).

Table 2.5 Comparison of the number of histidine residues present in apomyoglobin tryptic fragments with the number of HNE adducts observed (39)

Tryptic fragment	No. of Histidine	Adducted forms detected			
		non	1 HNE	2 HNE	3 HNE
T1	0	X			
T2	1	X	X		
T3	1	X	X		
T10	1	X	X		
T13	3	X	X	X	x
T14-15	1	X	X		
T16	2	X	X	X	
T17	1	X	X		
T18	0	X			
T21	0	X			

2.5 Determination of Lipid Peroxidation Products

There are several methods used for quantification of 4-hydroxynonenal (HNE) protein adducts such as enzyme-linked immunosorbent assay (ELISA)(37), isotope dilution GC/MS (41,42), and TBARS technique. The TBARS test is the most frequently used test to assess lipid peroxidation (mainly malondialdehyde and HNE with amino acid) because this technique is easy to perform and inexpensive. But this technique is less specific than the other (43).

For the determination the attachment sites of HNE adducts on protein, the methods frequency used are amino acid analysis or edman degradation (31-36), reversed-phase HPLC and MS such as fast atom bombardment (FAB), electrospray ionization (ESI) and tandem MS techniques (38,39,40). Although, edman degradation is one popular approach used, but it is a time consuming method and the blocked N-terminus protein failed to analyze by this method.

2.6 Myeloperoxidase System

Beside the oxidation of LDL by lipid peroxidation, myeloperoxidase also could promote the oxidation and modification of LDL. Myeloperoxidase is a heme protein secreted by activated phagocytes. Myeloperoxidase uses hydrogen peroxide (H_2O_2) generated by phagocytes to generate potent microbicidal oxidants and tyrosyl radical, which trigger LDL oxidation in vivo. Catalytically active myeloperoxidase is present in human atherosclerotic lesions, where it colocalizes with lipid-laden macrophages, the cellular hallmark of the early atherosclerotic lesions.

The best-characterized product of myeloperoxidase is hypochlorous acid (HOCl)

$$Cl^- + H_2O_2 + H^+ \longrightarrow HOCl + H_2O$$

LDL exposed to reagent HOCl at neutral pH becomes aggregated and is rapidly taken up and degraded by macrophages. Myeloperoxidase system oxidizes L-tyrosine to yield 3-chlorotyrosine that found in human atherosclerotic tissue and in LDL isolated from vascular lesions. The isotope dilution gas chromatography-mass spectrometry method is developed to measure tissue levels of 3-chlorotyrosine (44-48).

The difference between the two oxidation systems that is the hypochlorite (HOCl) mediated protein oxidation, HOCl directly modifies apoB into a form that is readily taken up by macrophages despite the lack of lipid peroxidation. While the copper mediated protein oxidation, lipids peroxidation products are required to initiate apoB carbonyl formation (49).

However, the oxidative modifications of LDL in two system share the similar biological consequences that is the modification of apoB-100, lead to an increase in net negative charge of apoB-100 and an accelerated uptake and apoB-100 degradation by macrophages as describe above.

3. Mass Spectrometry

The mass spectrometer is an instrument that serves for establishment of the molecular weight and structure of organic or inorganic compounds. The sample is volatilized within the spectrometer and gas-phase ions formed from it are separated according to their mass/charge (m/z) ratios. The ion currents corresponding to the different species are amplified and recorded. The peak intensities are plotted as ordinates, in arbitrary units or normalized with respect to the most important peak, which is assigned a value of 100. A mass spectrometer consists of the following basic units.

1. an ion source where ions are formed from the sample;
2. an analyzer which separates the ions according to their m/z values;
3. a detector which give the intensity of the ion current for each species;

Various methods of ionization can be used; the choice is dependent on the physical state, the volatility and thermal stability of the sample. Electron ionization (EI) gives satisfactory results for gas-phase molecules. Electron ionization is the oldest and, until recently, the most widely used method. The substance is volatized into the ionization chamber, where its molecules are bombarded with electrons and transformed into positively charged ions. For inorganic solids such as salts, thermal ionization, field desorption and laser desorption are used. Atom or ion bombardment is suitable for ionization of organic compounds of molecular weight up to about 10 kDa. Electrospray ionization (ESI) and matrix-assisted laser desorption ionization (MALDI) provide information on high molecular weight analytes such as proteins, peptides, etc.

The basic mass analyzers for mass spectrometry include the time-of-flight analyzer, cyclotron resonance analyzer, quadrupole, ion trap and electric and magnetic sectors. The quadrupole analyzers will be described in detail later.

3.1 Electrospray Ionization Mass Spectrometry

Electrospray ionization (ESI) is a liquid inlet system for mass spectrometry and acts as an ionization source. It is one method for effecting differential solvent removal. The solvent is passed along a short length of capillary tube, the end of which is held at a

high positive or negative electric potential (typically 3-5 kV). Nitrogen is used as both a nebulizing and counter-flowing gas to aid desolvation and the source region is heated to 60-80 °C (50,51) (figure 2.9).

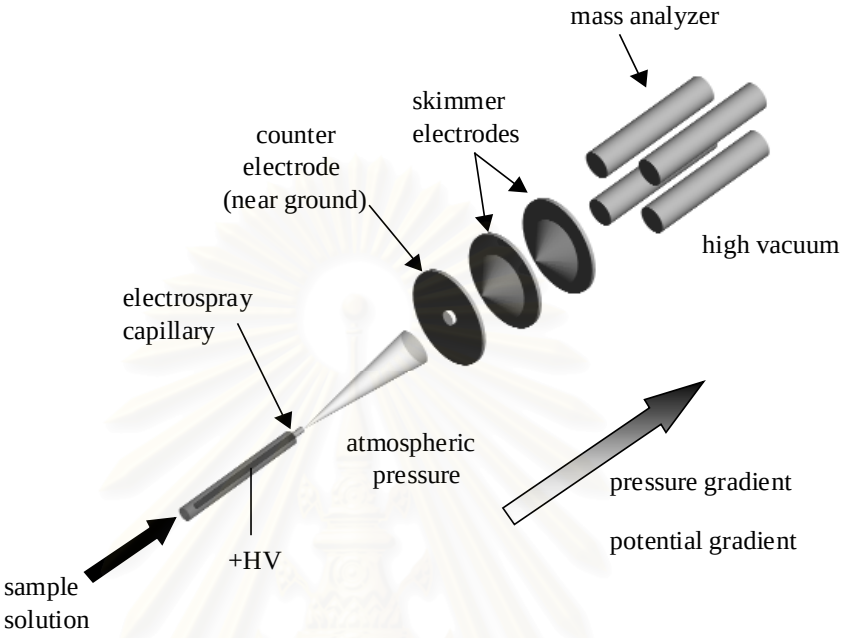

Figure 2.9 Schematic of electrospray ion source.

The exact mechanism of ESI process remains the subject of discussion. There are three major steps in the electrospray process

1. Production of charged droplets at the ESI capillary tip
2. Shrinkage of the charge droplets by solvent evaporation leading to very small highly charged droplets that are capable of producing gas-phase ions
3. Production of gas-phase ions from the very small and highly charged droplets.

Sample and solvent arrive at the charged capillary tip. When the capillary is the positive electrode, the positive ions in the solution will be drawn downfield in the solution toward the meniscus of the liquid and the negative ions will be drawn away from the surface (figure 2.10). The liquid emerging from the capillary is thus drawn into a “Taylor cone” under the influence of the steep potential gradient. At the cone tip, the surface charge density is such that repulsive forces exceed the surface tension and droplets form. The process that produces the small droplets is called budding and the diameter

of the droplet is dependent on potential, flow rate and solution properties (52). The charged droplet diameter decreases through desolvation while the charge remains constant due to the emission of ions from solution to the gas is highly endothermic process.

The decrease of droplet diameter via solvent evaporation process leads to an increase of the electrostatic repulsion of the charges at the surface until the droplets reach the stability limit (called the Rayleigh limit). Droplet fission occurs to produce the smaller-size stable droplet (53) and this process is repeated (figure 2.10).

There are two main mechanisms proposed for the formation of gas-phase ions from small and highly charged droplets. The first mechanism suggests the ultimate formation of very small droplets that contain only a single ion (50). Solvent evaporation will lead to a gas-phase ion. After the decrease of the droplet diameter, the second mechanism occurs that is single direct ion emission from droplets becomes energetically favorable and this process is called “ion evaporation” (54).

The high electric field in the electrospray source produces multiply charged ions. For which

$$m/z = \frac{M + nH}{n}$$

where, M = molecular weight,

n = number of charges and

H = mass of proton

Two adjacent ions in a multiply charged ion series appear at m/z of A_1 and A_2; $n_1 = n_2 + 1$, where n_1 is the number of charges on A_1 and

n_2 is the number of charges on A_2.

Then, $\frac{M + n_1H}{n_1} = A_1$ and $\frac{M + n_2H}{n_2} = A_2$

Therefore, $n_2 = \frac{A_1 + H}{A_2 - A_1}$

Thus, mass and charge number may be independently determined.

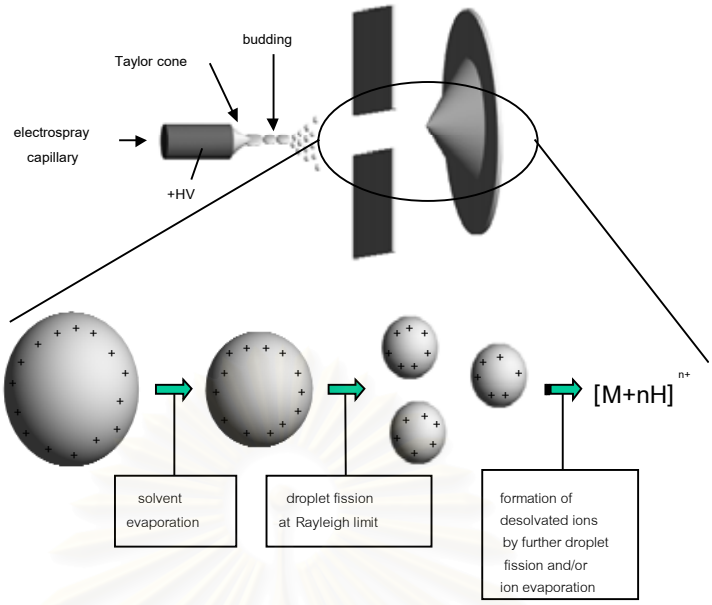

Figure 2.10 Schematic of ion formation during electrospray (adapted from 55).

3.2 Low Flow Electrospray (Nanoelectrospray)

First, the non-sheath probe was created for capillary electrophoresis/mass spectrometry (CE/MS) that can operate at typically less than 0.25 μl/min compared with conventional electrospray probe at 1-10 μl/min, incorporated with 25 μl gastight syringe and a fused-silica capillary. This was used to analyze horse-heart myoglobin (30 pmol; 1.02 μl) and oligonucleotide (1 pmol; 1.02 μl) at a flow rate of 0.2 μl/min (56).

Subsequently, a low flow-rate electrospray source was developed to the technique that called micro-electrospray. The source consisted of a 22.5 cm spray needle of 50 μm id with a 1 cm section of C-18 packing at the spray tip for desalting and sample preconcentration. Optimal flow rate of the source was 300-900 nl/min. To increase the sensitivity, the tip of the spray needle was placed to within approximately 3 mm of the sample cone. And was used to analyze peptides at the zeptomole (10^{-21} mole) level (57,58).

Nanoelectrospray, an off-line low-flow electrospray source was developed later. This type of source is different from others in design. The process of nanoelectrospray provides sufficient “pumping” of sample to the spray tip. The capillary needle is a gold-coated pulled glass capillary with an orifice of 1-2 μm that is used for electric charging

of the sample. Consequently, the nanoelectrospray source can analyze samples of 0.2 - 2 μl for long periods (59).

3.3 Quadrupole Mass Analyzer

The quadrupole mass analyzer consists of four metal rods held in strict alignment parallel and at a fixed distance from one another (figure 2.11). Opposite rods are connected in pairs both radio frequency (RF) and direct current (DC) generators. The trajectory of ions will pass in the z-direction between the four rods

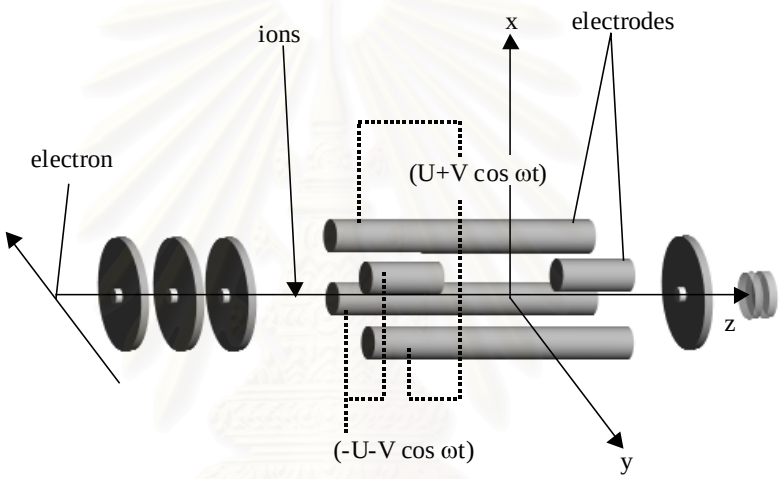

Figure 2.11 Schematic of quadrupole rods.

In mass spectrometry, resolution is defined as M/ΔM, where M is the mass of the ion and ΔM is the smallest increment of mass that can be distinguished by the analyzer. For the quadrupole mass analyzer, ΔM is commonly about one dalton over the entire mass range.

During quadrupole mass analyzer scanning, there are changing voltages (U,V) and a fixed frequency (ω). By continuously increasing U and V, ions of all of m/z will successively pass along the axis of the quadrupole rods to enable recording of mass spectra.

Quadrupole instruments are popular because they are compact, relatively inexpensive and easy to operate. Moreover, the advantages compared with the magnetic sector are ease of data system control and ease of interfacing with a wide

range of inlet systems. Although the quadrupole mass filter does not provide a high resolution, it does constitute an integral part of more sophisticated instruments such as the tandem quadrupole and the instruments of hybrid geometry, specifically designed for tandem mass spectrometric analysis (60).

3.4 Tandem mass spectrometry

Tandem mass spectrometry is a method where a mass analyzer (MS1) is employed to isolated a precursor ion, which then undergoes fragmentation yielding product ions, subsequently analyzed by a second stage of mass analysis (MS2) (61).

Modes of scanning in tandem MS are classified in three modes.

1. Product ion scanning

Precursor ions are selected by MS1 and pass to the collision cell. Ions undergo collision with an inert gas (argon or helium) to cause dissociation and the resulting fragment (product) ions are separated in MS2.

2. Precursor ion scanning

MS2 is set to pass only the product ions of a specified m/z ratio. All ions from the ion source are scanned by MS1 and passed sequentially into the collision cell. Those ions that fragment to give product ions of interest are revealed by the transmission of the product ions through MS2.

3. Constant neutral loss

MS1 scans the spectrum of ions from the source and MS2 scans the same mass but offset by Δm, where Δm is the difference in m/z between the precursor and product ions.

Tandem mass spectrometry can be separated into two types, tandem-in-space and tandem-in-time. **Tandem-in-space** mass spectrometers incorporate many different combinations of mass analyzers. Common types are described in table 2.6.

Table 2.6 Analytical characteristics of some tandem-in-space mass spectrometers.

Instrument	CAD Energy Regime	Precursor Resolution	Product Resolution
Tandem quadrupole	low	Unit	Unit
Sector/quadrupole	low	> 10,000 possible	Unit
Hybrid 4-sector	high	1,000 typical > 10,000 possible	1,000-2,000
sector/Tof hybrid	high or low	1,000 typical > 10,000 possible	10000 (62)
quadrupole/Tof hybrid	low	1,000 typical Unit	2000 (63)

Low energy CAD; E_{lab} less than 200 eV

High energy CAD; E_{lab} greater than 1000 eV

The most common tandem-in-space instrument is the tandem quadrupole mass spectrometer. It can be used for precursor ion scanning and constant neutral loss scanning unlike tandem-in-time instruments. In principle, this advantage applies to other tandem-in-space instruments. A limitation of tandem-in-space instruments is that the stages of mass spectrometry possible are equal to the number of mass analyzers.

Tandem-in-time mass spectrometers, precursor ion trapping, ion activation, and product ion analysis are achieved in a single volume mass analyzer. Some tandem-in-time mass spectrometers are shown in table 2.7

Table 2.7 Analytical characteristics of some tandem-in-time mass spectrometers.

Instrument	CAD Energy Regime	Precursor Resolution	Product Resolution
Quadrupole ion trap	Low	unit at m/z < 1,400	Unit
Fourier transform ion cyclotron resonance	Low	<1,000 typical <20,000 possible	40,000

There is no theoretical limit on the number of stages of analysis on this type of mass spectrometer. The practical limit depends on the trapping efficiency and the sensitivity of the detector. A disadvantage of tandem-in-time instruments is the inability to directly record precursor ion or constant neutral loss spectra.

3.5 Collisionally Activated Dissociation (CAD)

Collisionally activated dissociation (CAD) process is a two-step process (61,64,65). The first is collision between the ion and the target molecules. Ion translational energy is converted to internal energy so that the ion is elevated from the ground state to an excited state. The second step is the unimolecular decomposition of the activated ion.

The maximum translational energy of target molecules converted into internal energy under inelastic conditions is given by the collision energy in the centre-of-mass frame of reference (E_{cm}) ,

$$E_{cm} = E_{lab} \frac{m}{(m_t + m_p)}$$

where m_t is the target mass,

m_p is the projectile (precursor) mass and

E_{lab} = ion kinetic energy in the laboratory frame of reference.

Collision energy is categorized into two groups: high-energy (E_{lab} in the keV range) and low-energy (E_{lab} up to 200 eV).

High-Energy Collisionally Activated Dissociation (keV) is generally performed using sector or hybrid instruments. Ions are accelerated by a potential of a few kV and collided with target gas molecules. Helium is the most common target gas but is not always very efficient in transferring energy into internal energy. Consequently, fragment yield can be increased by using a heavier gas such as argon or xenon (see equation above) through this may be offset by greater ion scattering. The increase in internal energy following high-energy collision averages at 1-3 eV but can reach up to 15 eV

Low-Energy Collisionally Activated Dissociation (up to 200 eV) is commonly operated using hybrids or tandem quadrupole mass spectrometers. The normal collision cell is a quadrupole (or other multipole) in RF-only mode. The type of collision gas is more significant than it is for high-energy CAD and is usually a heavier gas such as argon or xenon.

Apart from the energy level, there are several other differences between low energy CAD and high energy CAD. The time that ions spend in the collisional region in low energy CAD is around 10-100 μs while it is less than 1 μs in high energy CAD. Moreover, the collision properties of the multiple collision region in low energy CAD enable multiple collisions to be accommodated without excessive scattering losses.

3.6 Mass Spectrometry for Peptide Identification

The Edman degradation is one popular approach uses for protein sequencing, but the most frequent failure to obtain amino acid sequence results from a blocked N-terminus of the protein. Several other methods have appeared to facilitate the use of the sequence database to identify proteins. One increasingly popular approach uses mass spectrometry and computer algorithms to search sequence databases.

Protein identification using mass spectrometric data may take two approaches. The first one is using the mass measurement ability of mass spectrometers to detect the intact protein or peptides (66) following enzymatic digestion. The peptides derived from enzymatic digestion of the protein are compared to the molecular weights for a known predicted sequence. The second type of the protein identification using mass

spectrometric data uses tandem mass spectrometry and CAD to obtain peptide amino acid sequence (67).

Analysis of peptide sequences by CAD in tandem mass spectrometry has become a useful technique in biological compound analysis. This technique is based on cleavage of bonds along the peptide backbone to produce fragment ions indicative of amino acid sequence. Roepstorff and Fohlman set a systematic nomenclature for designating sequence ions (68). The A, B and C ion-type contain the original peptide N-terminus and X, Y and Z ion-type contain the original peptide C-terminus (figure 2.12). A subscript number indicates the number of amino acid residues of the fragment and apostrophes indicate the number of additional proton.

Other types of ions are also present that is derived solely from cleavage of the peptide backbone: internal fragment ions and immonium ions (derived from individual amino acid residues are labeled using the single letter code for the amino acid concerned) are shown in figure 2.13. The $(A_rY_s)'_t$ and $(B_rY_s)'_t$ system was used to describe internal fragmentation. The subscripted letter outside of the parenthesis (t) indicates the number of amino acid residues of the fragment ion. In addition, the total number of amino acids in the peptide chain is given by r+s-t. The abundance of internal fragment ions is dependent on the sequence of peptide and the CAD method. Internal fragments were suggested more commonly observed following low energy CAD (27). The time available for decomposition is longer in the low energy CAD than high energy CAD and there is a higher probability for multiple collisions to occur.

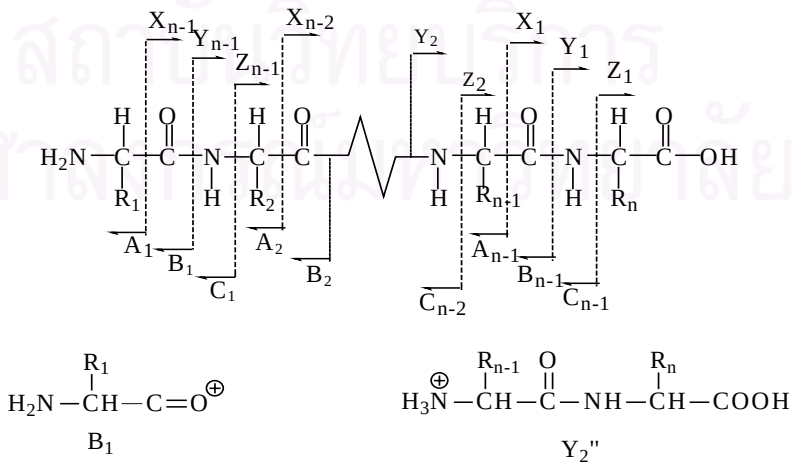

Figure 2.12 The nomenclature of the common peptide fragment ions developed by Roepstorff and Fohlman (1984).

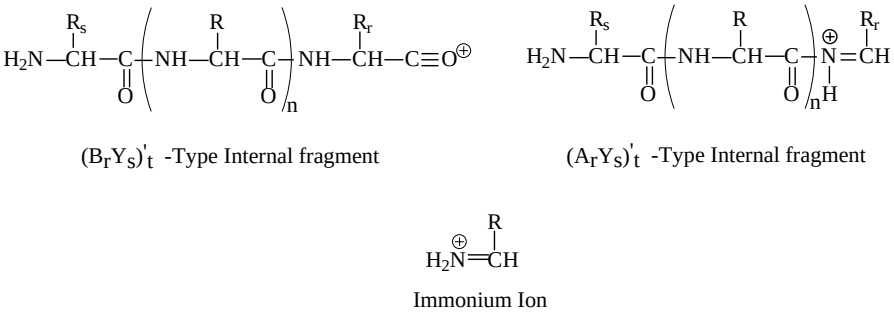

Figure 2.13 Other ions derived solely from cleavage of peptide backbone.

Biemann revised the nomenclature system from Roepstorff and Fohlman. In Biemann's system, lower case letters were used to avoid confusion with single letter codes for amino acids and certain hydrogen migrations were assumed (figure 2.14) (69). Usually, a, b, y, z or immonium type ions are observed in both low and high energy CAD.

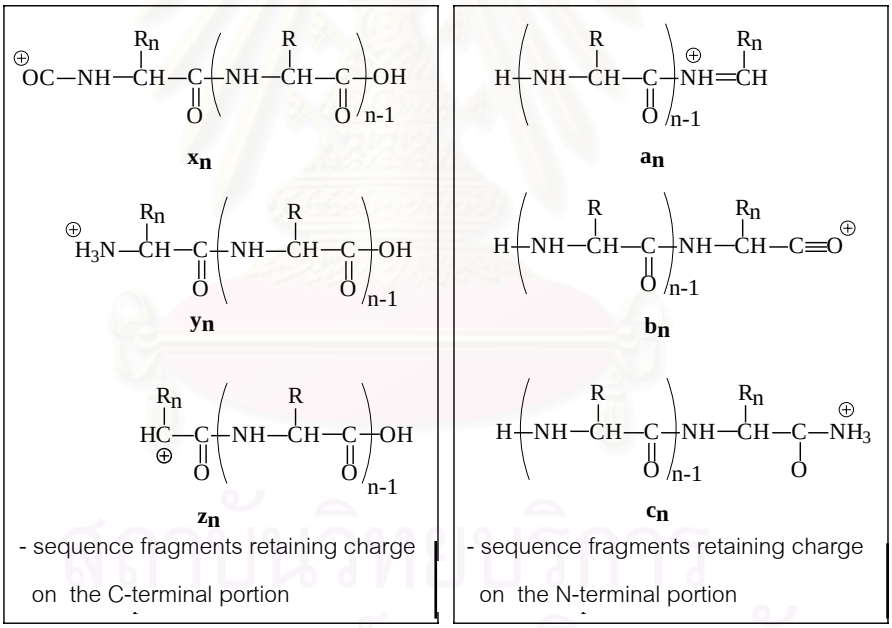

Figure 2.14 The nomenclature of the common peptide fragment ions developed by Biemann (1988) (69).

In conclude there are two groups of information that can be obtained from tandem mass spectrometry. The first one is the molecular weight of the peptide. The second group is the fragmentation information, which gained by dissociation of the peptide ion.

Chapters III

Experimental

1. Materials

Low-density lipoprotein (LDL) sample was obtained from the blood of a healthy person. Angiotensin II, trypsin (L-1-tosylamide-2-phenylethylchloromethyl ketone-treated), bovine serum albumin (BSA), sodium borohydride ($NaBH_4$), and spectroscopic grade trifluoroacetic acid (TFA), were obtained from Sigma. Acetonitrile (ACN) HPLC-grade and all ACS reagent grade chemical - formic acid (HCOOH), potassium bromide (KBr), ethylenediamine tetraacetic acid (EDTA), copper sulphate ($CUSO_4$), sodium chloride (NaCl), disodium hydrogen phosphate (Na_2HPO_4), sodium dihydrogen phosphate (NaH_2PO_4), dipotassium hydrogen phosphate (K_2HPO_4), potassium dihydrogen phosphate (KH_2PO_4), chloroform ($CHCl_3$), and methanol (MeOH) were obtained from Merck chemical.

2. Methods (40)

2.1 Preparation of Plasma from Blood

The blood plasma (EDTA 1 mg/ml blood) from fasting healthy volunteer was centrifuged at 3,000 rpm at 4 ^{o}C for 15 min to separate plasma and blood cells. The plasma constituted the top (yellow liquid) layer in the centrifuge tube.

2.2 Preparation of LDL from Plasma

LDL was prepared by using sequential ultracentrifugation. First, Plasma (1.006 g/ml) was adjusted to a density of 1.019 g/ml for separation of V-LDL, I-LDL from plasma by addition of heavy density KBr solution (1.332 g/ml in 0.1 mM EDTA). The requisite volume was calculated using the equation

$$V_2 = \left(\frac{D - D_1}{D_2 - D} \right) . V_1$$

V_1 = volume of original solution (ml)

V_2 = volume of heavy density solution (ml)

D = required density (g/ml)

D_1 = original density

D_2 = density of heavy solution (1.332 g/ml)

The adjusted density plasma was transferred to centrifuge tube and then centrifuged at 100,000 rpm at 4 ^{o}C for 3 hours using a Hitachi himac CS100 ultracentrifuge, rotor model S100AT-5. Subsequently, the V-LDL and I-LDL in the top layer (pale yellow liquid) were discarded and then the plasma was readjusted to a density of 1.063 g/ml by addition of heavy density KBr solution. The readjusted density plasma was centrifuged at 100,000 rpm at 4 ^{o}C for 4 hours. Consequently, the LDL (density 1.019-1.063 g/ml) in the top layer was collected and dialyzed against 50 mM phosphate buffered saline (PBS) buffer (for 1 L of solution: 0.45g NaH_2PO_4, 1g Na_2HPO_4, 8g NaCl, adjusted to pH 7.4 with NaOH) for 24 hours at 4 ^{o}C in a dialysis bag (10,000 molecular weight cut-off).

2.3 Protein Quantification by the Bradford Method

The Bradford method is based on the binding of Coomossie blue G250 dye to protein not to amino acid. The cationic form of the dye absorbs in the UV with an absorbance maximum at 465 nm, and the anionic form absorbs at 595 nm. Dye in the acidic form binds to the protein to produce the complex anionic form and then the amount of complex can be quantified by measuring the absorbance at 595 nm (all of experiment used 1 mg/ml BSA as a standard).

2.4 Metal-catalyzed oxidation of LDL

The LDL solution (1.2 – 1.7 mg protein/ml) was diluted to a concentration of 1 mg/ml and then placed in a dialysis bag. The bag was immersed in PBS buffer that contained 10 μM $CuSO_4$, and allowed standing for 24 hour at 37 ^{o}C.

2.5 Reduction and Delipidation of Oxidized LDL

10 ml LDL suspension obtained after oxidation was transferred to a 50-ml tube and cooled to 0 °C and stirred vigorously using a magnetic stir bar. Then 1.4g K_2HPO_4 and 0.31g KH_2PO_4 were added to the cool slurry to yield a 1 M potassium phosphate suspension solution at pH 7.3. A single portion of 0.1g $NaBH_4$ was added to the suspension and stirring was continued until all the reducing agent had dissolved. The tube was capped and mixed by inversion several times. The tube was then uncapped and the suspension was allowed to warm to room temperature. The suspension was diluted with 20 ml H_2O. The oxidized LDL was delipidated by washing with $CHCl_3$: MeOH (2:1) and centrifuged for short period. The resulting apoprotein B-100 was dried under a stream of nitrogen.

2.6 Digestion of apo B-100 with trypsin

Apo B-100 was resuspended in buffer containing 0.1 M NH_4HCO_3, 1 mM $CaCl_2$, pH 8.3. Trypsin was added in ratio 1: 50 (enzyme: substrate, w/w). The suspension was stirred and maintained at 37 °C for 18 h at which time the digest was halted by lowering the pH to 2.5 by the addition of formic acid. The solution was briefly centrifuged prior to fractionation to remove the small amount of undissolved material.

2.7 Fractionation by HPLC of the tryptic digest of apo B-100

The supernatant from the tryptic digestion was fractionated by HPLC using a C18 column (4.6 x 150 mm) and eluted at 0.5 ml/min using a gradient of solvent A (0.1% v/v TFA in H_2O) and solvent B (ACN containing 0.01% v/v TFA). A linear gradient was used from 100% A to 65% A in 45 min and then from 65% A to 5% A in 10 minutes followed by a 10 minute hold at 5% A. The injection volume was 0.8 ml. Detection was by UV absorption at 217 nm. Fractions were collected over 1 minute into 1.5 ml eppendorf ® tubes and the fractions from 4 HPLC runs were combined and dried under reduced pressure. Prior to analysis by electrospray ionization mass spectrometer, each fraction was dissolved in 100 μl of electrospray solvent (0.1% v/v formic acid in acetonitrile: water (1:1, v/v)).

3. Instrumentation

3.1 High Performance Liquid Chromatography (HPLC)

All HPLC separations were performed using a gradient HPLC system of Shimadzu class - LC10 equipped with UV detector and Rheodyne 7725i injector. Chromatograms were recorded and processed using class-LC software version 1.6 (Shimadzu) running on a personal computer.

3.2 Electrospray Ionization Mass Spectrometry (ESI MS)

Electrospray ionization mass spectrometry was carried out using a tandem quadrupole Quattro II Micro, Micromass instrument. The heated capillary temperature was 150° C. Typical source cone voltages were 25-30 V and the electrospray capillary potential was 3.5 kV. For conventional mass spectra, resolution was set to give a peak width at half height of 0.6 m/z units for the monoisotopic peak of a singly charged ion. Product ion spectra were recorded with MS1 set to give a peak width at half height of 2-4 m/z-units, while MS2 was adjusted to give a peak width at half height of 0.9 - 1.5 m/z-units. Angiotensin II (10 μM) was used for calibration of conventional mass scanning and product ion scanning. In tandem MS experiments, argon at 1-3 mbar was used as collision gas and the collision offset was set between 20-40 V for product ion scanning. A built in syringe pump was used to infuse sample at a rate of 5-8 μl/min to the electrospray probe for all experiments. All spectra were recorded in multi-channel analyzer mode (MCA) with a scan rate of 100 m/z-units per second. Masslynx™ software was used for instrument control and data acquisition.

4. Determination of Modified Sites on Apoprotein B-100

Electrospray ionization mass spectrometry (ESI-MS) and ESI tandem MS techniques were used to determination the attachment sites of HNE adducts on apoprotein B-100. Precursor ion scanning of m/z 268 corresponding to the reduced form of immonium ion of HNE-modified histidine was used to screen for the HNE-adducted apoprotein B-100 tryptic fragment. The product ion scanning was used to determine amino acid sequence of this modified peptide.

Chapters IV

Results and Discussion

1. Protein Sequencing of Standard Peptide

Angiotensin II, Ang II, (10 μM) was used as standard for adjusts the condition of conventional mass scanning and product ion scanning. Stock standard Ang II (1 mg/ml) 10 μl was diluted to 1000 μl in electrospray solvent (0.1 % v/v formic acid in ACN: H_2O (1:1,v/v)). For product ion scanning cone voltage and collision offset were varied between 20-40 V. The results did not show significant difference between them, but the most appropriate cone voltage was 30 V and collision energy was 25 V.

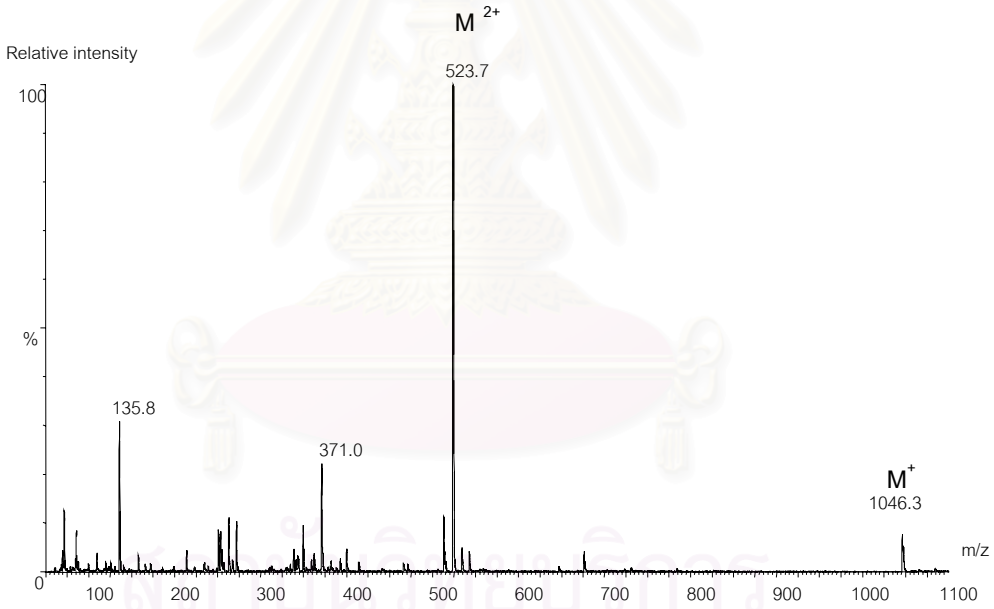

Figure 4.1 ESI conventional mass spectrum of Angiotensin II (10 μM), cone voltage was set at 30 V.

From the acquired data, the observed molecular mass $(M+H)^+$ of Angiotensin II is 1046.3 Da while the calculated molecular mass $(M+H)^+$ is 1046.2 Da. And peak of double charge of Ang II was observed at m/z 523.7. To determine the sequence of Ang II, product ion scanning of m/z 523.7 (M^{2+}) was performed (figure 4.2).

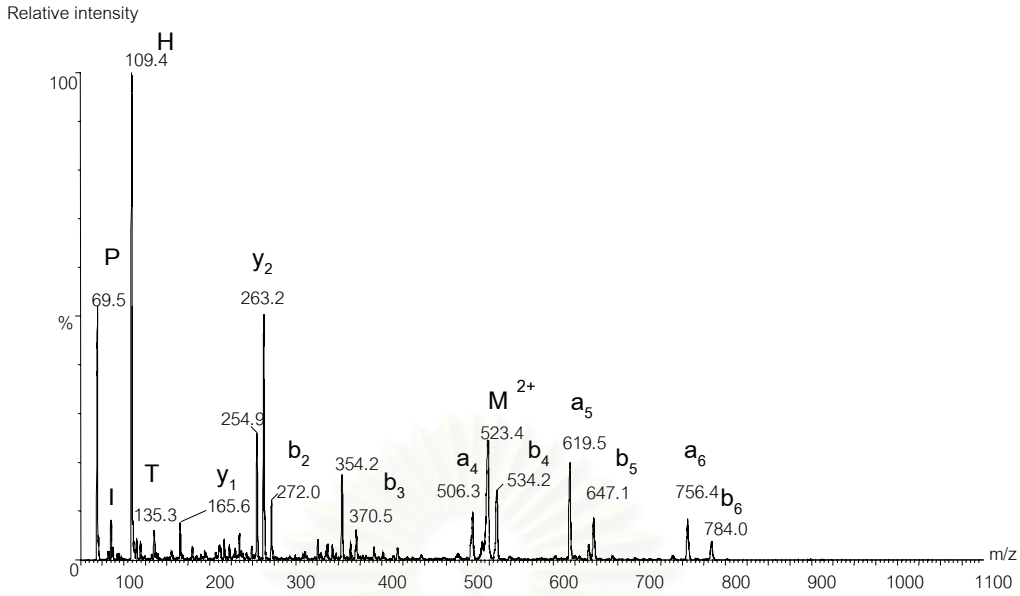

Figure 4.2 ESI tandem mass spectrum of Angiotensin II. Almost complete singly b-ion series was observed. The sequence of Ang II (DRVYIHPF) was obtained from product ion scanning of m/z 523.7 (M^{2+}), cone voltage was set at 30 V and collision offset was set at 25 V.

2. Results of Native Apoprotein B-100

LDL was isolated from human plasma (1 mg EDTA/1 ml bloods) by sequential ultracentrifugation, and divided into two portions. For the first portion, native apoB-100 was extracted with $CHCl_3$: MeOH (2:1) from native LDL and digested by trypsin. Later, the tryptic peptides were separated and purified by reverse phase HPLC using gradient elution (ACN/H_2O) with UV detector at 217 nm (figure 4.3) and fractions were collected over 1 minute. Finally, mass spectrometry was used to determine the sites of modification on apoB-100. For the second portion, LDL was oxidized by $CuSO_4$ and reduced HNE protein adducts with $NaBH_4$, after that oxidized apoB-100 was extracted, digested, separated and analyzed same as native apoB-100.

.

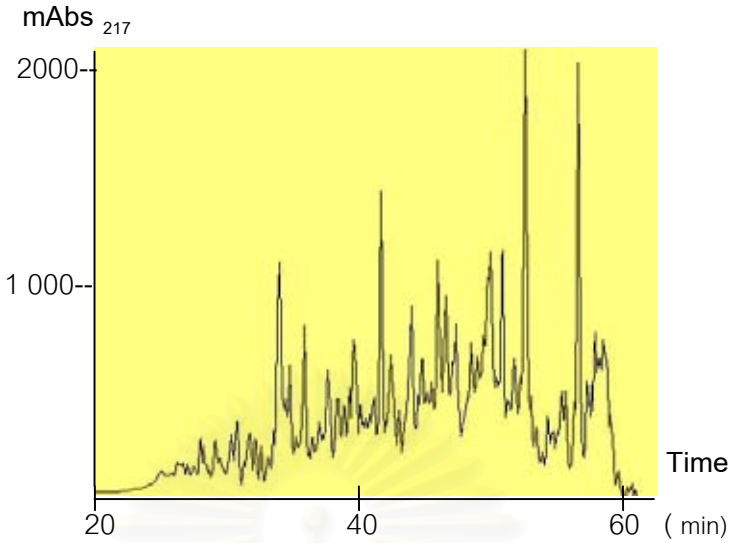

Figure 4.3 HPLC chromatogram of native apoB-100 tryptic digest eluted from C18-reverse phase HPLC using gradient elution ACN/$H_2$0 during 65 minutes.

Total HPLC fractions of native apoB-100 were extensively analyzed by ESI-MS and ESI tandem MS. Conventional ESI-MS was used in MS scan mode to screen for all native tryptic peptides in each fraction. Tandem MS was used in precursor ion scanning and product ion scanning mode.

The precursor ion scanning of m/z 268 was used to detect the reduced form of immonium ion of HNE-modified histidine in apoB-100 tryptic digest. The results obtained from precursor ion scanning mode were compared to the values predicted for tryptic peptides from the sequence of native apo B-100 and product ion scanning was used to confirm the sequence of these peptides.

The results from precursor ion scanning MS, peak at 268 m/z corresponding to immonium ion of HNE-modified histidine were not detected in native apoB-100. But peak at 268 m/z corresponding to the loss of water or ammonia group from peptide fragmentation also detected in native apoB-100 tryptic peptides of HPLC fraction 26, 30 and 38. The results are shown in figure 4.4 – 4.9.

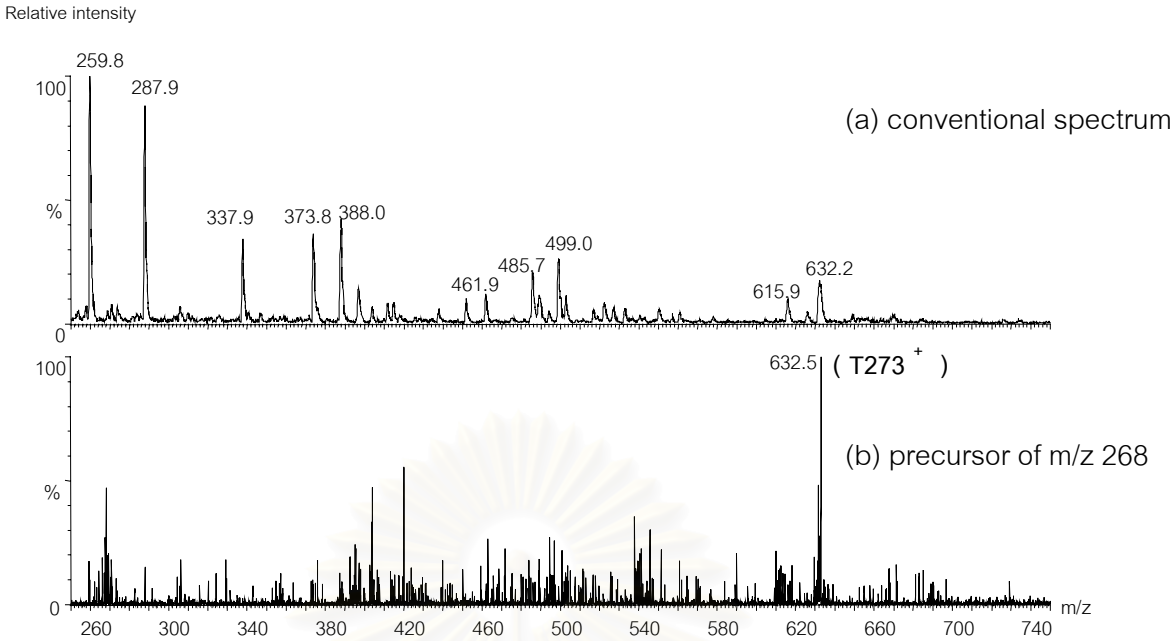

Figure 4.4 ESI MS and tandem MS of native apoB-100 from HPLC fraction 26 :
a) conventional mass spectrum, b) precursor ion scanning of m/z 268

Native apoB-100 tryptic peptides from HPLC fraction 26 showed numerous expected of native apo B-100 (figure 4.4a) and from ESI precursor spectrum (figure 4.4b) showed that the peptide at m/z 632.5 could fragment and yield the residue mass at m/z 268 that might correspond to peak of immonium ion of HNE-modified histidine. Molecular mass of 632.5 Da was compared to values predicted for tryptic peptides from the sequence of native apoB-100 and molecular mass of 632.7 Da of T273 was found to be in good agreement. The product ion scanning of m/z 632.3 was used to confirm the sequence of this peptide (figure 4.5). The complete amino acid sequence of T273, EVTQR, was obtained from the presence of a series of singly charged y-type ions. The peak at m/z 268 corresponds to the lost of two NH_3 groups (-34 Da) from y_2 ion at m/z 303.0 not due to the immonium ion of HNE-modified histidine.

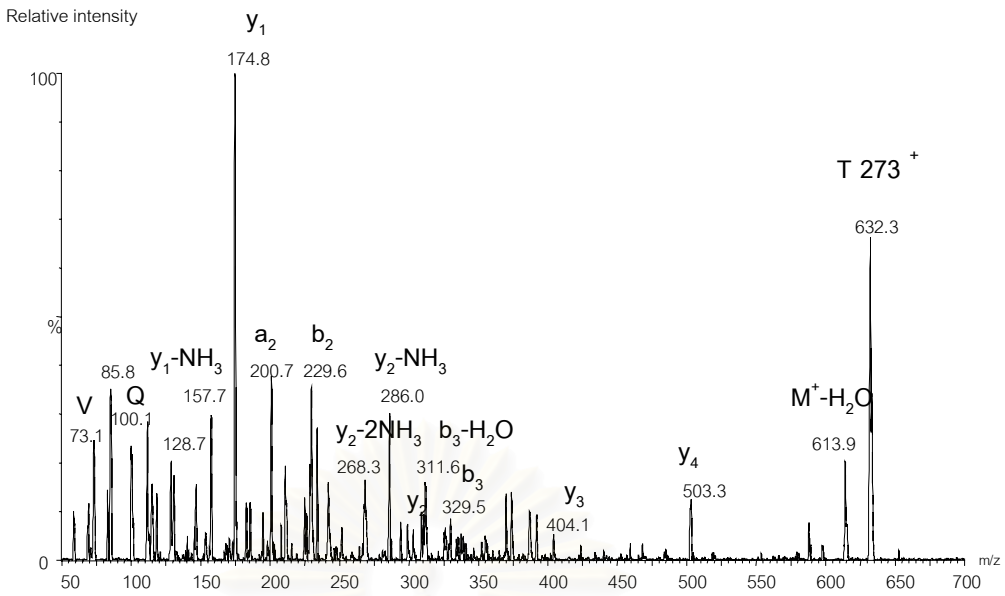

Figure 4.5 ESI tandem MS of HPLC fraction 26 of native apoB-100 tryptic peptides. Product of CAD of m/z 632.3, attributed to T273 with the sequence EVTQR.

The same as native apoB-100 tryptic peptides from HPLC fraction 26, mass spectrum of tryptic peptides from HPLC fraction 30 and 38 also show the precursors at m/z 268. So the resultant peptides were compared to values predicted for tryptic peptides from the sequence of native apoB-100 and product ion scanning was used to confirm the sequence of these peptides as shown in figure 4.6 - 4.9.

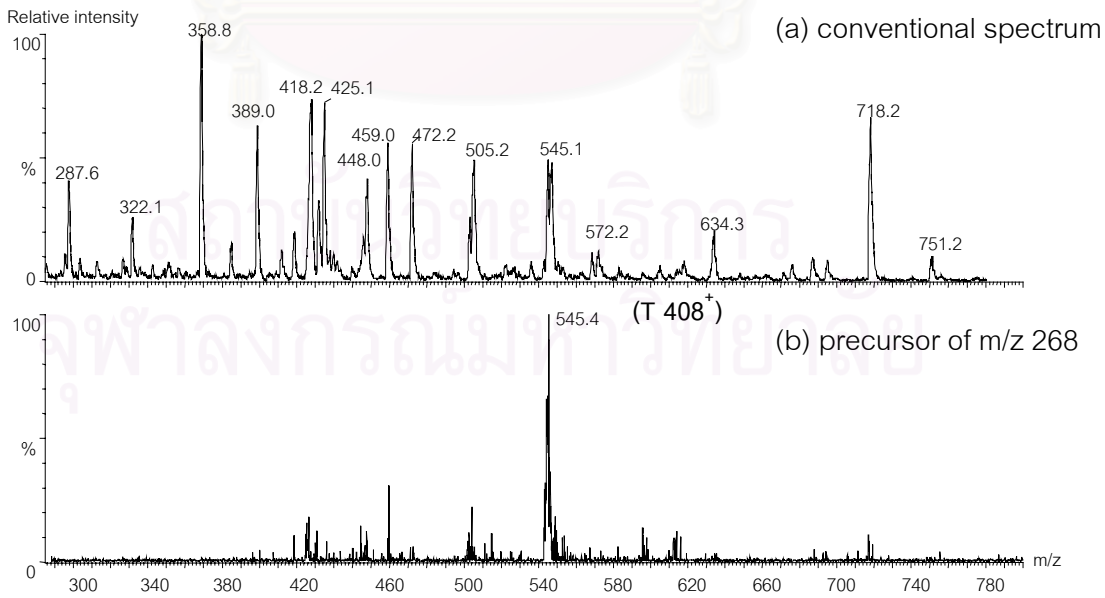

Figure 4.6 ESI MS and tandem MS of native apoB-100 from HPLC fraction 30 :

a) conventional mass spectrum, b) precursor ion scanning of m/z 268

The ESI precursor spectrum of m/z 268 (figure 4.6 b) indicated that the peptide at m/z 545.4 could fragment and yield the residue mass at m/z 268. Molecular mass of 545.4 Da was compared to values predicted for tryptic peptides from the sequence of native apoB-100 and molecular mass of 545.7 Da of T408 was found to be in good agreement. Product ion scanning of m/z 545.3 was used to confirm the sequence of this peptide (figure 4.7).

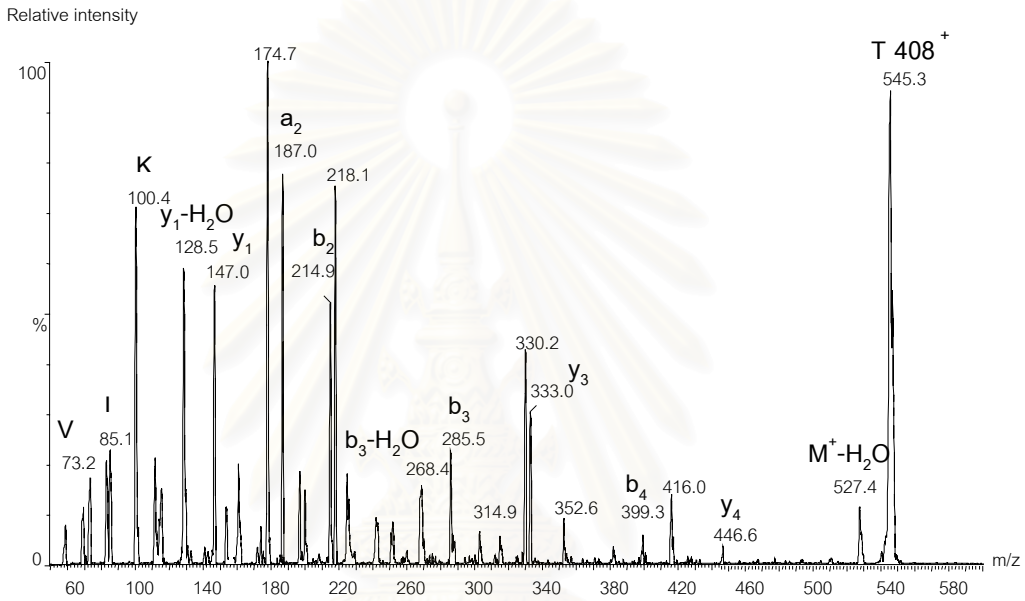

Figure 4.7 ESI tandem MS of HPLC fraction 30 of native apoB-100 tryptic peptides. Product of CAD of m/z 545.3, attributed to T408 with the sequence VLADK.

The complete amino acid sequence of T408, VLADK, was obtained from the presence of a series of singly charged y-type ions. And peak at m/z 268 corresponds to the lost of H_2O group (-18 Da) from b_3 ion at m/z 285.5 instate of the immonium ion of HNE-modified histidine.

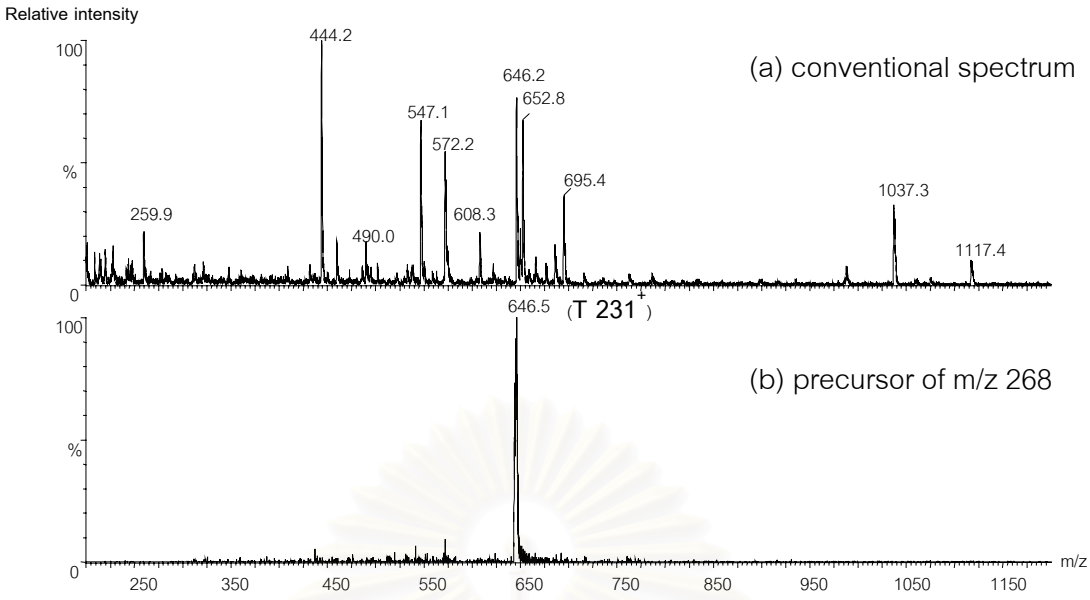

Figure 4.8 ESI MS and tandem MS of native apoB-100 from HPLC fraction 38 : a) conventional mass spectrum, b) precursor ion scanning of m/z 268

The ESI precursor spectrum of m/z 268 (figure 4.8 b) indicated that the peptide at m/z 646.5 could fragment and yield the residue mass at m/z 268. Molecular mass of 646.5 Da was compared to values predicted for tryptic peptides from the sequence of native apoB-100 and molecular mass of 646.8 Da of T231 was found to be in good agreement. Product ion scanning of m/z 646.6 was used to confirm the sequence of this peptide (figure 4.9).

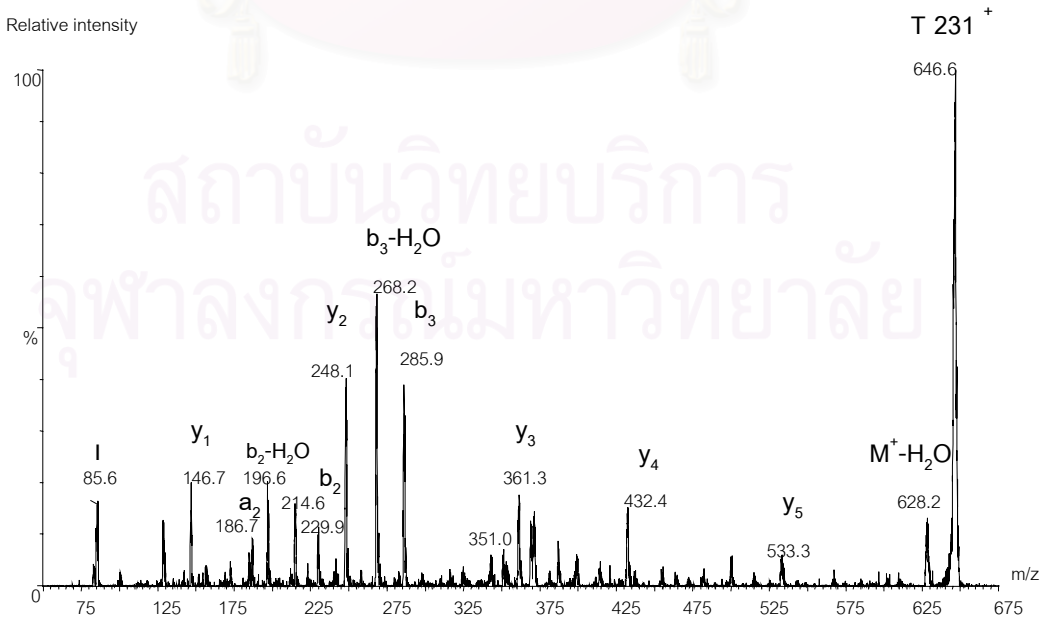

Figure 4.9 ESI tandem MS of HPLC fraction 38 of native apoB-100 tryptic peptides. Product of CAD of m/z 646.6, attributed to T231 with the sequence LTALTK.

The complete amino acid sequence of T231, LTALTK, was obtained from the presence of a series of singly charged y-type ions. The peak at m/z 268 corresponds to the lost of H_2O group (-18 Da) from b_3 ion at m/z 285.9 instate of the immonium ion of HNE-modified histidine.

The observation of the lost of neutral, NH_3 or H_2O, from the precursor peak commonly found from process in collisionally induced dissociation (CAD). These losses are observed for both the b- and y- ion series if that ion contains a particular amino acid. The type of neutral loss occurred depend on the amino acid composition of those peptides.

Table 4.1 Neutral losses observed from ions with different amino acid compositions(70).

Amino acid - Letter code	Neutral loss
Serine – S	18
Threonine - T	18
Cysteine - C	34
Asparagine - N	17
Aspartic acid - D	18
Glutamine - Q	17
Lysine - K	17
Glutamic acid - E	18
Methionine - M	48
Arginine - R	17

2.1 Native Apoprotein B-100 Sequencing

Many sequences of native apoB-100 tryptic digest was obtained from tandem MS, product ion scanning mode, the collision energy was adjusted between 20-40 V depend on amino acid structure of those peptides. The examples shown in figure 4.10 - 4.12.

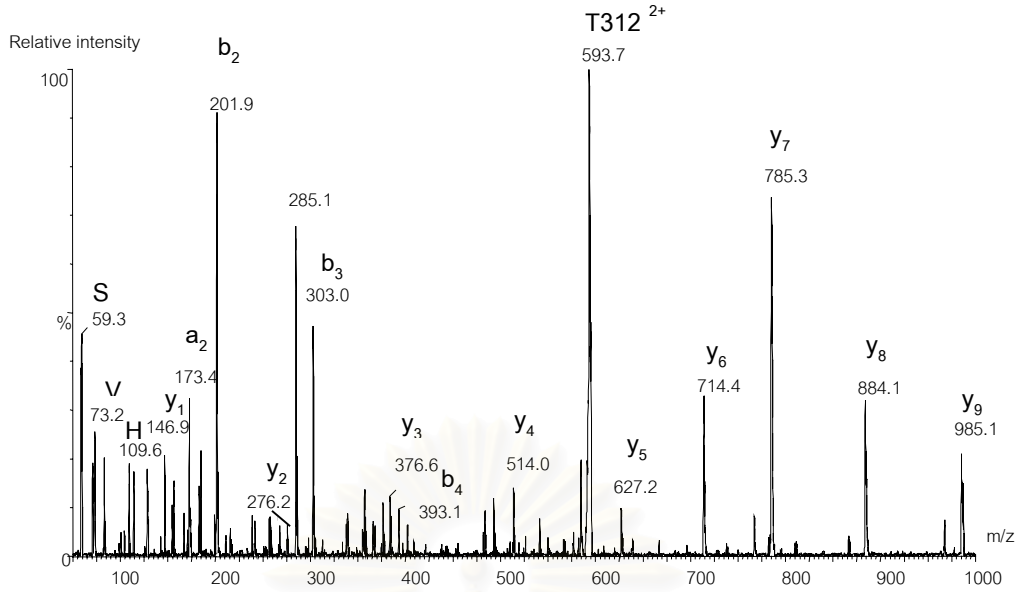

Figure 4.10 ESI product ion scanning of m/z 593.7 (T312 $^{2+}$) from HPLC fraction 36. The complete sequence of T312 (SNTVASLHTEK) was obtained with collision voltage 25 V.

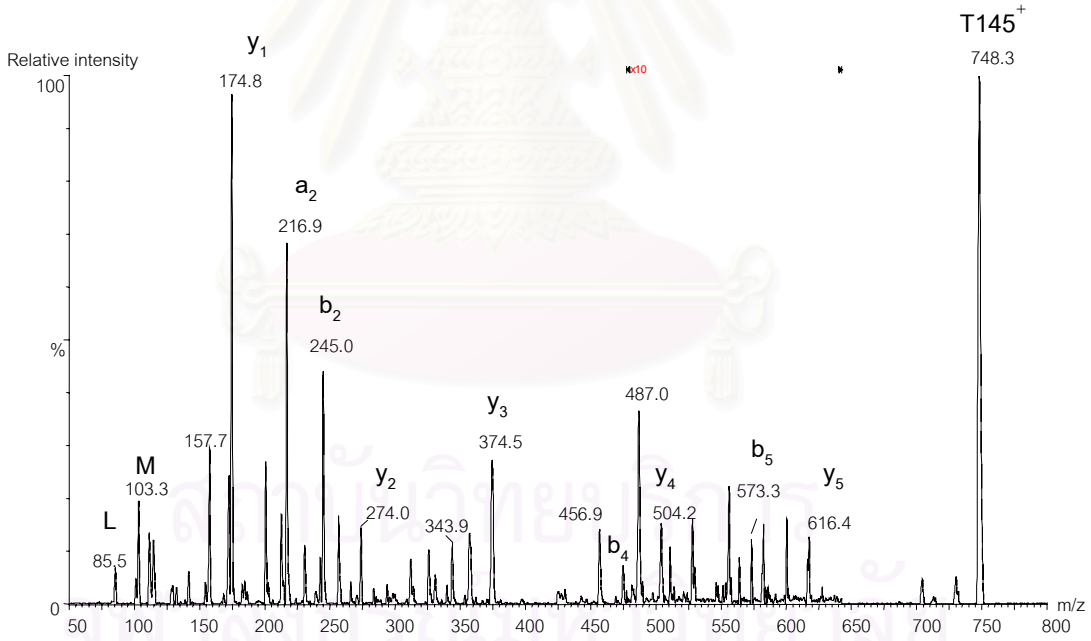

Figure 4.11 ESI product ion scanning of m/z 748.4 (T145 $^{+}$) from HPLC fraction 39. The complete sequence of T145 (MLETVR) was obtained with collision voltage 40 V.

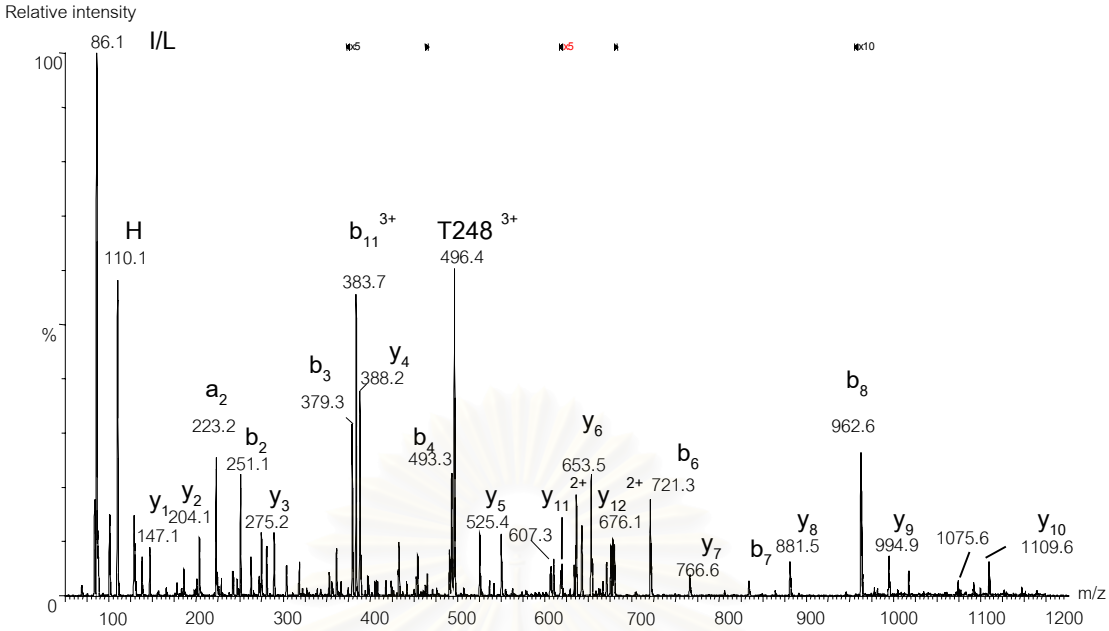

Figure 4.12 ESI product ion scanning of m/z 496.4 (T248 $^{3+}$) from HPLC fraction 44. The complete sequence of T248(HIQNIDIQHLAGK) was obtained with collision voltage 20 V.

From the results above, the observed molecular mass of native apoB-100 tryptic digest peptides was compared to values predicted for tryptic peptides from the sequence of native apoB-100 in Table 4.2. Mass error of these peptides are between 0.2 - 0.5 Da.

Table 4.2 Observed peptides in the tryptic digestion of native apoB-100.

Fragment No.	Sequence	No. of Charge	Theory (Da)	Observed (Da)
T273	EVTQR	1	632.7	632.3
T408	VLADK	1	545.7	545.3
T231	LTALTK	1	646.8	646.6
T312	SNTVASLHTEK	2	594.2	593.7
T145	MLETVR	1	748.9	748.4
T248	HIQNIDIQHLAGK	3	496.6	496.4

3. Results of Oxidized Apoprotein B-100

LDL, isolated from human plasma (1 mg EDTA/1 ml bloods) by sequential ultracentrifugation, was oxidized in an oxygen-saturated buffer containing a 10 μM concentration of $CuSO_4$ (37 °C, 24 hours). After oxidation, oxidized LDL was reduced using $NaBH_4$ to stabilize HNE adducts formed during oxidation. Oxidized apoB-100 was extracted with $CHCl_3$: MeOH (2:1) from oxidized LDL and digested by trypsin. Later, the tryptic peptides were separated and purified by reverse phase HPLC using gradient elution (ACN/H_2O) with UV detector at 217 nm (figure 4.13). The HPLC fractions were collected at 1 minute interval from the column and the fractions were subjected to mass spectrometric analysis using conventional scanning and precursor ion scanning of m/z 268 ions, which corresponds to a reduced form of the HNE-modified histidine immonium ions. The resultant precursor ions of m/z 268 were compared to the values predicted for tryptic peptides from the sequence of native apo B-100, and modified apo B-100 where each histidine is replaced by an HNE-adducted histidine residue. The molecular weight of tryptic peptides, which contain more than one histidine residue were calculated for all possible combinations of native and HNE-adducted residues. The m/z values of the $[M+nH]^{n+}$ ions where n = 1 to 5 were calculated for each peptide. Those precursor ions that corresponded to m/z values of predicted HNE-adducted tryptic fragments were subjected to product ion analyses to confirm the proposed amino acid sequence.

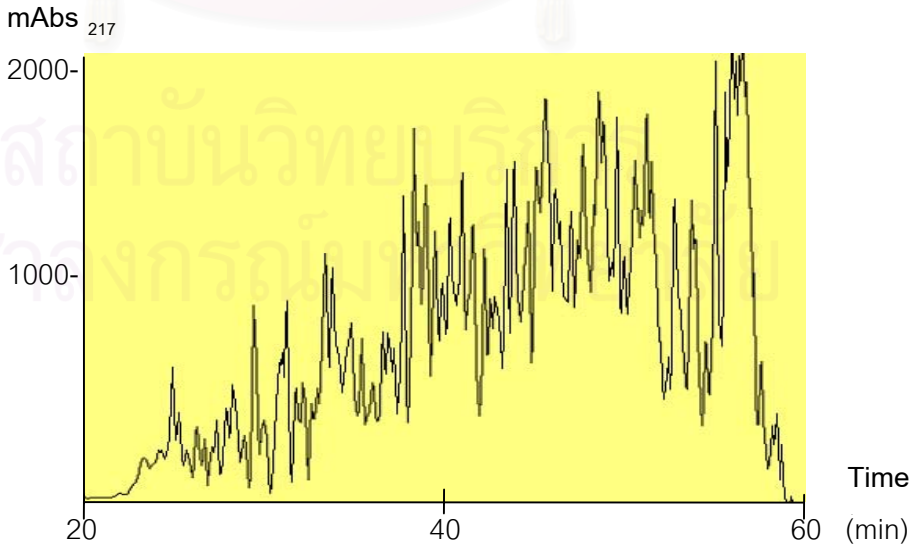

Figure 4.13 The HPLC chromatogram of oxidized apo B-100 tryptic digest from C-18 reverse phase HPLC using gradient elution with ACN/H_2O, 65 minutes.

Total HPLC fractions of oxidized apoB-100 were extensively analyzed by ESI-MS and ESI tandem MS as describe before. Oxidized apoB-100 tryptic peptides from HPLC fraction 29 showed numerous expected of native apo B-100 (figure 4.14a). While electrospray precursor spectrum (figure 4.14b) showed the peptide at m/z 505.8 and m/z 1010.3 could fragment and yield the residue mass at m/z 268 that might correspond to peak of immonium ion of HNE-modified histidine. The ions at m/z 505.8 and 1010.3 were found to be in good agreement with the expected value for the $[M+H]^{2+}$ ion (505.6) and $[M+H]^{+}$ (1010.3) of HNE-adducted of T198, respectively. The product ion scanning was used to confirm the sequence of this peptide (figure 4.15, 4.16).

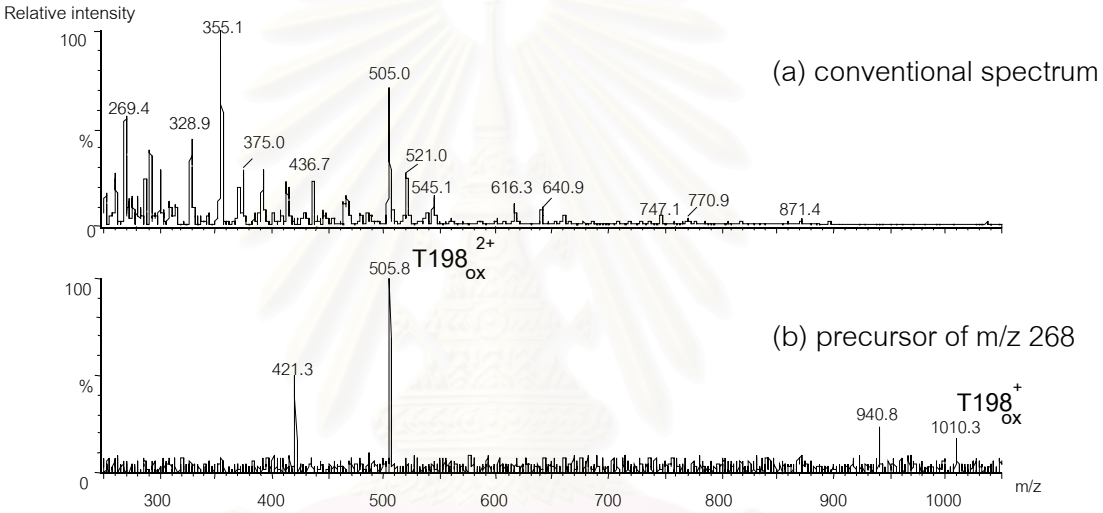

Figure 4.14 ESI MS and tandem MS of HPLC fraction 29 of oxidized apoB-100 :

a) conventional mass spectrum, b) precursors of m/z 268

The product ion spectrum obtained from the ion at m/z 1010.3 (figure 4.15) produced limited sequence information with only the presence of a C-terminal arginine residue confirmed, though ions of m/z 431.8 and 502.8 can be attributed to y_4 and y_5 ions for the expected sequence. The presence of leucine (or isoleucine) and histidine were confirmed by the presence of the immonium ions at m/z 86 and 110, respectively. The ion at m/z 110, corresponds to a native histidine immonium ion, is attributable to a second generation product from the HNE-modified immonium ion. HNE-modified T198 corresponds to the amino acid sequence, $LH^{*}VAGNLK$ (where H^{*} is an HNE-modified histidine residue). The lack of further sequence information was a reflection of the low abundance of the precursor ion.

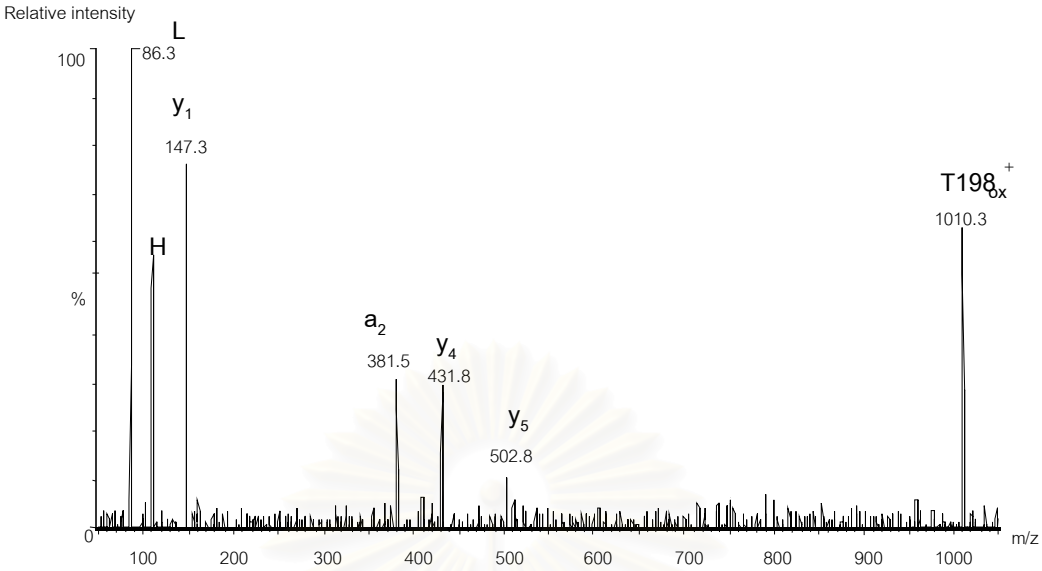

Figure 4.15 ESI tandem MS of HPLC fraction 29 of oxidized apoB-100. Products of CAD of m/z 1010.3, attributed to HNE-adducted T198 with the sequence LH*VAGNLK (where * indicates adduction by HNE)

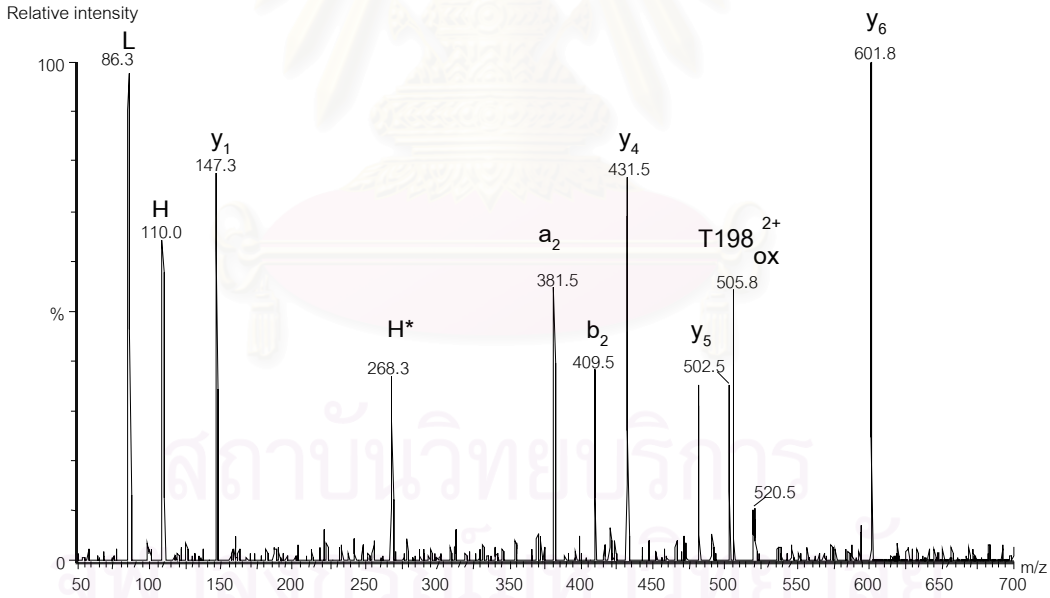

Figure 4.16 ESI tandem MS of HPLC fraction 29 of oxidized apoB-100. Products of CAD of m/z 505.8, attributed to HNE-adducted T198 with the sequence LH*VAGNLK (where * indicates adduction by HNE)

For the product ion scanning experiment of m/z 505.8 (figure 4.16) contained sufficient structural information to fully confirm the sequence from the presence of a

series of singly charged y-type ions. Taking into account both results from the figure 4.15 and 4.16, the amino acid sequence of T198 has been confirmed.

A further HPLC fraction 37 also apparently contained HNE-modified histidine peptides. The conventional ESI mass spectrum of fraction 37 was complicated (figure 4.17a) but the spectrum of precursors of m/z 268 only showed three significant ions at m/z 567.5, 662.8 and 850.5 (figure 4.17b). These ions were not detected in the conventional ESI mass spectrum. The ions at m/z 567.5 and 850.5 correspond to the triply and doubly protonated forms of HNE-adducted T103 (expected m/z 850.5 and 567.3 for triply and doubly charged ions), respectively, with the expected sequence LLSGGNTLH*LVSTTK. Product ion scanning was used to confirm the sequence of this modified peptide (figure 4.18, 4.19).

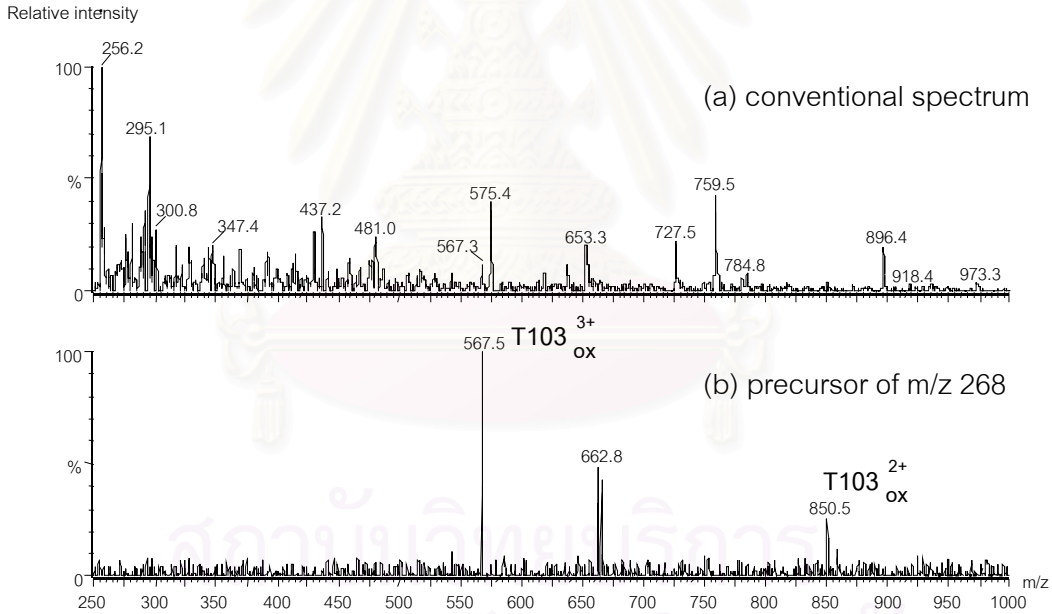

Figure 4.17 ESI MS and tandem MS of HPLC fraction 37 of oxidized apoB-100 : a) conventional mass spectrum, b) precursors of m/z 268

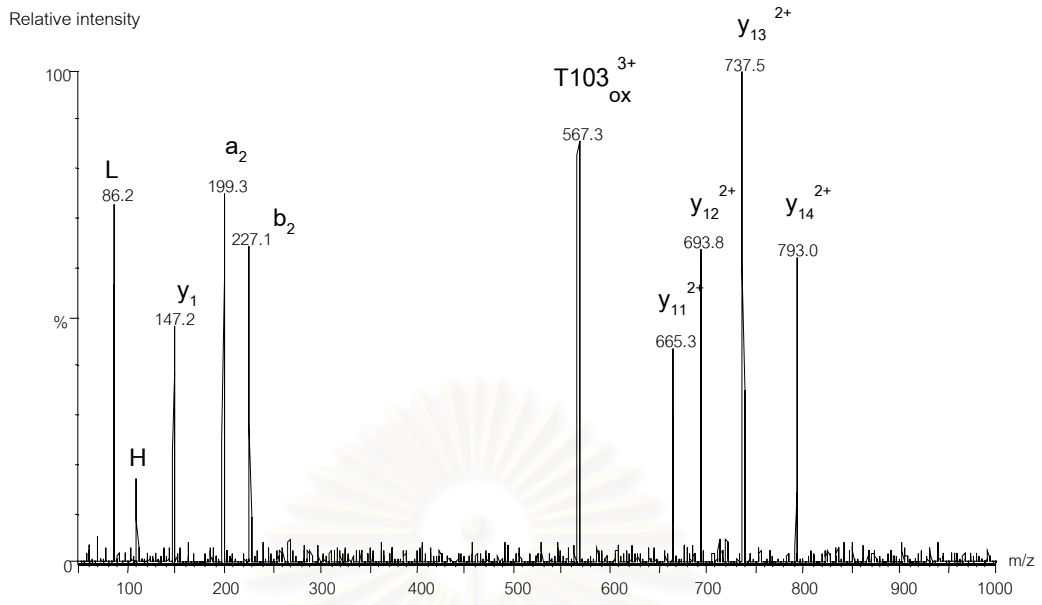

Figure 4.18 ESI tandem MS of HPLC fraction 37 of oxidized apoB-100. Products of CAD of m/z 567.3, attributed to HNE-adducted T103 with the sequence LLSGGNTLH*LVSTTK (where * indicates adduction by HNE)

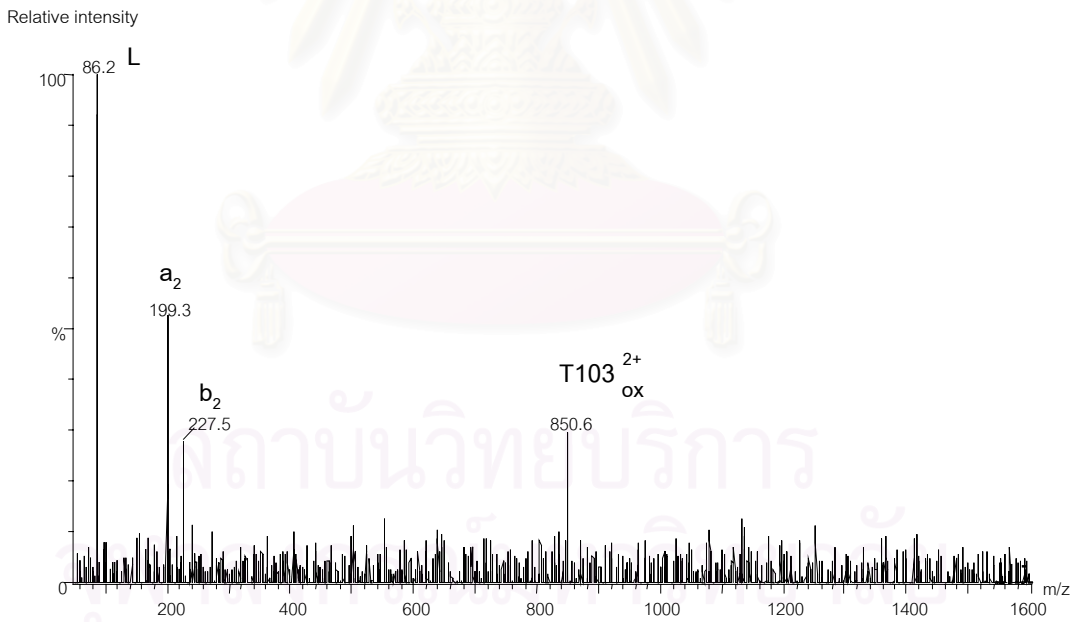

Figure 4.19 ESI tandem MS of HPLC fraction 37 of oxidized apoB-100. Products of CAD of m/z 850.6, attributed to HNE-adducted T103 with the sequence LLSGGNTLH*LVSTTK (where * indicates adduction by HNE)

The product ion spectrum obtained from the ion at m/z 567.5, yielded only partial sequence information (figure 4.18). The products that are observed in this spectrum confirmed the amino acid sequence of the first four N-terminal residues (y_{11} to y_{14}) and the C-terminal lysine (y_1). Moreover, this spectrum contains information on the immonium ions of leucine and histidine. The product ion spectrum obtained from the doubly charged ion at m/z 850.5 (figure 4.19) contained very few sequence ions but the ions observed (a_2 and b_2) were consistent with the predicted amino acid sequence. Indeed, the poor yield of sequence ions was associated with the low abundance of the precursor ion and the expected poor fragmentation efficiently of a peptide containing two basic sites having only two ionizable protons. None of the other significant ions (m/z 662.8 and 665.3) that are observed in the precursor ion spectrum of fraction 37 (figure 4.17) corresponded to the predicted HNE-adducted tryptic fragments.

In this study, the analysis of apoB-100 tryptic digests derived from oxidized LDL gave two modified peptides, T198 and T103 with the sequence LH*VAGNLK and LLSGGNTLH*LVSTTK (where * indicates adduction by HNE), consequently. Both of the modified peptides were identified previous study (40,71). The modified peptides detected in previous work are T4/325, T90, T103, T224, T362, T429, T430 (40) and T4/325, T103, T198, T224, T250, T373 (71).

Interestingly, in HNE modified apomyoglobin (39) all of histidine residue were modified, but in HNE modified LDL only some histidine residues observed to be modified. Due to apoB-100 is associated with the lipid core to form LDL. Some amino acid sequences of apoB-100 will reside on the surface but some part of the sequence will be buried in the lipid core. The location of individual residues may affect the tendency to lipid conjugation. A second factor is the pKa of individual histidine residues with the slightly different of pKa values. This may affect HNE conjugate formation. A failure to observe specific sites of modification, even though they exist, might be attributable to poor recoveries of the modified tryptic peptide or low response factors during mass spectrometric detection.

Chapters V
Conclusion

As known, when the structure of apoB-100 was modified, the LDL receptor can not recognize and uptake cholesterol result in scavenger receptor increases recognition and accelerated uptakes of cholesterol by macrophages, leading to the formation of atherosclerotic plaque. The main objective of this research was the characterization of lipid/protein conjugates in oxidized LDL. Then mass spectrometry was used to investigate the modification of histidine by the lipid peroxidation, HNE.

The ESI mass spectrometry and tandem mass spectrometry have been used to study samples. Scanning for precursors of m/z 268 (corresponding to the reduced form of the immonium ion of HNE-modified histidine) proved effective for identifying peptides containing modified histidine residues. All of the adducted tryptic peptides yield precursors of m/z 268, indicating that HNE modification involved Michael addition.

The analysis of apoB-100 tryptic digests derived from oxidized LDL was found to be successful and allowed identification of two modified peptides as before (40,71) that is T198 and T103 with the sequence LH*VAGNLK and LLSGGNTLH*LVSTTK (where * indicates adduction by HNE), consequently.

From precursor ion scanning of m/z 268 MS, the native apoB-100 was also detected, but peak of m/z 268 in native apoB-100 due to the lost of neutral, NH_3 or H_2O, from the precursor peak.

In this research, the lipid/protein conjugates in oxidized LDL (in vitro) was investigated. The results from the investigation of oxidized LDL represent evidence supporting an important hypothesis concerning the initiation of atherosclerosis. The future work related to the determination of HNE-conjugates to LDL removed from atherosclerotic plaques of the human body should be included.

References

1. Zubay , G. 1993. Biochemistry. Third edition. England : Wm. C. Brown Publishers,
2. Mathews, C. K., Van Holde, K. E., and Alhern, K. G. 2000. Biochemistry. Third edition. New York : Addison-Wesley Publishing Company,
3. Voet, D., and Voet, J. G. 1995. Biochemistry. Second edition. New york : John Wiley & Sons, Inc.,
4. Orten, J. M., and Neuhaus, O. W. 1982. Human Biochemistry. Tenth edition. St. Louis : The C. V. Mosby Company,
5. Cotran, R. S., Robbins, S. L., Kumar, V. 1994. Robbins Pathologic basic of disease. Fifth edition. USA : W.B. Saunders Company,
6. Hevonoja, T., Pentikäinen, M. O., Hyvönen, M. T., Kovanen, P. T., Ala-Korpela, M. 2000. Structure of low density lipoprotein (LDL) particles: Basis for understanding molecular changes in modified LDL. Biochim. Biophys. Acta 1488 : 189-210.
7. Esterbauer, H., Dieber-Rotheneder, M., Waeg, G., Striegl, G., and Jürgens, G. 1990. Biochemical, Structural, and Functional Properties of Oxidized L0w-Density Lipoprotein. Chem. Res. Toxicol. 3 : 77-92.
8. Anderson, R. G. W., Brown, M. S., and Goldstein, J. L. 1977. Role of the coated and endocytic vesicle in the uptake of receptor-bound low density lipoprotein in human fibroblasts. Cell 10 : 351-364.
9. Brown, M. S., Basu, S. K., Falck, J. R., Ho, Y. K., and Goldstein, J. L. 1980. The scavenger cell pathway for lipoprotein degradation: specificity of the binding site that mediates the uptake of negative-charge LDL by macrophages. J. Supramol. Struct. 13(1) : 67-81.
10. Brown, M. S., and Goldstein, J. L. 1983. Lipoprotein metabolism in the macrophage: Implication for cholesterol deposition in atherosclerosis. Annu. Rev. Biochem 52 : 223-261.
11. Hajjar, D. P., and Haberland, M. E. 1997. Lipoprotein Trafficking in Vascular Cells. J. Biol. Chem. 272 : 22975-22978.

12. Dhaliwal, B. S., Steinbrecher, U. P. 1999. Scavenger receptors and oxidized low density lipoproteins. Clinica. Chimica. Acta 286 : 191-205.
13. Benditt, E. P., and Schwartz, S. M. 1988. Pathology. Emanuel, Rubin, John, L. Farber, Blood vessels, 452-477. Philadelphia : J.B. Lippincott Company,
14. Rosenfeld, M. E. 2000. An overview of the evolution of the atherosclerotic plaque: from fatty streak to plaque rupture and thrombosis. Z Kardiol 89 : VII/2-VII6.
15. Toborek, M., and Kaiser, S. 1999. Endothelial cell functions, Relationship to atherogenesis. Basic. Res. Cardiol. 94 : 295-314.
16. Epstein, F. H. 1999. Atherosclerosis-An Inflammatory Disease. N Engl. J. Med. 340 : 115-126.
17. Schwenke, D. C., and Carew, T. E. 1989. Initiation of atherosclerotic lesions in cholesterol-fed rabbits. I. Focal increases in arterial LDL concentration precede development of fatty streak lesions. Arteriosclerosis 9(6) : 895-907.
18. Schwenke, D. C., and Carew, T. E. 1989. . Initiation of atherosclerotic lesions in cholesterol-fed rabbits. I I. Selective retention of LDL vs.selective increases in LDL permeability in susceptible sites of arteries. Arteriosclerosis 9(6) : 908-18.
19. Rice-Evans, C., Bruckdorfer, K. R. 1995. Oxidative Stress, Lipoproteins and Cardiovascular Dysfunction. London : Portland Press Research Monograph,
20. Goldstein, J. L., Ho, Y. K., Basu, S. K., Brown, M. S. 1979. Binding site on macrophages that mediates uptake and degradation of acetylated low density lipoprotein, producing massive cholesterol deposition. Proc. Natl. Acad. Sci. USA 76 : 333-37.
21. Quinn, M. T., Parthasarathy, S., Fong, L. G., Steinberg, D. 1987. Oxidatively modified low density lipoproteins: a potential role in recruitment and retention of monocyte/macrophages during atherogenesis. Proc. Natl. Acad. Sci. USA 84 : 2995-8.
22. Aviram, M. 1993. Modified forms of low density lipoprotein and atherosclerosis. Atherosclerosis 98(1) : 1-9.
23. Spitelller, G. 2003. Are lipid peroxidation processes induced by changes in the cell wall structure and how are these processes connected with diseases? Med. Hypotheses 60 : 69-83.

24. Esterbauer, H.,Wag, G., and Puhl, H. 1993. Lipid peroxidation and its role in atherosclerosis. British Medical Bulletin 49 : 566-576.

25. Abuja, P. M., and Esterbauer, H. 1995. Simulation of Lipid Peroxidation in Low-Density Lipoprotein by a Basic "Skeleton" of Reactions. Chem. Res. Toxicol. 8 : 753-763.

26. Pryor, W. A., Porter, N. A. 1990. Suggested mechanisms for the production of 4-hydroxy-2-nonenal from the autoxidation of polyunsaturated fatty acids. . Free Radic. Biol. Med. 8 : 541-43.

27. Jessup, W., Mander, E. L., and Dean, R.T. 1992. The intracelllar storage and turn over of apolipoprotein B of oxidized LDL in macrophages. Biochim. Biophys. Acta 1126(2) : 167-77.

28. Jurgens, G., Lang, J., and Esterbauer, H. 1986. Modification of human low-density lipoprotein by the lipid peroxidation product 4-hydroxynonenal. Biochim. Biophys. Acta 875(1) : 103-14.

29. Hoff, H.F., O' Neil, J., Chisolm 3rd,G. M., Cole, T.B., Quehenberger, O., Esterbauer , H., and Jurgens, G. 1989. Modification of low density lipoprotein with 4-hydroxynonenal induces uptake by macrophages. Arterioscler 9(4) : 538-49.

30. Steinbrecher, U., P. 1986. Oxidation of Human Low Density Lipoprotein Results in Derivatization of Lysine Residues of Apolipoprotein B by Lipid Peroxide Decomposition Products. J. Biol. Chem. 262 : 3603-3608.

31. Bean, M. F., Carr, S. A., Thorne, G. C, Reilly, M. H., Gaskell, S. J. 1991. Tandem mass spectrometry of peptides using hybrid and four- sector instruments: a comparative study. Anal. Chem. 63 : 1473-81.

32. Malle, E., Ibovnik, A., Leis, H. J., Kostner, G. M., Verhallen, P. F., Sattler, W. 1995. Lysine modification of LDL or Lipoprotein(a) by 4-hydroxynonenal or malondialdehyde decreases platelet serotonin secretion without affecting platelet aggregability and eicosanoid formation. Arteroscler. Thromb. Vasc. Biol. 15 : 377-84.

33. Requena, J. R., Fu, M. X., Ahmed, M. U., Jenkins, A. J., Lyons, T. J., Thorpe, S. R. 1996. Lipoxidation products as biomarkers of oxidative damage to proteins during lipid peroxidation reactions. Nephrology dialysis transplantation 11 : 48-53.

34. Steinbrecher, U. P., Parthasarathy, S., Leake, D. S., Witztum, J. L., Steinberg, D. 1984. Modification of low density lipoprotein by endothelial cells involves lipid peroxidation and degradation of low density lipoprotein phospholipids. Proc. Natl. Acad. Sci. USA 81 : 3883-87.

35. Steinbrecher, U. P. 1987. Oxidation of human low density lipoprotein results in derivatization of lysine residues of apolipoprotein B by lipid peroxide decomposition products. J. Biol. Chem. 262 : 3603-08.

36. Jurgens, G., Lang, J., Esterbauer, H. 1986. Modification of human low-density lipoprotein by lipid peroxidation product 4-hydroxynonenal. Biochim. Biophys. Acta 875 : 103-14.

37. Uchida, K., Toyokuni, S., Nishikawa, S., Oda, K., Hiai, H., Stadtman, E. R. 1994. Michael Addition-Type 4-hydroxy-2-nonenal Adducts in Modified Low-Density Lipoprotein: Markers for Atherosclerosis. Biochemistry 33 : 12487-94.

38. Uchida, K., Stadtman, E. R. 1992. Modification of histidine residues in proteins by reaction with 4-hydroxynonenal. Proc. Natl. Acad. Sci. USA 89 : 4544-48.

39. Bolgar, M. S., and Gaskell, S. J. 1996. Determination of the Sites of 4-hydroxy-2-nonenal Adduction to Protein by Electrospray Tandem Mass Spectrometry. Anal.Chem 68 : 2325-2330.

40. Bolgar, M. S., Yang, C. Y., Gaskell, S. J. 1996. First Direct Evidence for Lipid/Protein Conjugation in Oxidized Human Low Density Lipoprotein. J. Biol. Chem. 271 : 27999-28001.

41. Bruenner, B. A., Jones, A. D., German, J. B. 1995. Direct characterization of protein adducts of the lipid-peroxidation product 4-hydroxy-2-nonenal using electrospray mass-spectrometry. Chem. Res. Toxicol. 8 : 552-59.

42. Bruenner, B. A., Jones, A. D., German, J. B. 1996. Simultaneous Determination of Multiple Aldehydes in Biological Tissues and Fluids Using Gas Chromatography/Stable Isotope Dilution Mass Spectrometry. Anal. Biochem. 241 : 212-19.

43. Moore, K., Riberts, L. J. 1998. Measurement of Lipid Peroxidation. Free. Rad. Res. 28 : 659-71.

44. Jacob, S. J., Cistola, D. C., Hsu, F. H., Muzaffar, S., Mueller, D. M., Hazen, S. L., and Heinecke, J. W. 1996. Human Phagocytes Employ the Myeloperoxidase-Hydrogen Peroxide System to Synthesize Dityrosine, Trityrosine, Pulcherosine, and Isodityrosine by a tyrosyl Radical-dependent Pathway. J. Biol. Chem. 271 : 19950-19956.

45. Chisolm III, G. M., Hazen, S. L., Fox, P. L, and Cathcart, M. K. 1999. The Oxidation of Lipoproteins by Monocytes-Macrophages. J. Biol. Chem. 274 : 25959-25962.

46. Dedy-Dupont, G., Deby, C., Lamy, M. 1999. Neutrophil myeloperoxidase revisited: it ‘ s role in health and disease. Intensivmed 36 : 500-513.

47. Leeuwenburgh, C., Rasmussen, J. E., Hsu, F. F., Mueller, D. M., Pennathur, S., and Heinecke, J. W. 1997. Mass spectrometric Quantification of Markers for Protein Oxidation by Tyrosyl Radical, Copper, and Hydroxyl Radical in Low Density Lipoprotein Isolated from Human Atherosclerotic Plaques. J. Biol. Chem. 272 : 3520-3526.

48. Hazen, S. L., and Heinecke, J. W. 1997. 3-Chlorotyrosine, a Specific Marker of Myeloperoxidase-catalyzed Oxidation, Is Markedly Elevated in Low Density Lipoprotein Isolated from Human Atherosclerotic Intima. J. Clin. Invest 99 : 2075-2081.

49. Yan, L. J., Lodge, J. K., Traber, M. G., Matsugo, S., and Packer, L. 1997. Comparison between copper-mediated and hypochlorite-mediated modifications of human low density lipoproteins evaluated by protein carbonyl formation. J. Lipid Res. 38 : 992-1001.

50. Dole, M., Mack, L. L., Hines, R. L., Mobley, R. C., Furguson, L. D., Alice, M. B. 1968. Molecular Beams of Macroions. J. Chem. Phys. 49 : 2240-49.

51. Fenn, J. B., Mann, M., Meng, C. K., Wong, S. F., Whitehouse, C. M. 1989. Electrospray ionization for mass spectrometry of large biomolecules. Science 246 : 64-71.

52. Kebarle, P., Ho, Y. 1997. Electrospray ionization mass spectrometry. Cole, R. B., fundamentals, instrumentation, and applications, 3-63. New York : John Wiley & Sons, Inc.,

53. Kebarle, P., Tang, L. 1993. From ions in solution to ions in the gas phase. Anal. Chem. 65 : 972A-86A.

54. Thomson, B. A., Iribarne, J. 1979. Field induced ion evaporation from liquid surface at atmospheric pressure. J. Chem. Phys. 71 : 4451-63.

55. Gaskell, S. J. 1997. Electrospray : principles and practice. J. Mass Spectrom. 32 : 677-88.

56. Gale, D. C., Smith, R. D. 1993. Small-volume and low-flow-rate electrospray-ionization mass-spectrometry of aqueous samples. Rapid Commun. Mass Spectrom. 7 : 1017-21.

57. Andren, P. E., Emmett, M. R., Caprioli, R. M. 1994. Micro-electrospray-zeptomole-attomole per microleter sensitivity for peptides. J. Am. Soc. Mass Spectrom. 5 : 867-69.

58. Emmett, M. R., Caprioli, R. M. 1994. Micro-electrospray-mass-spectrometry-ultra-high-sensitivity analysis of peptides and proteins. J. Am. Soc. Mass Spectrom. 5 : 605-13.

59. Wilm, M. S., Mann, M. 1996. Analytical properties of the nanoelectrospray ion-source. Anal. Chem. 68 : 1-8.

60. March, R. E., Hughes, R. J. 1989. Quadrupole Storage Mass Spectrometry. New York : John Wiley & Sons,

61. Hoffmann, E. D. 1996. Tandem Mass Spectrometry. J. Mass Spectrom. 31 : 129-31.

62. Medzihradszky, K. F., Adams, G. W., Burlingame, A. L., Bateman, R. H., Green, M. R. 1996. Protein sequence and structural studies employing matrix-assisted laser desorption ionization high energy collision-induced dissociation. J. Am. Soc. Mass Spectrom. 7 : 1-10.

63. Morris, H. R., Paxton, T., Dell, A., Langhorne, J., Berg, M., Bordoli, R. S., Hoyes, J., Bateman, R. H. 1996. High sensitivity collisionally-activated decomposition tandem mass spectrometry on a novel quadrupole/orthogonal-accerelation time-of-flight mass spectrometry. Rapid Commun. Mass Spectrom. 10 : 889-96.

64. Hoffmann, E. D., Charette, J., Stroobant, V. 1994. Mass Spectrometry Principles and Applications. New York : John Wiley & Sons,

65. Mcluckey, S. A. 1992. Principles of collisional activation in analytical mass-spectrometry . J. Am. Soc. Mass Spectrom. 3 : 599-614.

66. Hunt, D. F., Yates, J. R., Shabanowitz, J., Winston, S., Hauer, C. R. 1986. Protein sequencing by tandem mass spectrometry. Proc. Natl. Acad. Sci.USA 83 : 6233-38.

67. Gibson, B. W., Biemann, K. 1984. Strategy for the mass spectrometric verification and correction of the primary structures of proteins deduced from their DNA sequences. Proc. Natl. Acad. Sci.USA 81 : 1956-60.

68. Roepstorff, P., Fohlman, J. 1984. Proposal for a Common Nomenclature for Sequence Ions in Mass-Spectra of Peptides. Biomed. Mass Spectrom. 11 : 601.

69. Biemann, K. 1988. Contributions of mass spectrometry to peptide and protein structure. Biomed. Environ. Mass Spectrom. 16 : 99-111.

70. Kinter, M., and Sherman, N., E. 2000. Protein Sequencing and Identification Using Tandem Mass Spectrometry. New York : John Wiley & Sons,

71. Polkit, Sangvanich. 2000. The analysis of oxidized low-density lipoprotein by mass spectrometry. Doctor of philosophy thesis Department of Chemistry Faculty of Science University of Manchester institute of Science and Technology.

72. Siuzdak, G. 1996. Mass Spectrometry for Biotechnology. California : ACADAMIC PRESS,

APPENDIX A

Table A1. Amino acids and their Masses organized according to molecular weight (72).

Amino acid	Letter code (3 letters)	Letter code(1 letter)	Mass
Glycine	Gly	G	57
Alanine	Ala	A	71
Serine	Ser	S	87
Proline	Pro	P	97
Valine	Val	V	99
Threonine	Thr	T	101
Cysteine	Cys	C	103
Isoleucine	Ile	I	113
Leucine	Leu	L	113
Asparagine	Asn	N	114
Aspartic acid	Asp	D	115
Glutamine	Gln	Q	128
Lysine	Lys	K	128
Glutamic acid	Glu	E	129
Methionine	Met	M	131
Histidine	His	H	137
Phenylalanine	Phe	F	147
Arginine	Arg	R	156
Tyrosine	Tyr	Y	163
Tryptophan	Trp	W	186

Table A2. Masses of the low-mass ions characteristic of natural amino acids, most often immonium ions (72).

Amino acid	Characteristic mass
Serine (S)	60
Proline (P)	70
Valine (V)	72
Leucine (L)	86
Isoleucine (I)	86
Glutamine (Q)	101
Lysine (K)	101
Glutamic acid (E)	102
Methionine (M)	104
Histidine (H)	110
Phenylalanine (F)	120
Arginine (R)	129
Tyrosine (Y)	136
Tryptophan (W)	159

Amino acid sequence of apolipoprotein B-100

```
      1           11          21          31          41          51
1     MDPPRPALLA  LLALPALLLL  LLAGARAEEE  MLENVSLVCP  KDATRFKHLR  KYTYNYEAES  60
61    SSGVPGTADS  RSATRINCKV  ELEVPQLCSF  ILKTSQCTLK  EVYGFNPEGK  ALLKKTKNSE  120
121   EFAAAMSRYE  LKLAIPEGKQ  VFLYPEKDEP  TYILNIKRGI  ISALLVPPET  EEAKQVLFLD  180
181   TVYGNCSTHF  TVKTRKGNVA  TEISTERDLG  QCDRFKPIRT  GISPLALIKG  MTRPLSTLIS  240
241   SSQSCQYTLD  AKRKHVAEAI  CKEQHLFLPF  SYNNKYGMVA  QVTQTLKLED  TPKINSRFFG  300
301   EGTKKMGLAF  ESTKSTSPPK  QAEAVLKTLQ  ELKKLTISEQ  NIQRANLFNK  LVTELRGLSD  360
361   EAVTSLLPQL  IEVSSPITLQ  ALVQCGQPQC  STHILQWLKR  VHANPLLIDV  VTYLVALIPE  420
421   PSAQQLREIF  NMARDQRSRA  TLYALSHAVN  NYHKTNPTGT  QELLDIANYL  MEQIQDDCTG  480
481   DEDYTYLILR  VIGNMGQTME  QLTPELKSSI  LKCVQSTKPS  LMIQKAAIQA  LRKMEPKDKD  540
541   QEVLLQTFLD  DASPGDKRLA  AYLMLMRSPS  QADINKIVQI  LPWEQNEQVK  NFVASHIANI  600
601   LNSEELDIQD  LKKLVKEALK  ESQLPTVMDF  RKFSRNYQLY  KSVSLPSLDP  ASAKIEGNLI  660
661   FDPNNYLPKE  SMLKTTLTAF  GFASADLIEI  GLEGKGFEPT  LEALFGKQGF  FPDSVNKALY  720
721   WVNGQVPDGV  SKVLVDHFGY  TKDDKHEQDM  VNGIMLSVEK  LIKDLKSKEV  PEARAYLRIL  780
781   GEELGFASLH  DLQLLGKLLL  MGARTLQGIP  QMIGEVIRKG  SKNDFFLHYI  FMENAFELPT  840
841   GAGLQLQISS  SGVIAPGAKA  GVKLEVANMQ  AELVAKPSVS  VEFVTNMGII  IPDFARSGVQ  900
901   MNTNFFHESG  LEAHVALKAG  KLKFIIPSPK  RPVKLLSGGN  TLHLVSTTKT  EVIPPLIENR  960
961   QSWSVCKQVF  PGLNYCTSGA  YSNASSTDSA  SYYPLTGDTR  LELELRPTGE  IEQYSVSATY  1020
1021  ELQREDRALV  DTLKFVTQAE  GAKQTEATMT  FKYNRQSMTL  SSEVQIPDFD  VDLGTILRVN  1080
1081  DESTEGKTSY  RLTLDIQNKK  ITEVALMGHL  SCDTKEERKI  KGVISIPRLQ  AEARSEILAH  1140
1141  WSPAKLLLQM  DSSATAYGST  VSKRVAWHYD  EEKIEFEWNT  GTNVDTKKMT  SNFPVDLSDY  1200
1201  PKSLHMYANR  LLDHRVPETD  MTFRHVGSKL  IVAMSSWLQK  ASGSLPYTQT  LQDHLNSLKE  1260
1261  FNLQNMGLPD  FHIPENLFLK  SDGRVKYTLN  KNSLKIEIPL  PFGGKSSRDL  KMLETVRTPA  1320
1321  LHFKSVGFHL  PSREFQVPTF  TIPKLYQLQV  PLLGVLDLST  NVYSNLYNWS  ASYSGGNTST  1380
1381  DHFSLRARYH  MKADSVVDLL  SYNVQGSGET  TYDHKNTFTL  SCDGSLRHKF  LDSNIKFSHV  1440
1441  EKLGNNPVSK  GLLIFDASSS  WGPQMSASVH  LDSKKKQHLF  VKEVKIDGQF  RVSSFYAKGT  1500
1501  YGLSCQRDPN  TGRLNGESNL  RFNSSYLQGT  NQITGRYEDG  TLSLTSTSDL  QSGIIKNTAS  1560
1561  LKYENYELTL  KSDTNGKYKN  FATSNKMDMT  FSKQNALLRS  EYQADYESLR  FFSLLSGSLN  1620
1621  SHGLELNADI  LGTDKINSGA  HKATLRIGQD  GISTSATTNL  KCSLLVLENE  LNAELGLSGA  1680
1681  SMKLTTNGRF  REHNAKFSLD  GKAALTELSL  GSAYQAMILG  VDSKNIFNFK  VSQEGLKLSN  1740
1741  DMMGSYAEMK  FDHTNSLNIA  GLSLDFSSKL  DNIYSSDKFY  KQTVNLQLQP  YSLVTTLNSD  1800
1801  LKYNALDLTN  NGKLRLEPLK  LHVAGNLKGA  YQNNEIKHIY  AISSAALSAS  YKADTVAKVQ  1860
1861  GVEFSHRLNT  DIAGLASAID  MSTNYNSDSL  HFSNVFRSVM  APFTMTIDAH  TNGNGKLALW  1920
1921  GEHTGQLYSK  FLLKAEPLAF  TFSHDYKGST  SHHLVSRKSI  SAALEHKVSA  LLTPAEQTGT  1980
1981  WKLKTQFNNN  EYSQDLDAYN  TKDKIGVELT  GRTLADLTLL  DSPIKVPLLL  SEPINIIDAL  2040
2041  EMRDAVEKPQ  EFTIVAFVKY  DKNQDVHSIN  LPFFETLQEY  FERNRQTIIV  VVENVQRNLK  2100
2101  HINIDQFVRK  YRAALGKLPQ  QANDYLNSFN  WERQVSHAKE  KLTALTKKYR  ITENDIQIAL  2160
2161  DDAKINFNEK  LSQLQTYMIQ  FDQYIKDSYD  LHDLKIAIAN  IIDEIIEKLK  SLDEHYHIRV  2220
2221  NLVKTIHDLH  LFIENIDFNK  SGSSTASWIQ  NVDTKYQIRI  QIQEKLQQLK  RHIQNIDIQH  2280
2281  LAGKLKQHIE  AIDVRVLLDQ  LGTTISFERI  NDVLEHVKHF  VINLIGDFEV  AEKINAFRAK  2340
2341  VHELIERYEV  DQQIQVLMDK  LVELTHQYKL  KETIQKLSNV  LQQVKIKDYF  EKLVGFIDDA  2400
2401  VKKLNELSFK  TFIEDVNKFL  DMLIKKLKSF  DYHQFVDETN  DKIREVTQRL  NGEIQALELP  2460
2461  QKAEALKLFL  EETKATVAVY  LESLQDTKIT  LIINWLQEAL  SSASLAHMKA  KFRETLEDTR  2520
2521  DRMYQMDIQQ  ELQRYLSLVG  QVYSTLVTYI  SDWWTLAAKN  LTDFAEQYSI  QDWAKRMKAL  2580
2581  VEQGFTVPEI  KTILGTMPAF  EVSLQALQKA  TFQTPDFIVP  LTDLRIPSVQ  INFKDLKNIK  2640
2641  IPSRFSTPEF  TILNTFHIPS  FTIDFVEMKV  KIIRTIDQMQ  NSELQWPVPD  IYLRDLKVED  2700
2701  IPLARITLPD  FRLPEIAIPE  FIIPTLNLND  FQVPDLHIPE  FQLPHISHTI  EVPTFGKLYS  2760
2761  ILKIQSPLFT  LDANADIGNG  TTSANEAGIA  ASITAKGESK  LEVLNFDFQA  NAQLSNPKIN  2820
2821  PLALKESVKF  SSKYLRTEHG  SEMLFFGNAI  EGKSNTVASL  HTEKNTLELS  NGVIVKINNQ  2880
2881  LTLDSNTKYF  HKLNIPKLDF  SSQADLRNEI  KTLLKAGHIA  WTSSGKGSWK  WACPRFSDEG  2940
2941  THESQISFTI  EGPLTSFGLS  NKINSKHLRV  NQNLVYESGS  LNFSKLEIQS  QVDSQHVGHS  3000
3001  VLTAKGMALF  GEGKAEFTGR  HDAHLNGKVI  GTLKNSLFFS  AQPFEITAST  NNEGNLKVRF  3060
3061  PLRLTGKIDF  LNNYALFLSP  SAQQASWQVS  ARFNQYKYNQ  NFSAGNNENI  MEAHVGINGE  3120
3121  ANLDFLNIPL  TIPEMRLPYT  IITTPPLKDF  SLWEKTGLKE  FLKTTKQSFD  LSVKAQYKKN  3180
3181  KHRHSITNPL  AVLCEFISQS  IKSFDRHFEK  NRNNALDFVT  KSYNETKIKF  DKYKAEKSHD  3240
3241  ELPRTFQIPG  YTVPVVNVEV  SPFTIEMSAF  GYVFPKAVSM  PSFSILGSDV  RVPSYTLILP  3300
3301  SLELPVLHVP  RNLKLSLPHF  KELCTISHIF  IPAMGNITYD  FSFKSSVITL  NTNAELFNQS  3360
3361  DIVAHLLSSS  SSVIDALQYK  LEGTTRLTRK  RGLKLATALS  LSNKFVEGSH  NSTVSLTTKN  3420
3421  MEVSVAKTTK  AEIPILRMNF  KQELNGNTKS  KPTVSSSMEF  KYDFNSSMLY  STAKGAVDHK  3480
3481  LSLESLTSYF  SIESSTKGDV  KGSVLSREYS  GTIASEANTY  LNSKSTRSSV  KLQGTSKIDD  3540
3541  IWNLEVKENF  AGEATLQRIY  SLWEHSTKNH  LQLEGLFFTN  GEHTSKATLE  LSPWQMSALV  3600
3601  QVHASQPSSF  HDFPDLGQEV  ALNANTKNQK  IRWKNEVRIH  SGSFQSQVEL  SNDQEKAHLD  3660
3661  IAGSLEGHLR  FLKNIILPVY  DKSLWDFLKL  DVTTSIGRRQ  HLRVSTAFVY  TKNPNGYSFS  3720
3721  IPVKVLADKF  ITPGLKLNDL  NSVLVMPTFH  VPFTDLQVPS  CKLDFREIQI  YKKLRTSSFA  3780
3781  LNLPTLPEVK  FPEVDVLTKY  SQPEDSLIPF  FEITVPESQL  TVSQFTLPKS  VSDGIAALDL  3840
3841  NAVANKIADF  ELPTIIVPEQ  TIEIPSIKFS  VPAGIVIPSF  QALTARFEVD  SPVYNATWSA  3900
3901  SLKNKADYVE  TVLDSTCSST  VQFLEYELNV  LGTHKIEDGT  LASKTKGTLA  HRDFSAEYEE  3960
3961  DGKFEGLQEW  EGKAHLNIKS  PAFTDLHLRY  QKDKKGISTS  AASPAVGTVG  MDMDEDDDFS  4020
```

```
4021  KWNFYYSPQS  SPDKKLTIFK  TELRVRESDE  ETQIKVNWEE  EAASGLLTSL  KDNVPKATGV  4080
4081  LYDYVNKYHW  EHTGLTLREV  SSKLRRNLQN  NAEWVYQGAI  RQIDDIDVRF  QKAASGTTGT  4140
4141  YQEWKDKAQN  LYQELLTQEG  QASFQGLKDN  VFDGLVRVTQ  KFHMKVKHLI  DSLIDFLNFP  4200
4201  RFQFPGKPGI  YTREELCTMF  IREVGTVLSQ  VYSKVHNGSE  ILFSYFQDLV  ITLPFELRKH  4260
4261  KLIDVISMYR  ELLKDLSKEA  QEVFKAIQSL  KTTEVLRNLQ  DLLQFIFQLI  EDNIKQLKEM  4320
4321  KFTYLINYIQ  DEINTIFNDY  IPYVFKLLKE  NLCLNLHKFN  EFIQNELQEA  SQELQQIHQY  4380
4381  IMALREEYFD  PSIVGWTVKY  YELEEKIVSL  IKNLLVALKD  FHSEYIVSAS  NFTSQLSSQV  4440
4441  EQFLHRNIQE  YLSILTDPDG  KGKEKIAELS  ATAQEIIKSQ  AIATKKIISD  YHQQFRYKLQ  4500
4501  DFSDQLSDYY  EKFIAESKRL  IDLSIQNYHT  FLIYITELLK  KLQSTTVMNP  YMKLAPGELT  4560
4561  IIL
```

Note: bold letters are precursor sequence

APPENDIX B

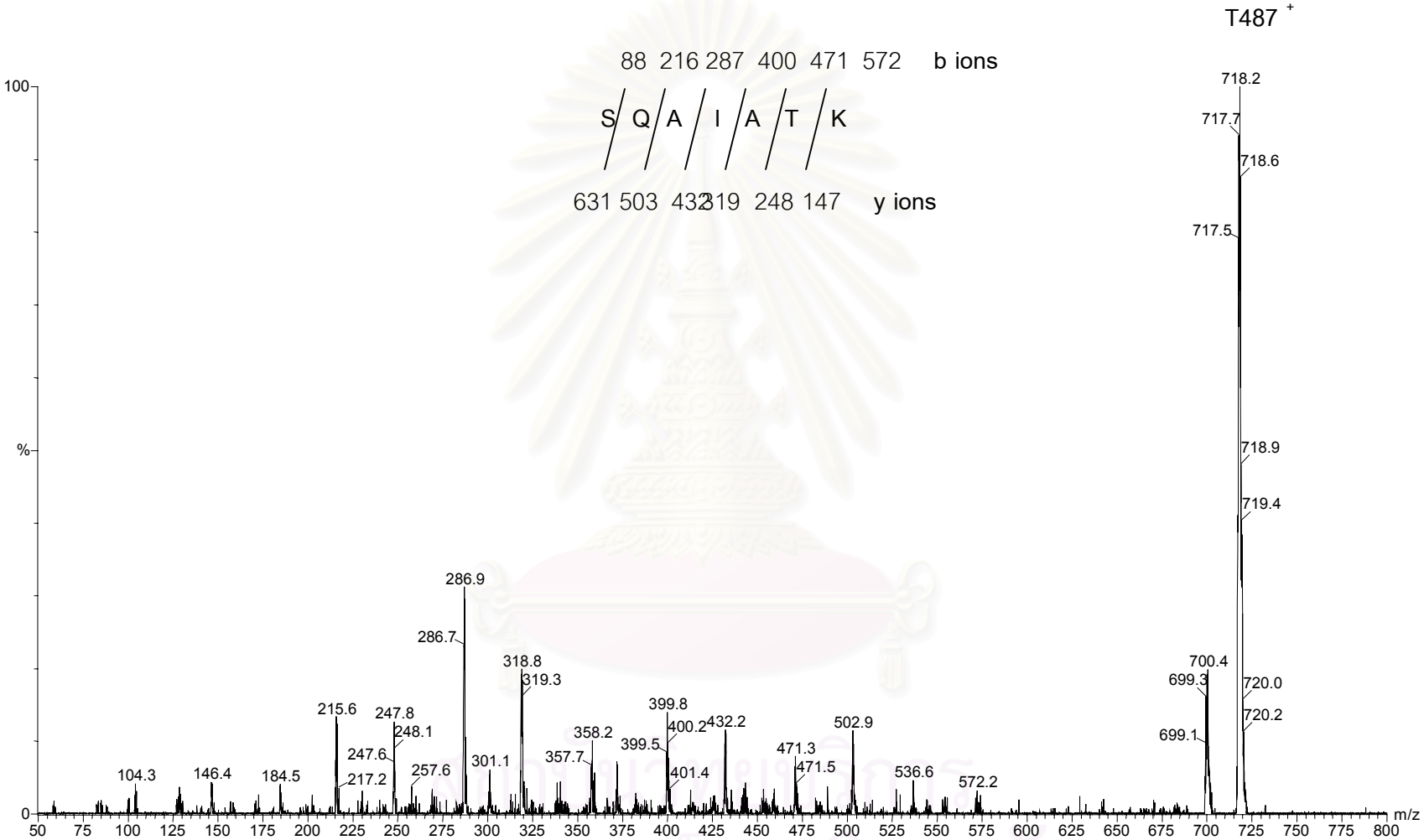

Figure B1. Product ion scanning of m/z 718.2 with the amino acid sequence SQAIATK of T487 was obtained.

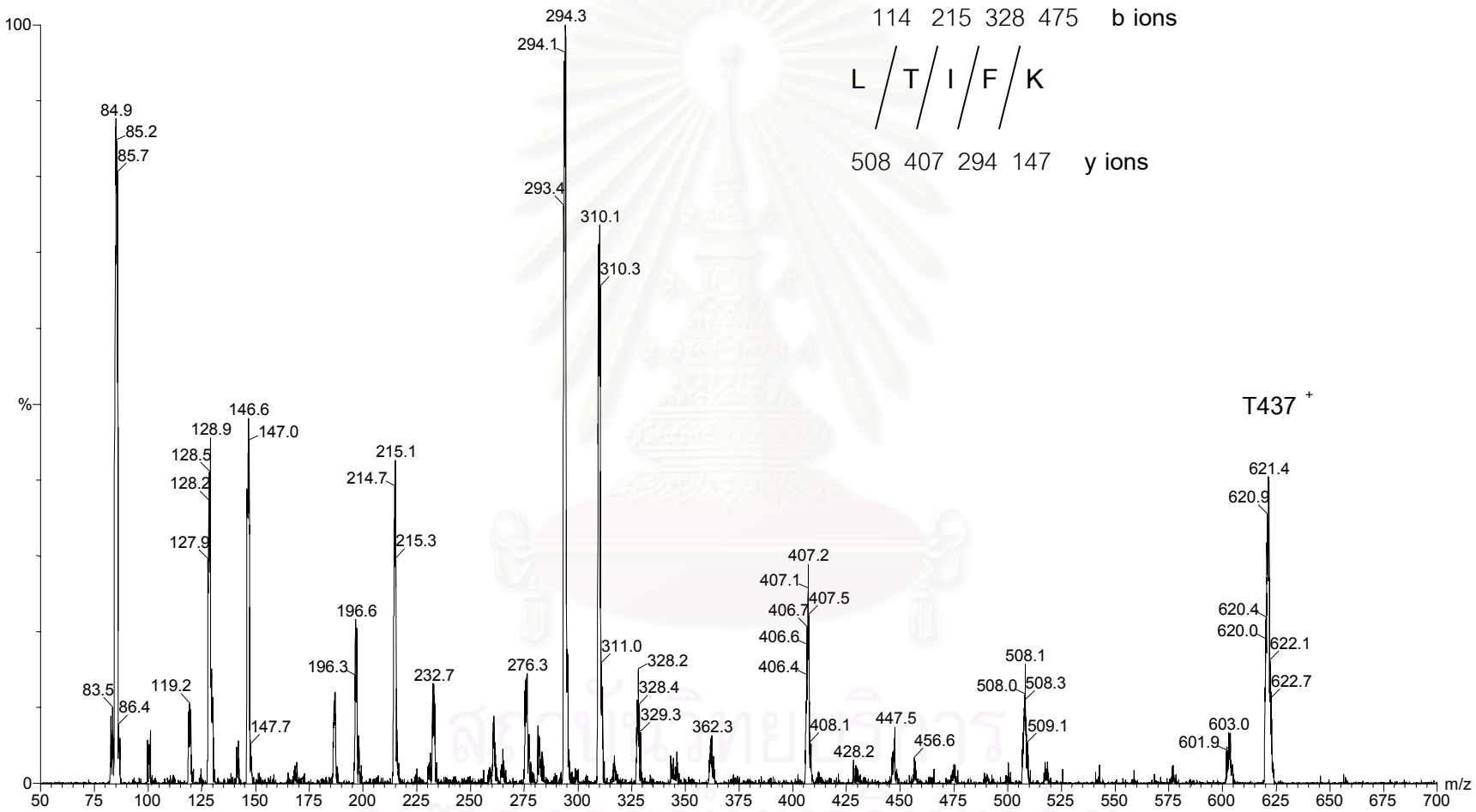

Figure B2. Product ion scanning of m/z 621.4 with the amino acid sequence LTIFK of T437 was obtained.

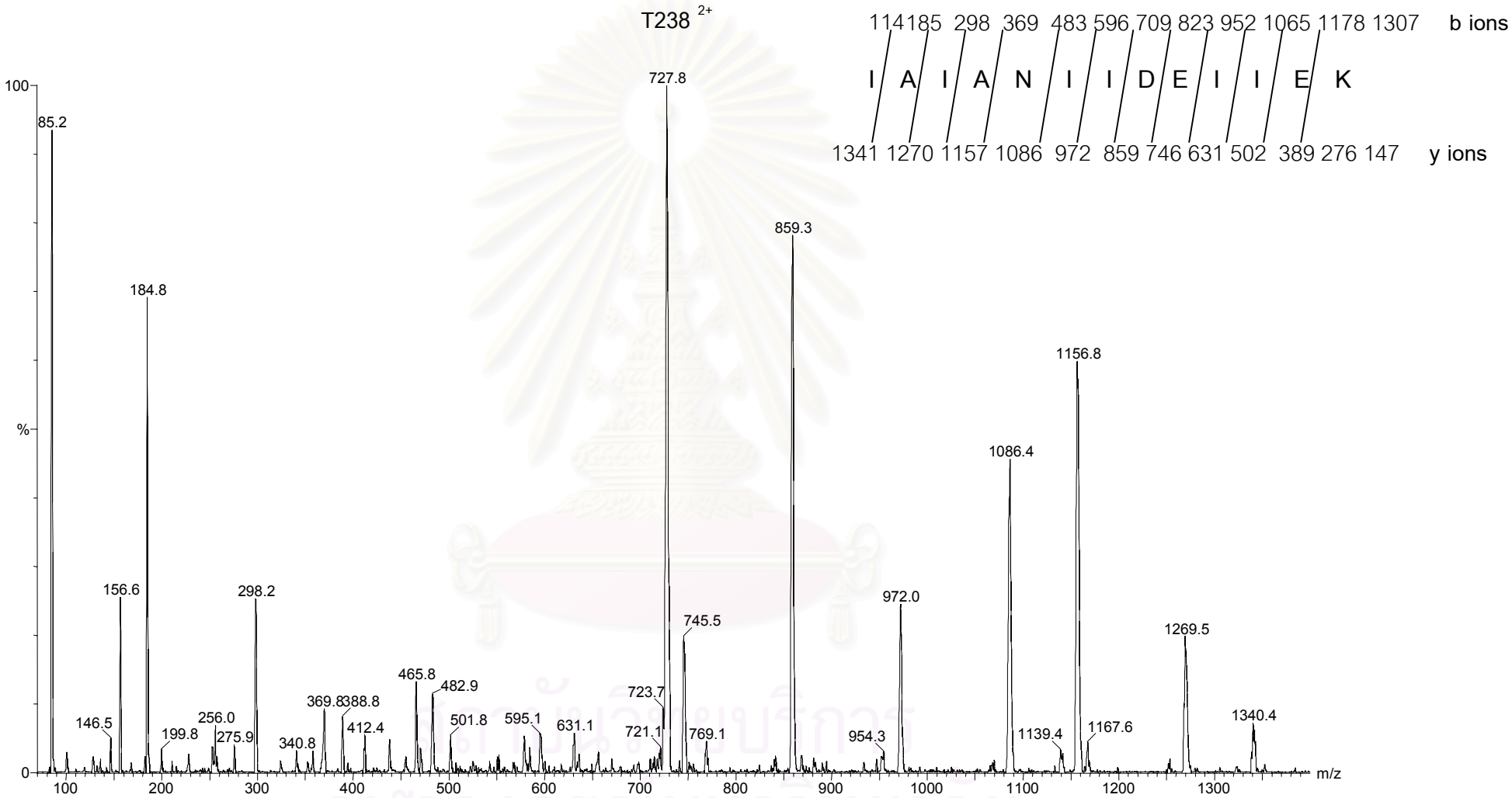

Figure B3. Product ion scanning of m/z 727.8 with the amino acid sequence IAIANIIDEIIEK of T238 was obtained.

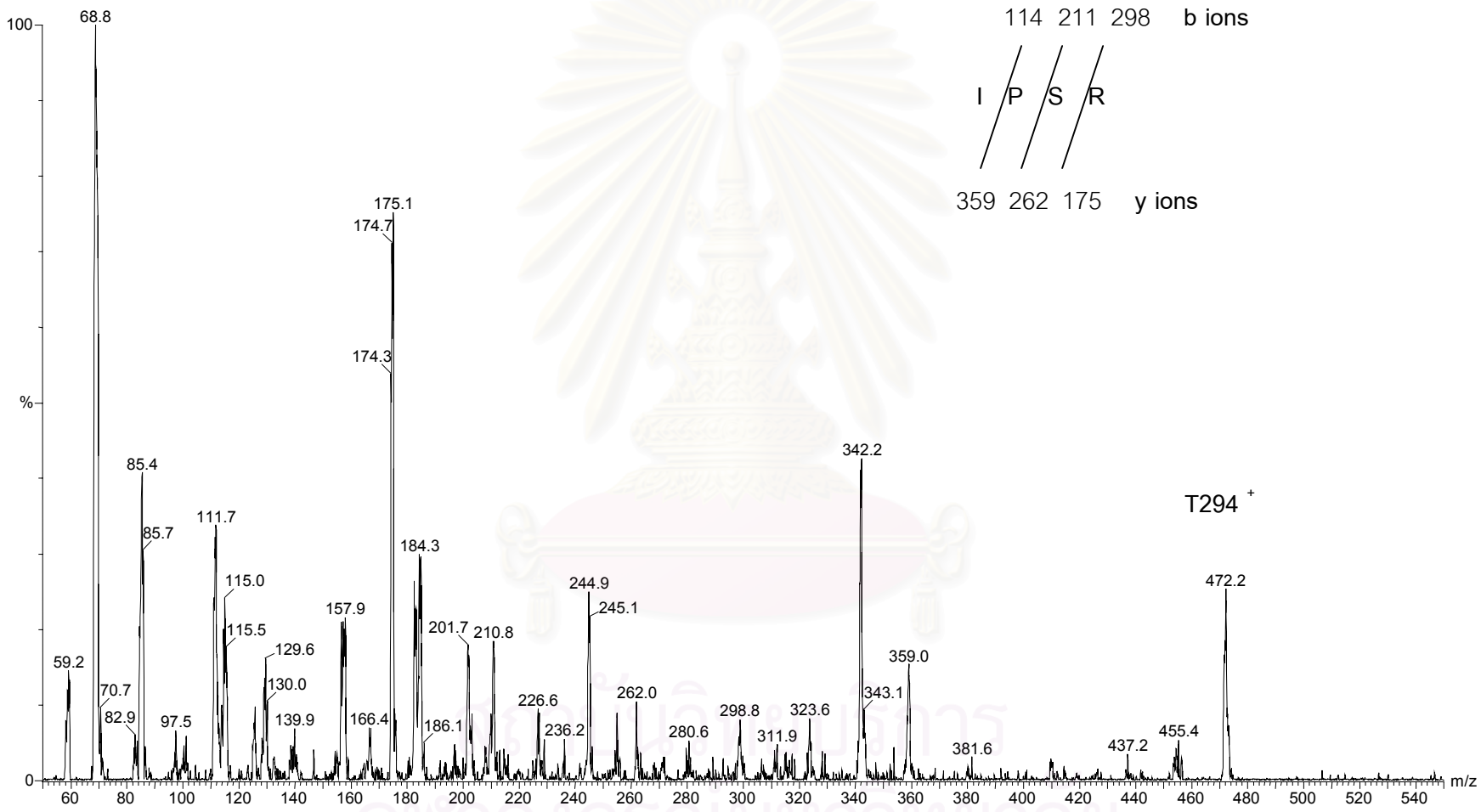

Figure B4. Product ion scanning of m/z 472.2 with the amino acid sequence IPSR of T294 was obtained.

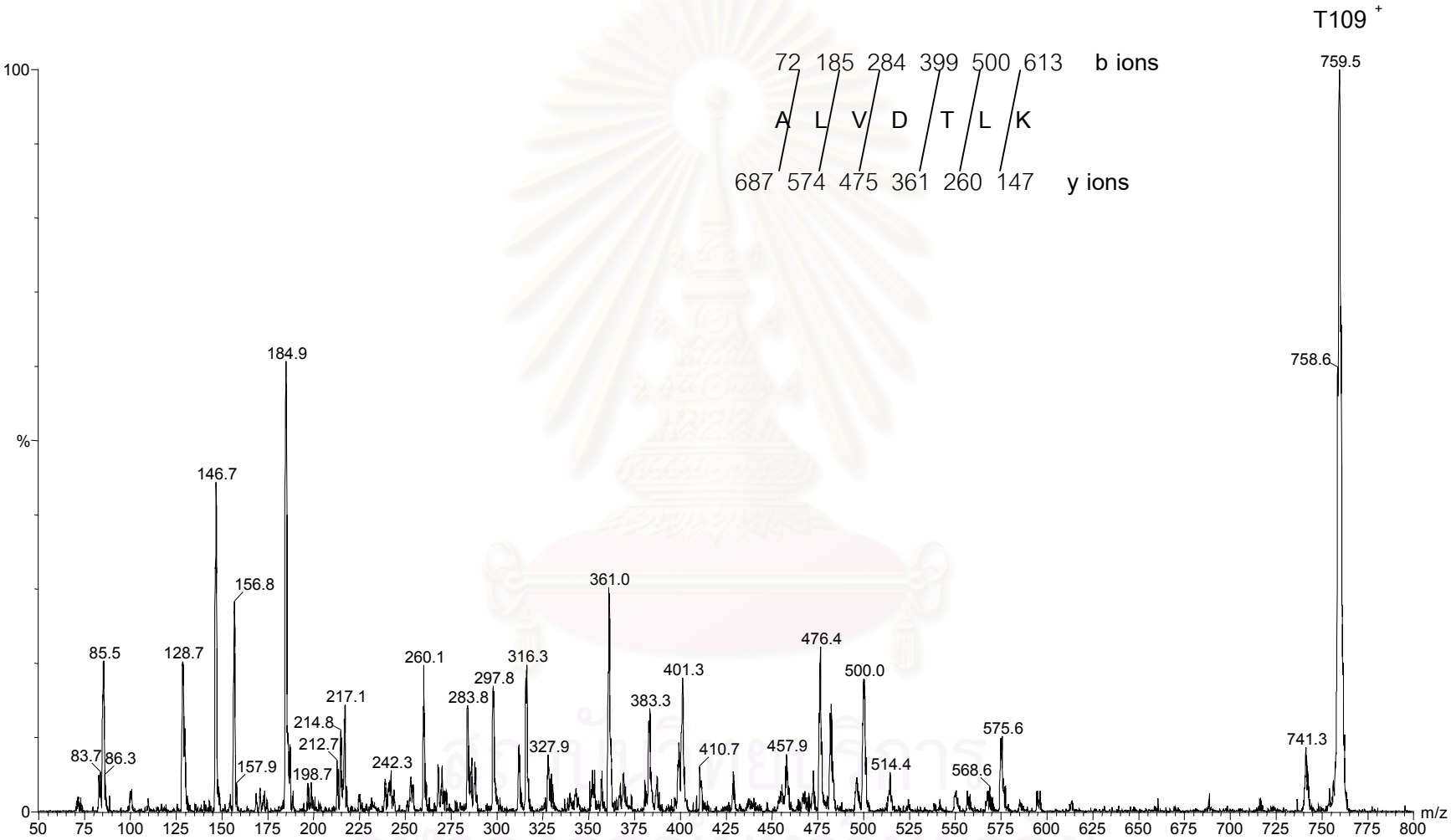

Figure B5. Product ion scanning of m/z 759.5 with the amino acid sequence ALVDTLK of T109 was obtained.

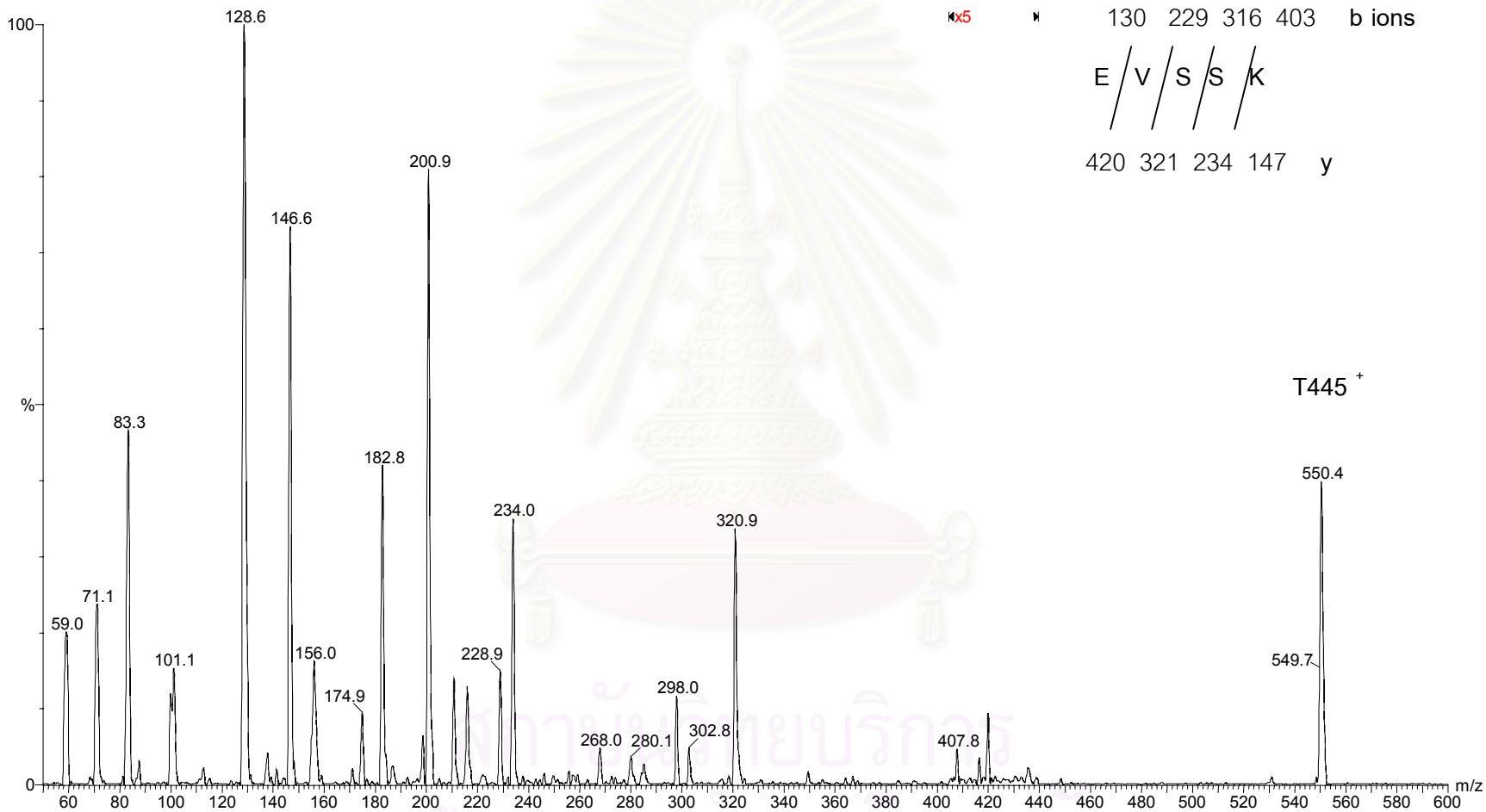

Figure B6. Product ion scanning of m/z 550.4 with the amino acid sequence EVSSK of T445 was obtained.

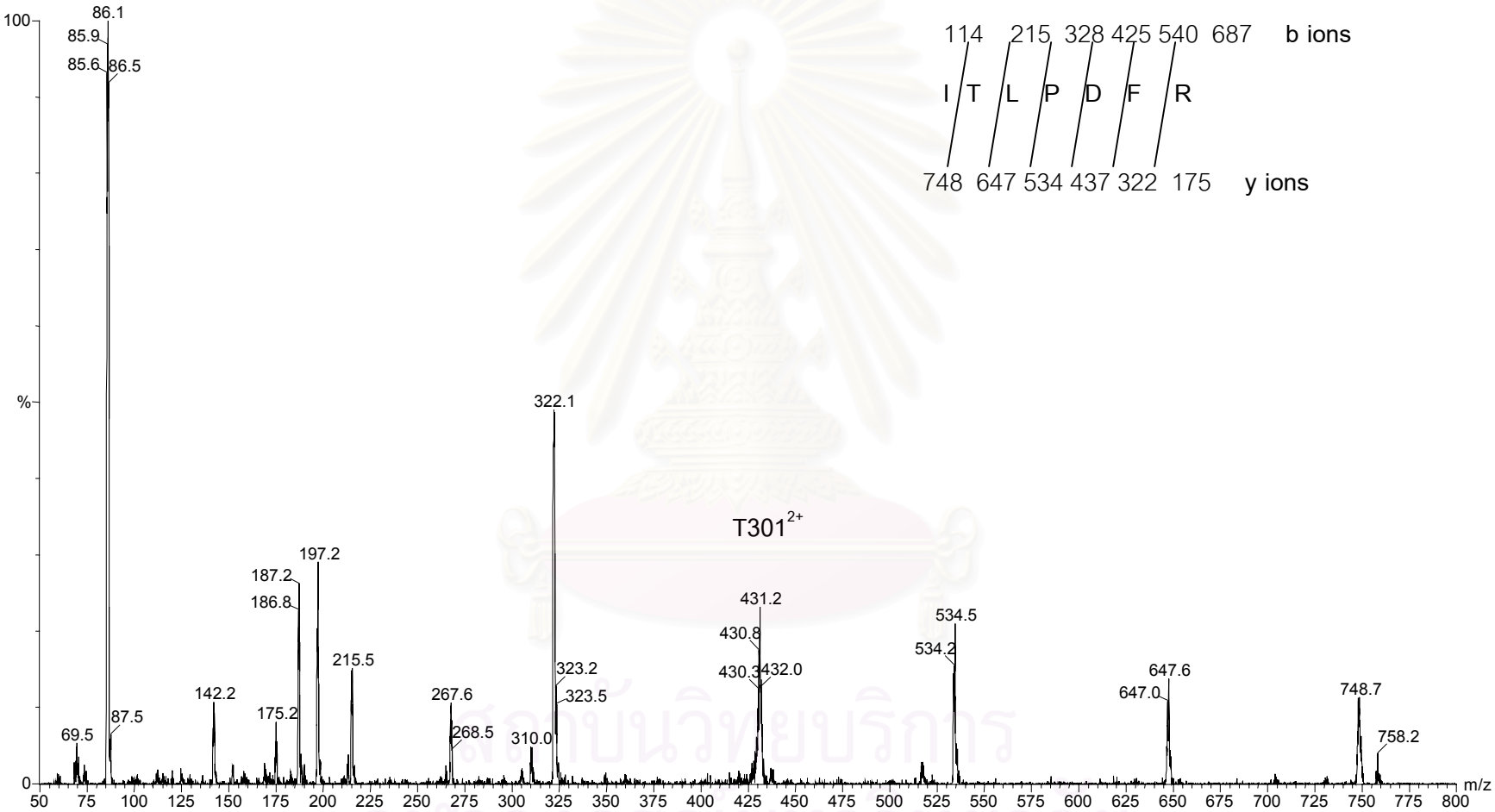

Figure B7. Product ion scanning of m/z 431.2 with the amino acid sequence ITLPDFR of T301 was obtained.

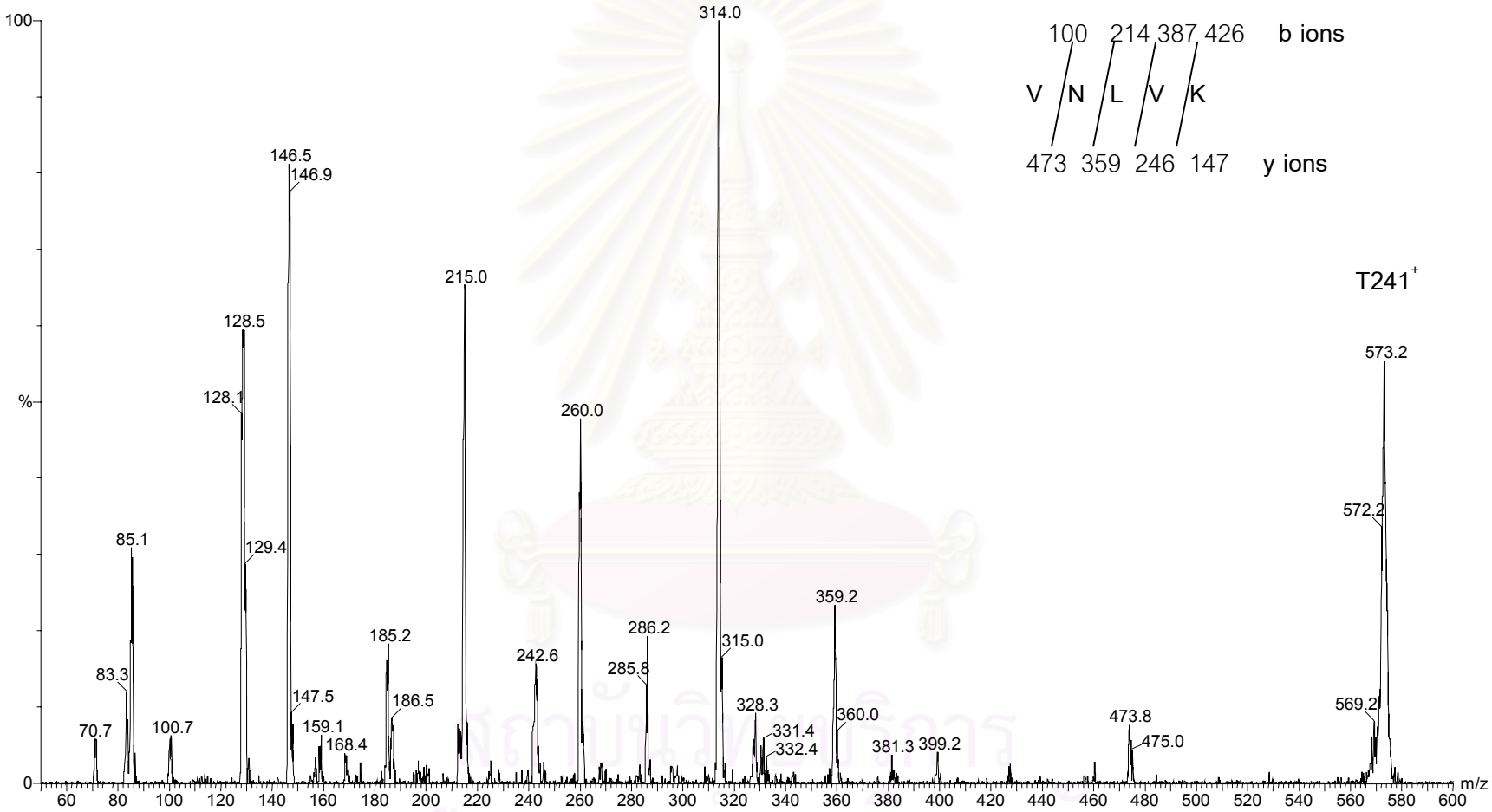

Figure B8. Product ion scanning of m/z 573.2 with the amino acid sequence VNLVK of T241 was obtained.

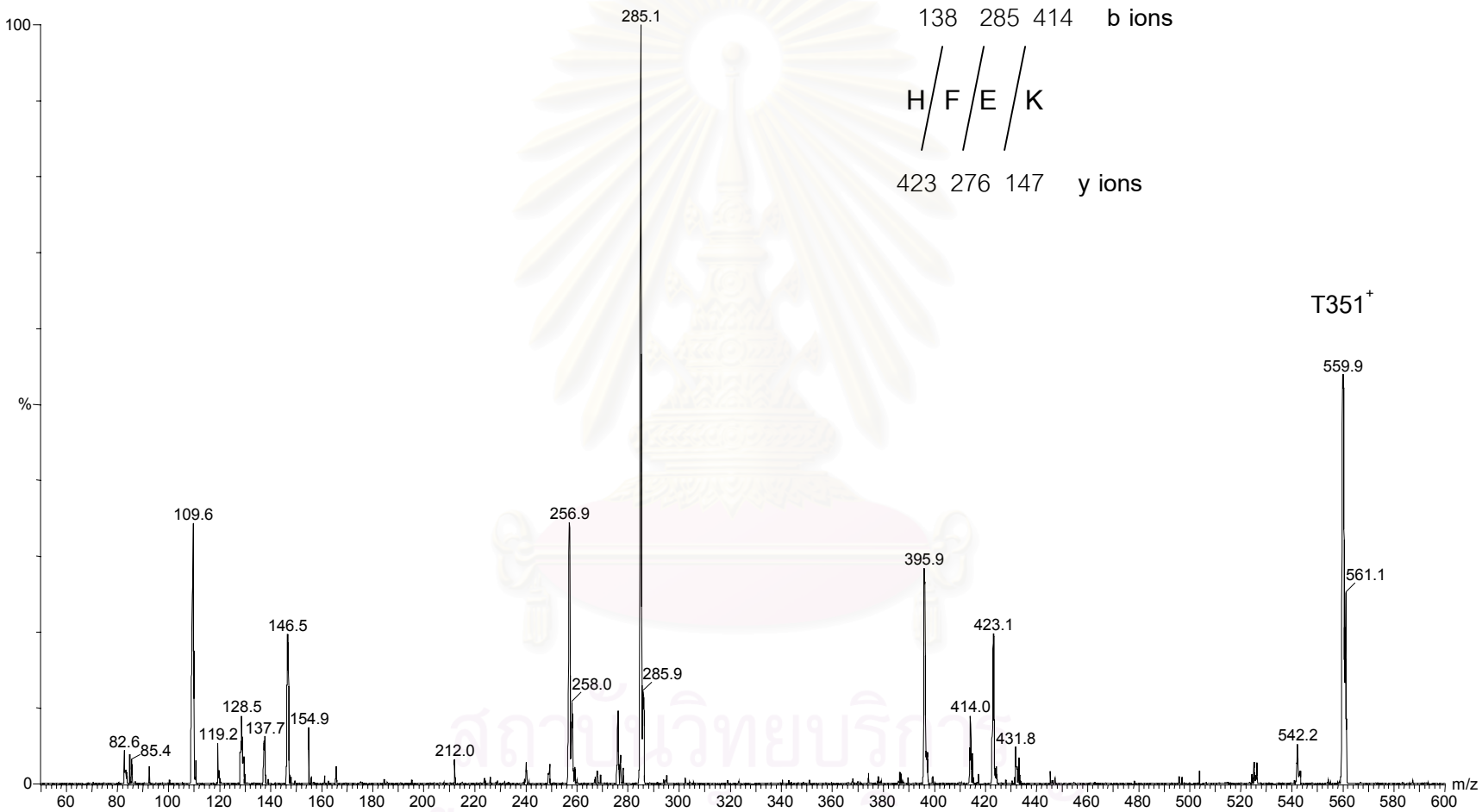

Figure B9. Product ion scanning of m/z 559.9 with the amino acid sequence HFEK of T351 was obtained.

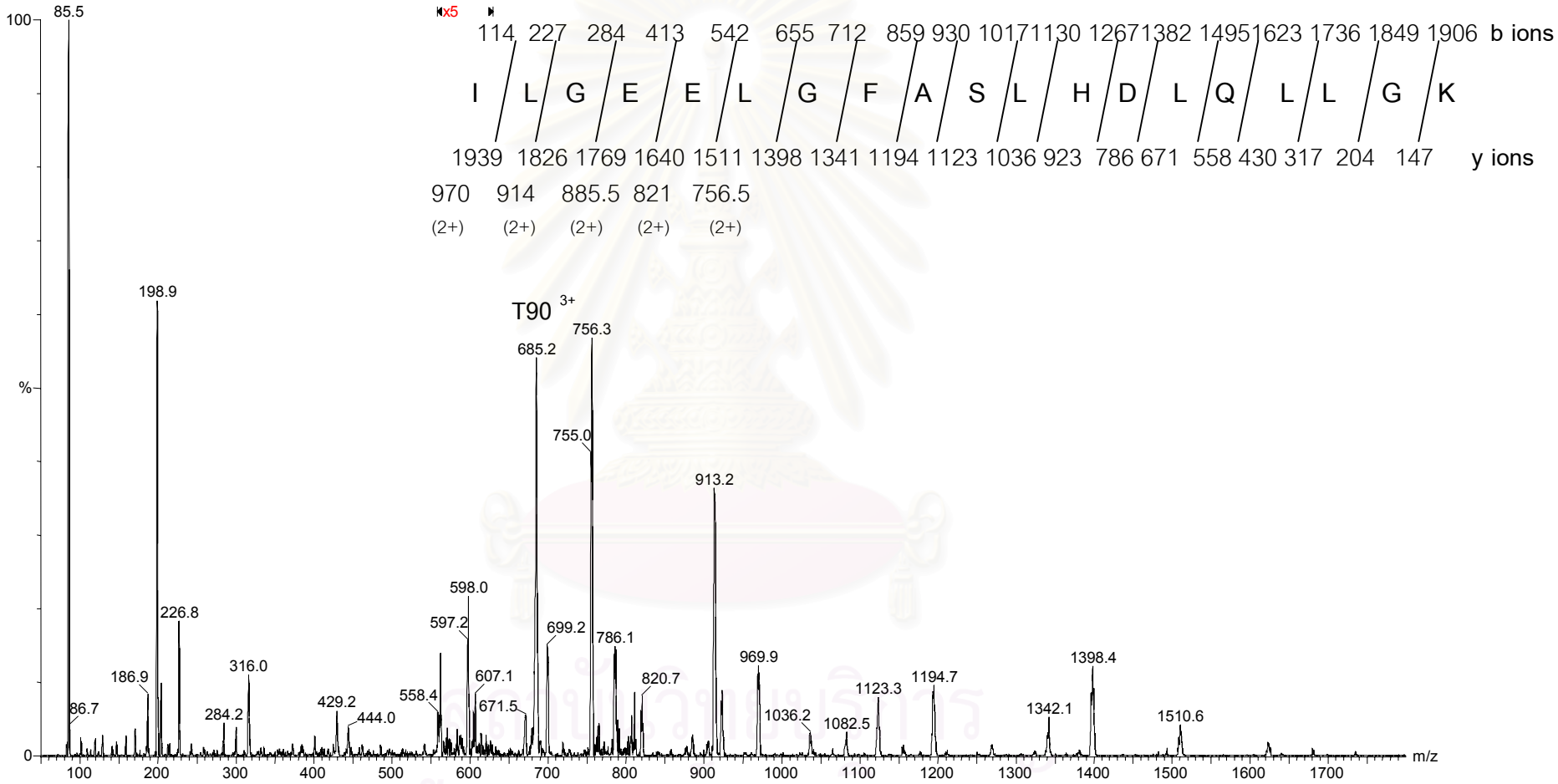

Figure B10. Product ion scanning of m/z 685.2 with the amino acid sequence ILGEELGFASLHDLQLLGK of T90 was obtained.

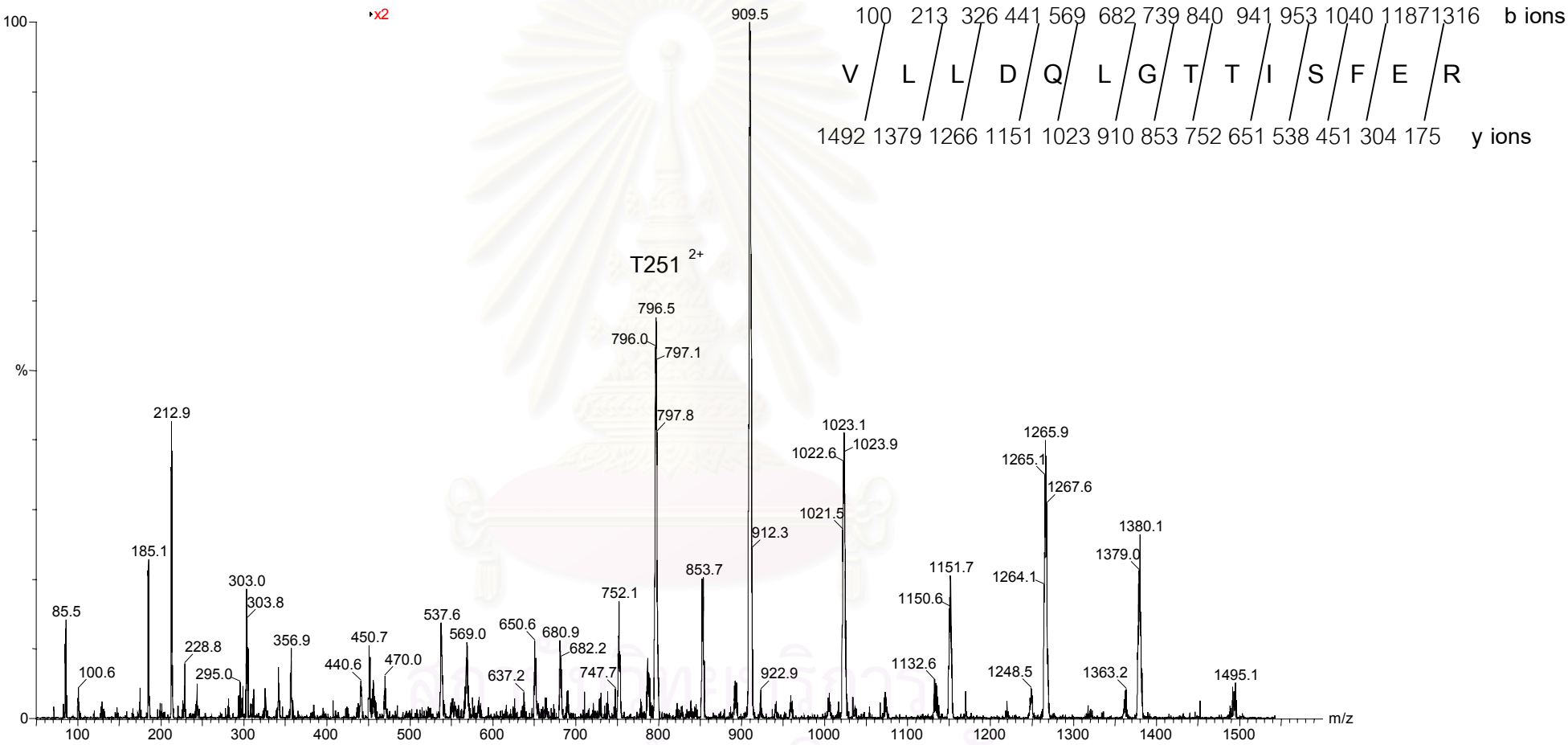

Figure B11. Product ion scanning of m/z 796.5 with the amino acid sequence VLLDQLGTTISFER of T251 was obtained.

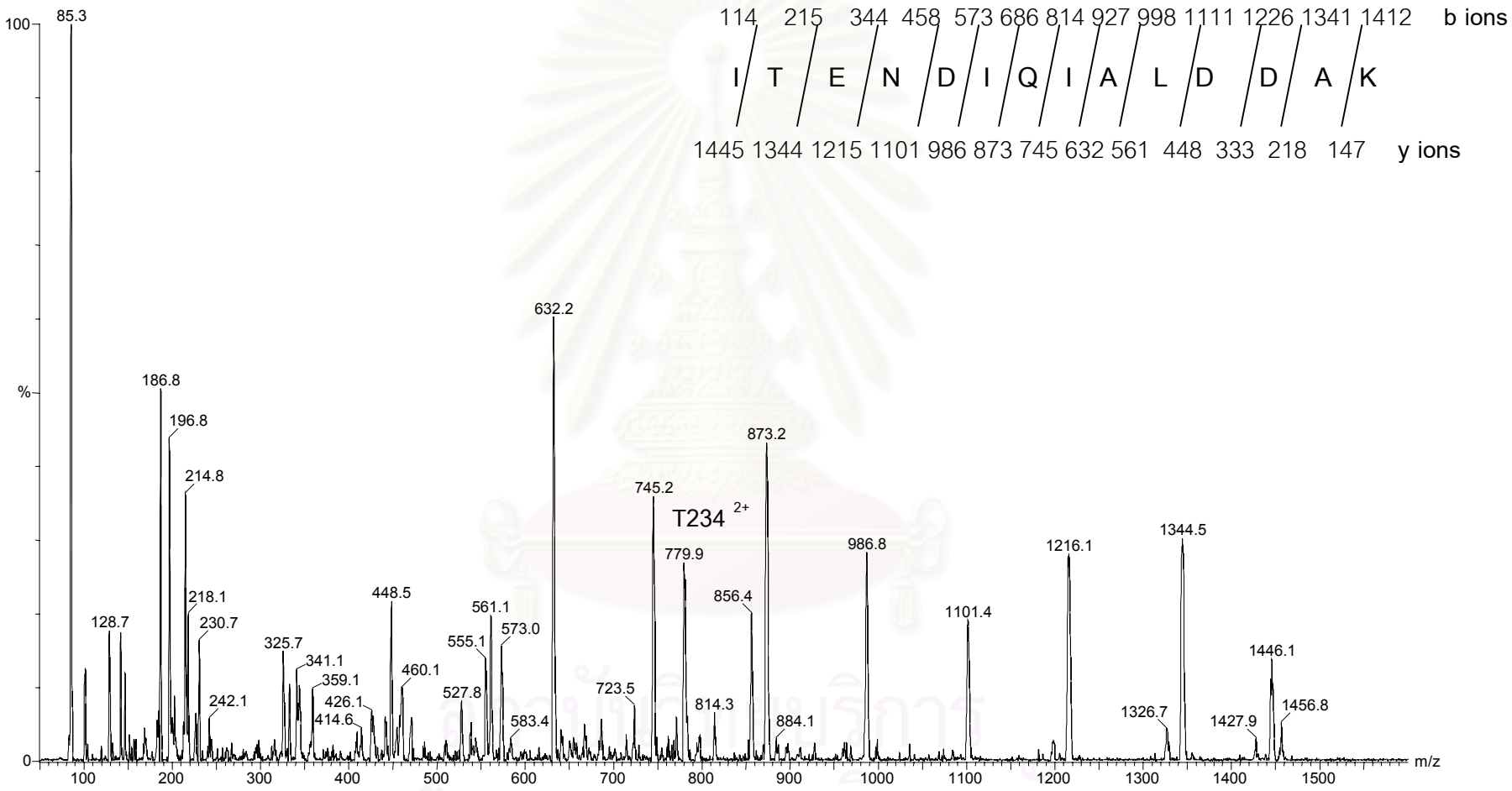

Figure B12. Product ion scanning of m/z 779.9 with the amino acid sequence ITENDIQIALDDAK of T234 was obtained.

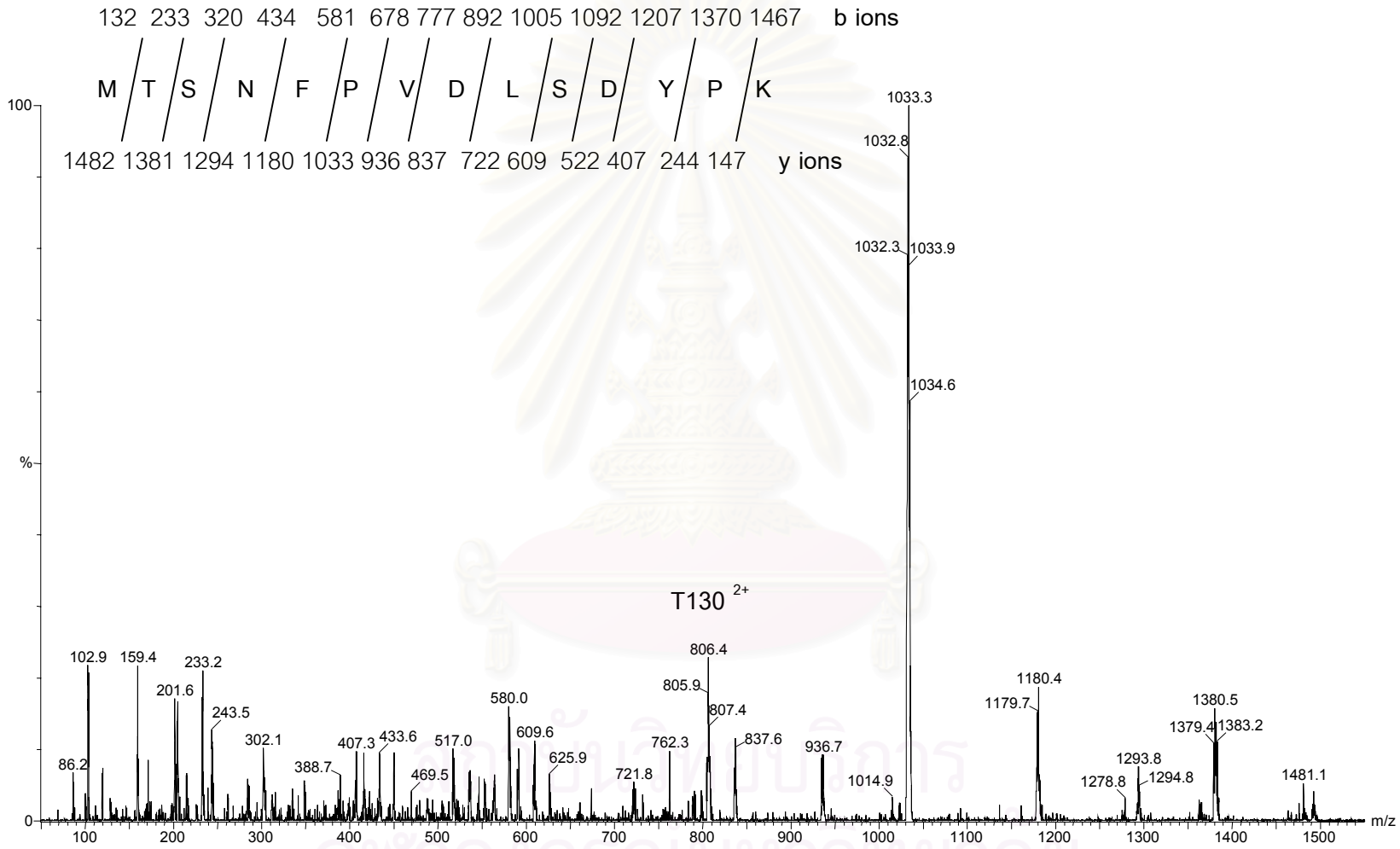

Figure B13. Product ion scanning of m/z 806.4 with the amino acid sequence MTSNFPVDLSDYPK of T130 was obtained.

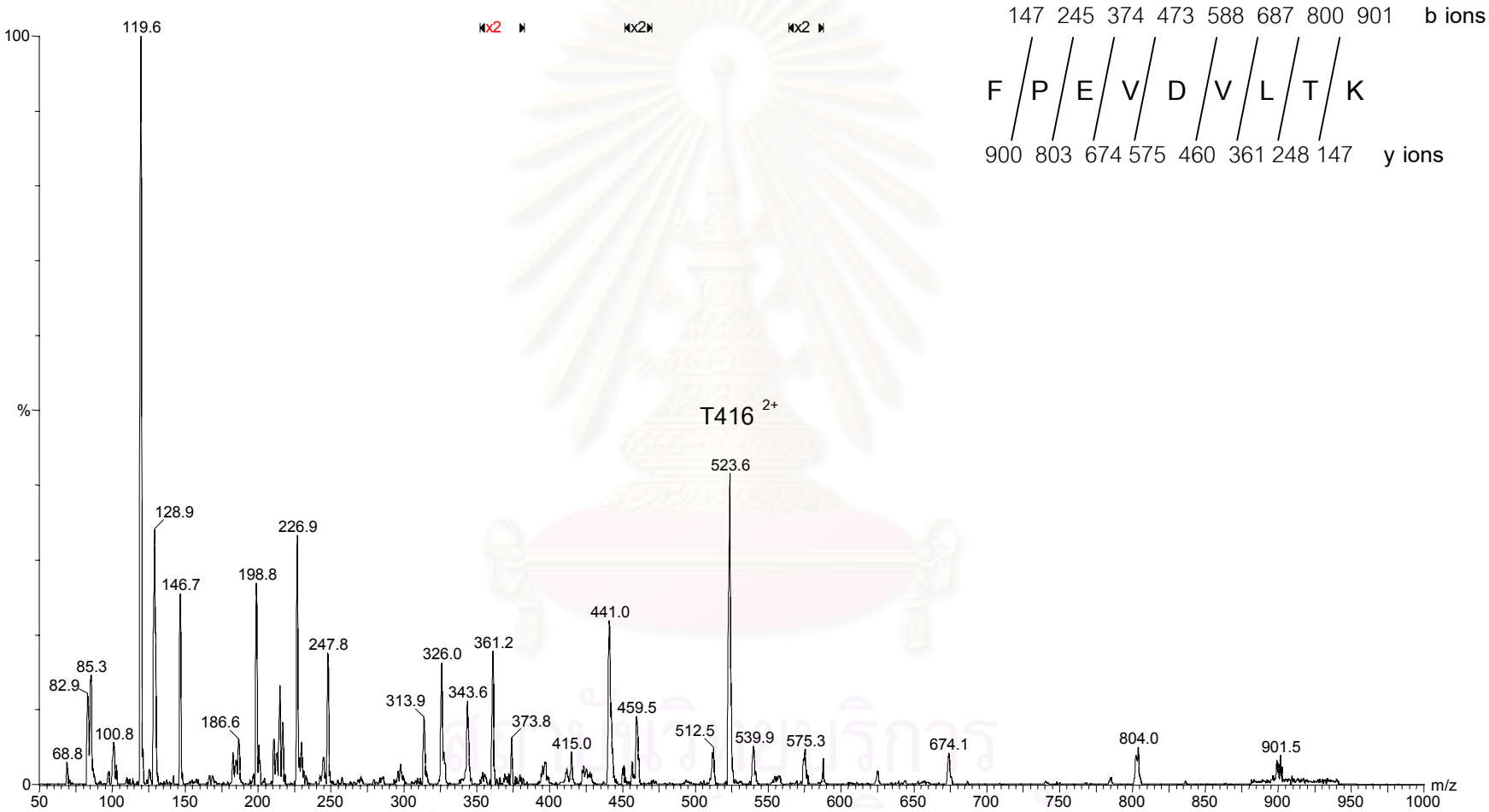

Figure B14. Product ion scanning of m/z 523.6 with the amino acid sequence FPEVDVLTK of T416 was obtained.

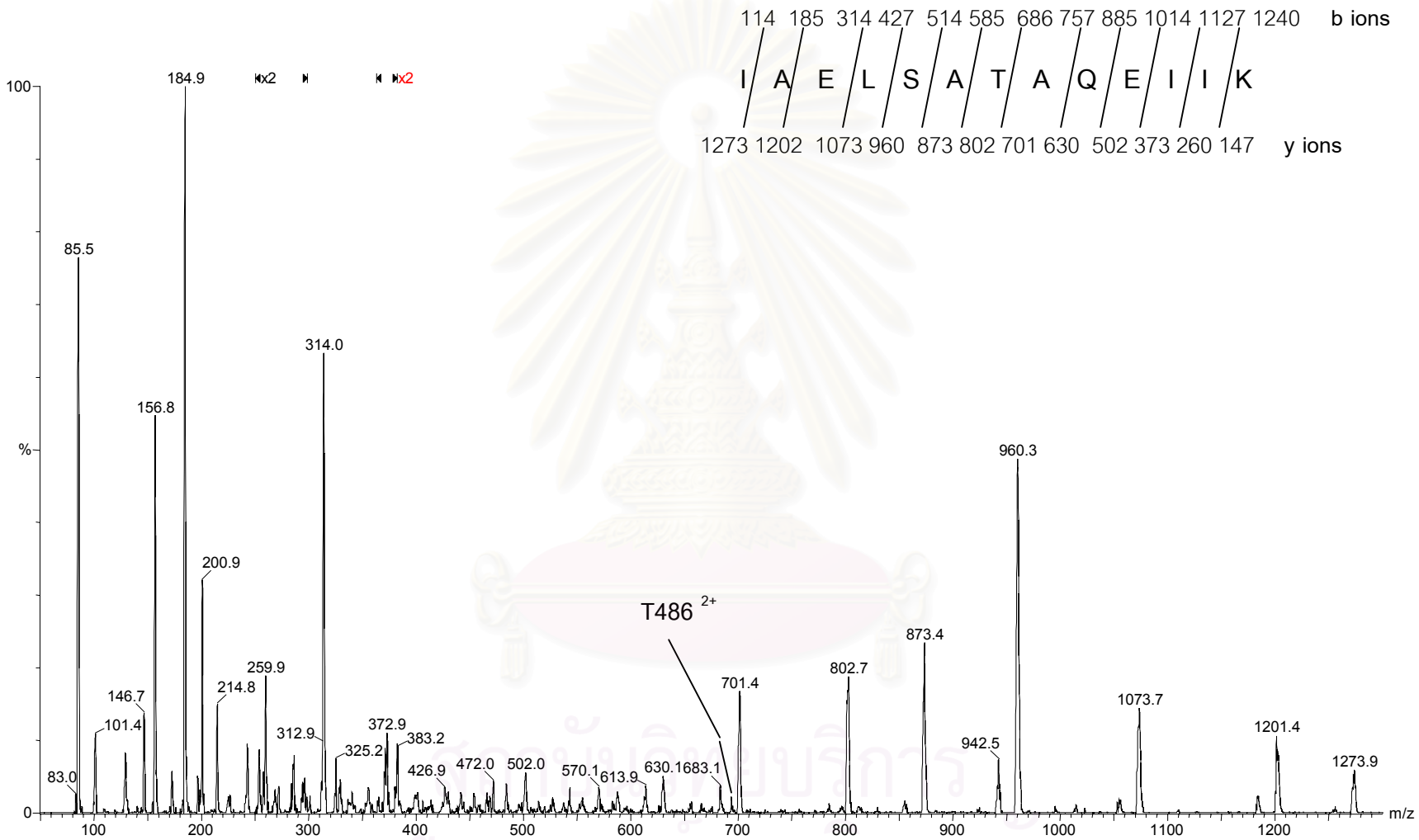

Figure B15. Product ion scanning of m/z 693.6 with the amino acid sequence IAELSATAQEIIK of T486 was obtained.

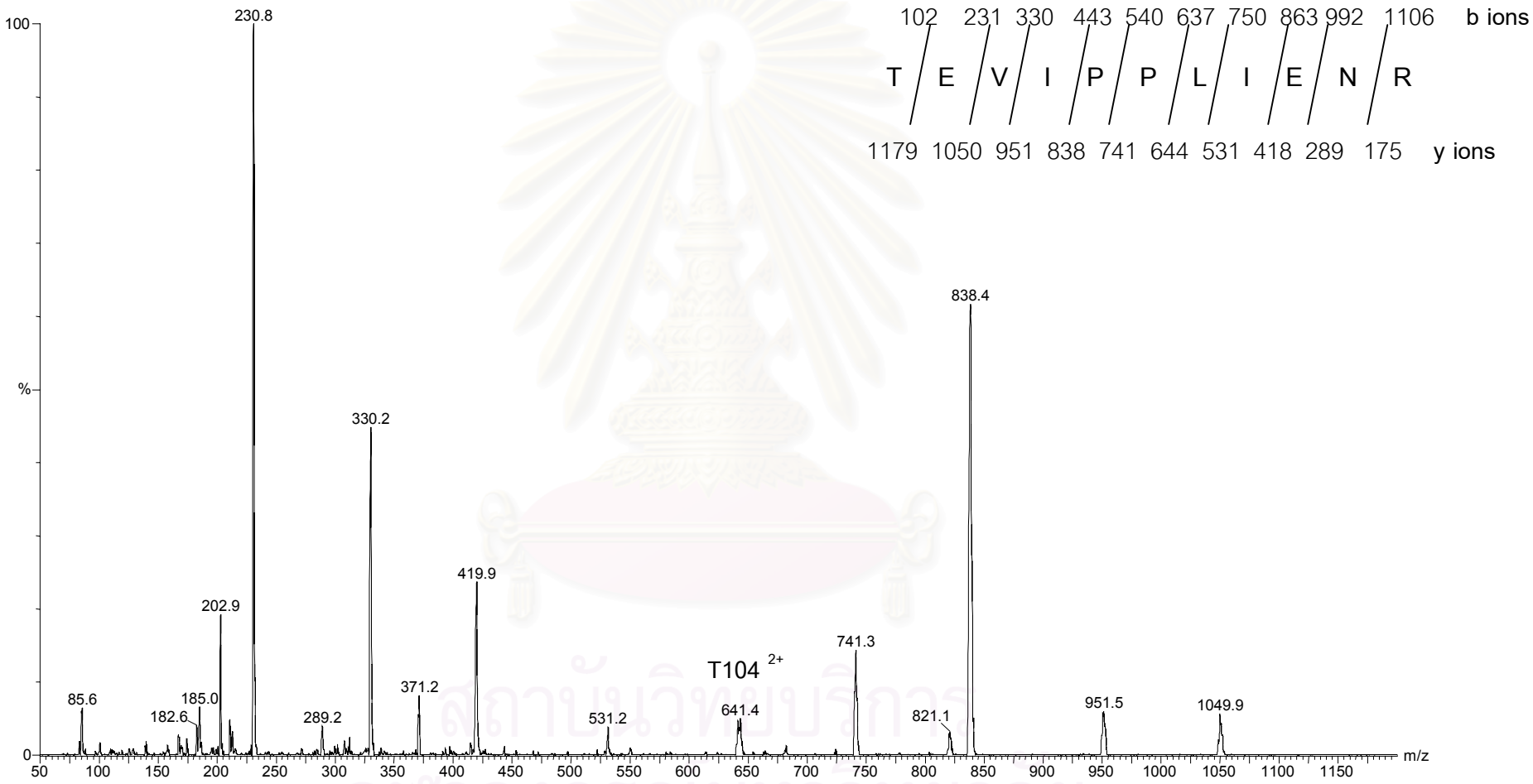

Figure B16. Product ion scanning of m/z 641.4 with the amino acid sequence TEVIPPLIENR of T104 was obtained.

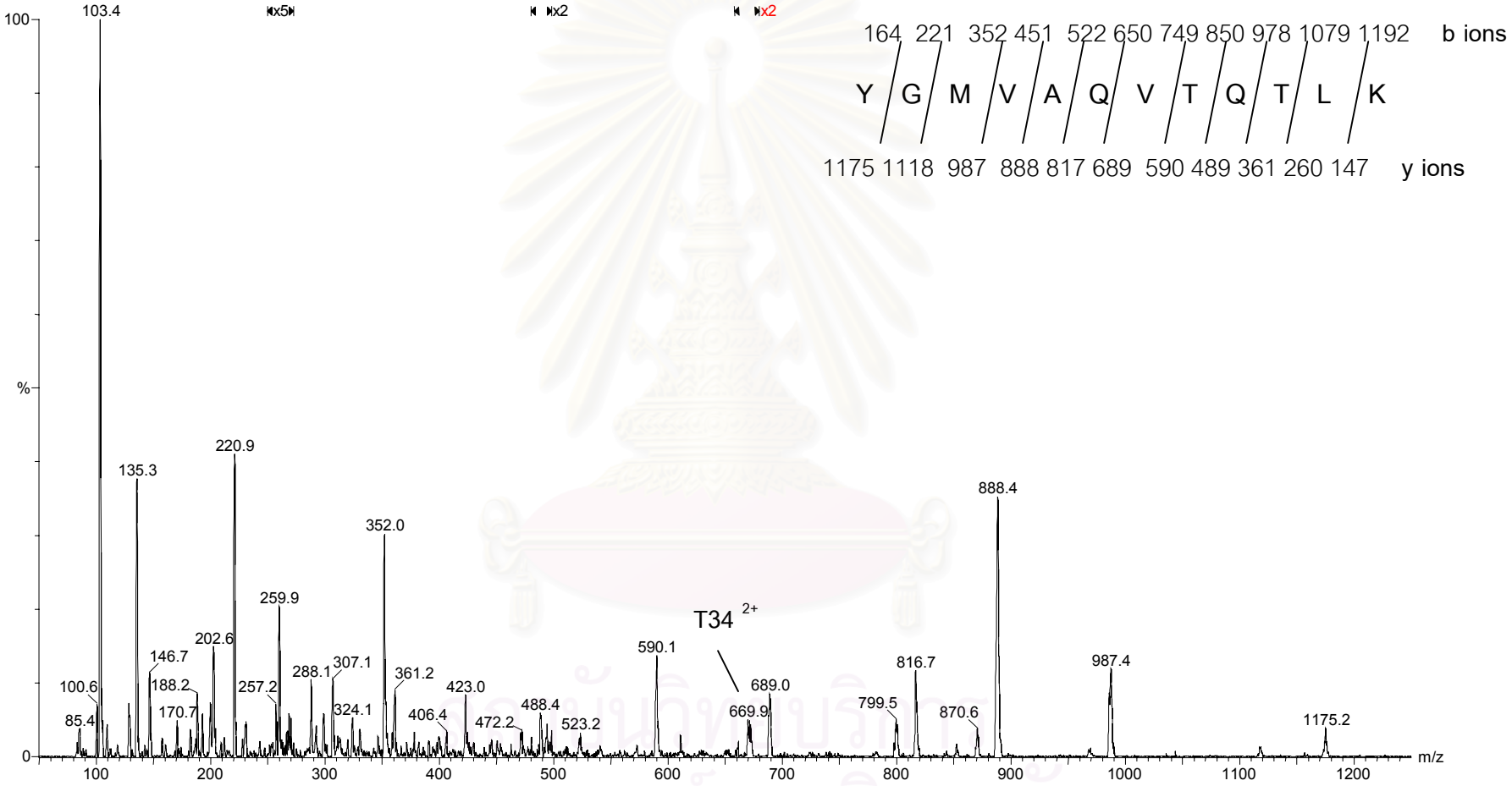

Figure B17. Product ion scanning of m/z 669.9 with the amino acid sequence YGMVAQVTQTLK of T34 was obtained.

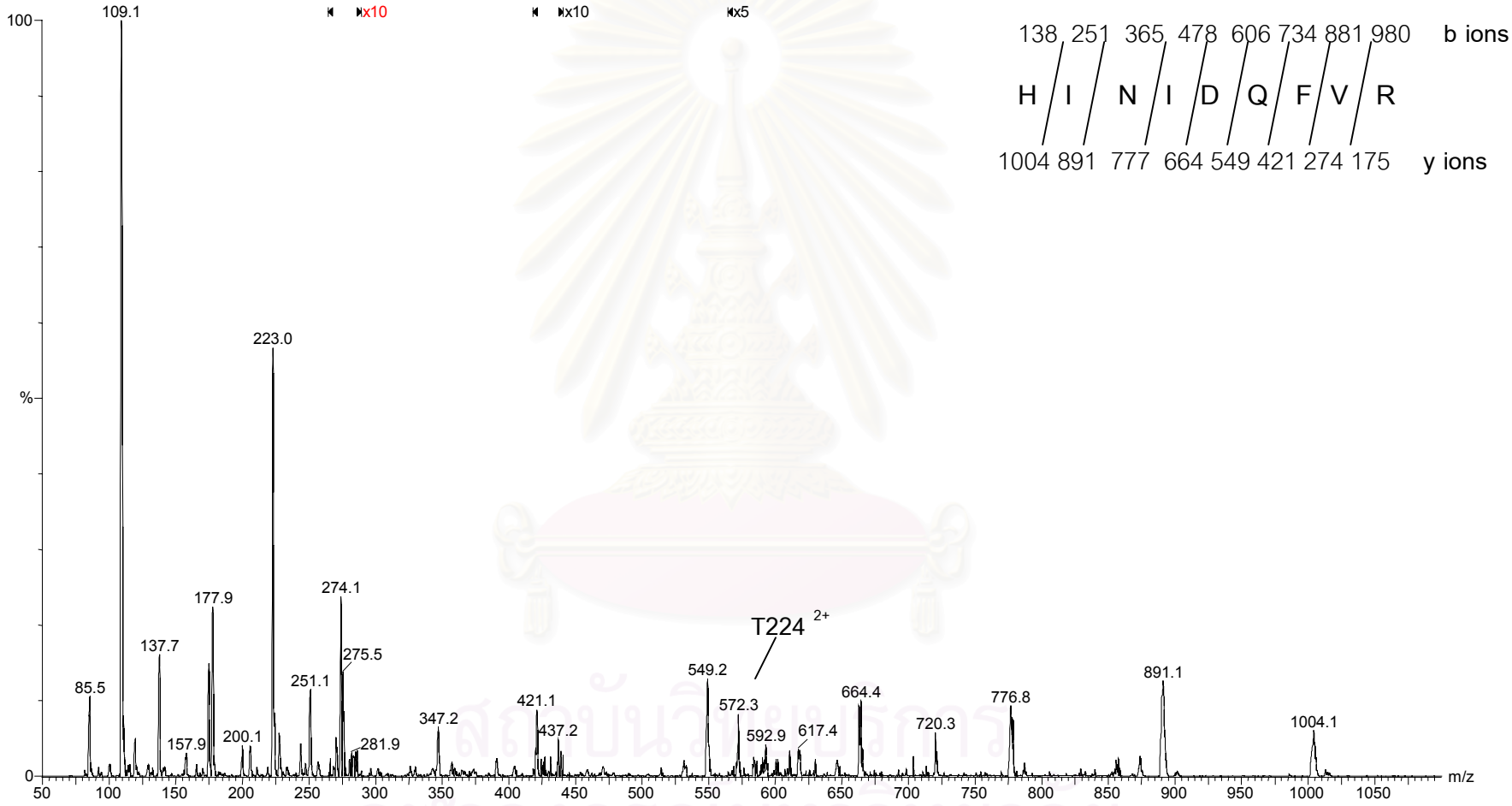

Figure B18. Product ion scanning of m/z 572.3 with the amino acid sequence HINIDQFVR of T224 was obtained.

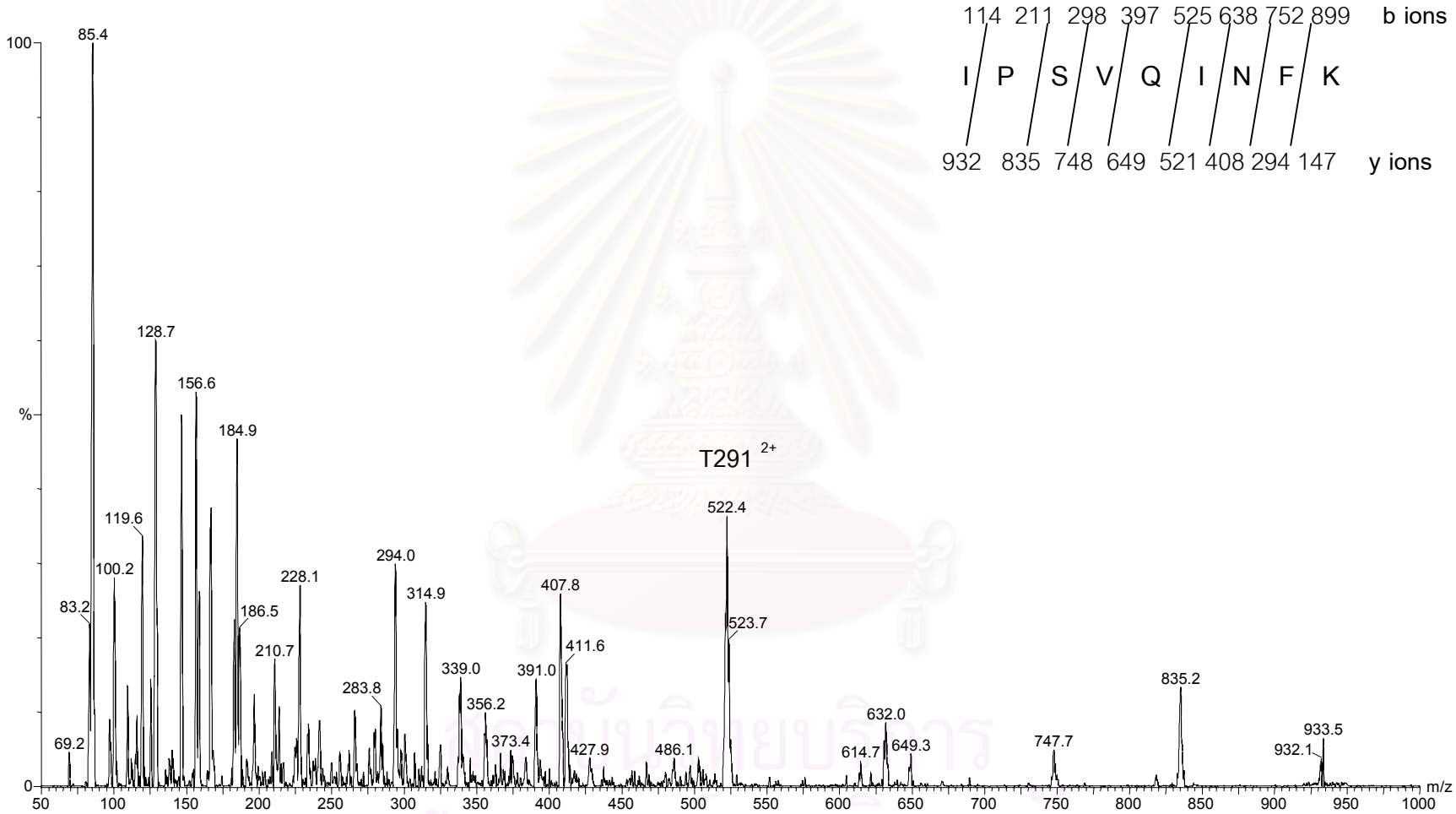

Figure B19. Product ion scanning of m/z 523.7 with the amino acid sequence IPSVQINFK of T291 was obtained.

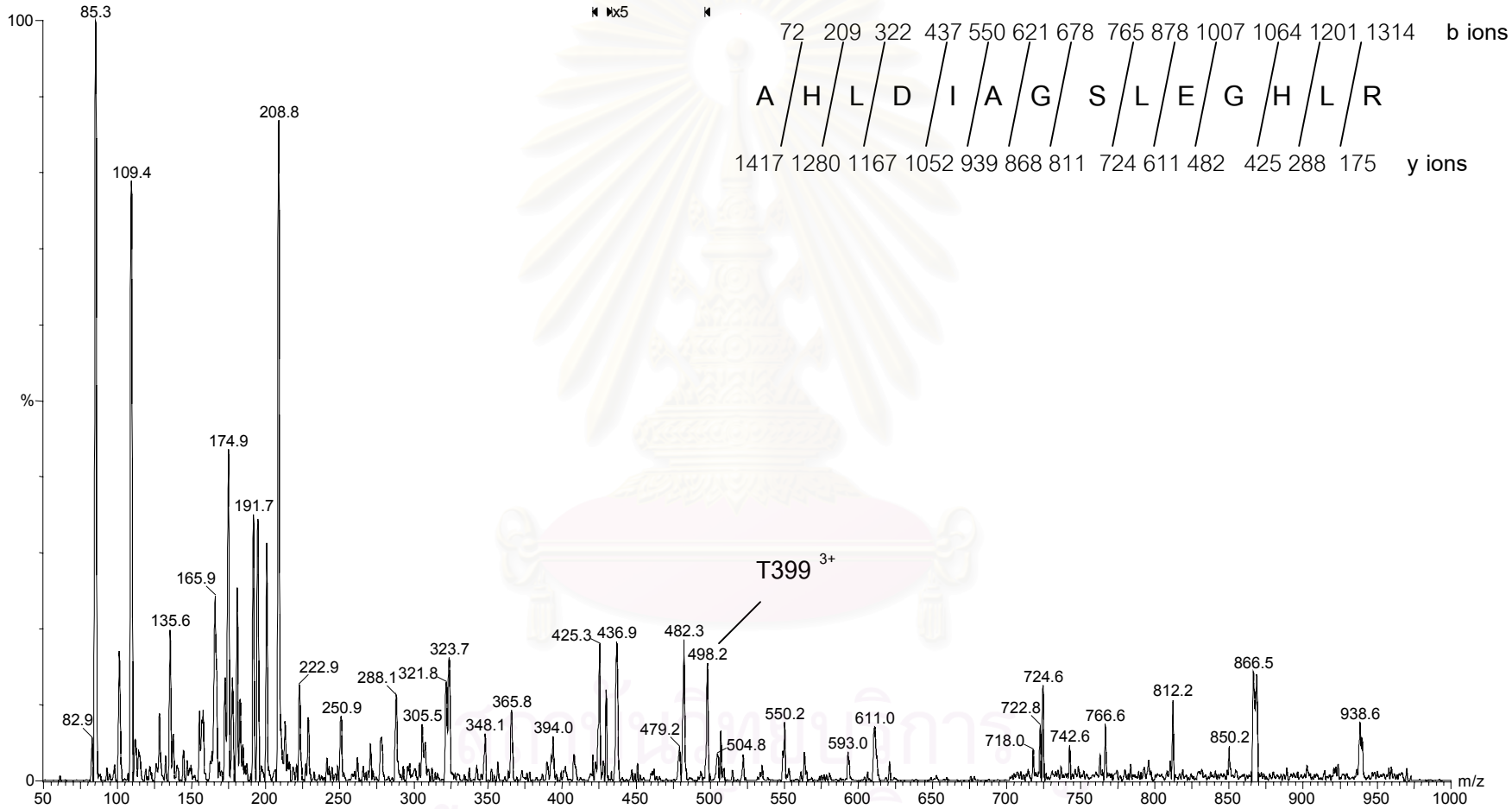

Figure B20. Product ion scanning of m/z 498.2 with the amino acid sequence AHLDIAGSLEGHLR of T399 was obtained.

BIOGRAPHY

Miss Siriporn Sangsuthum was born on 25 April 1972 at Chulalongkorn hospital, Bangkok. She graduated with bachelor degree of science, Department of General Science, Faculty of Science, Chulalongkorn University in 2538. Now, she is a scientist at Department of Clinical Chemistry, Faculty of Allied Health Sciences, Chulalongkorn University.